Novel Fluorescent Fluorenyl/Carbazolyl-Pyridinyl Alternating Copolymers: Synthesis, Characterization and Properties

PAN XIAOYONG

(*B.Sc.*, *U*niversity of Science and Technology of China)

A THESIS SUBMITTED FOR THE DEGREE OF

MASTER OF SCIENCE

DEPARTMENT OF CHEMISTRY

NATIONAL UNIVERSITY OF SINGAPORE

2006

Acknowledgements

I wish to express my gratitude to my supervisors, Associate Professor Siu-Choon Ng and Professor Hardy S. O. Chan for their constant guidance and encouragement throughout this project.

I would like to express my appreciation to Mr. Zhou Xuedong, Dr. Liu Shouping and Dr. Xiao Changyong for their kind assistance in the preparation and characterization of copolymers.

I would like to express my heartfelt thanks to all graduate students and technologists in our group. In particular, I would like to thank Lai Xianghua, Chen Daming, Xia Haibing, Tang Weihua, Liu Xiao and Zhang Sheng, for their advice and friendship.

I would also like to thank the staff of Central Instrumental Lab, Thermal Analysis Lab, Honours Lab and Chemical Store for their help to obtain spectra, special chemicals and to use the computers.

Finally, I would like to express my gratitude to the National University of Singapore for the award of a research scholarship and for providing me with the opportunity and the facilities to carry out the research work reported in this thesis.

Table of Contents

Summary

A few series of novel, soluble fluorescent alternating polymers were designed and synthesized. They were poly[2,7-(9,9-bis(2-ethylhexyl)fluorenyl)-alt-(pyridinyl)] &poly[2,7-(9,9-bis(2-ethylhexyl)fluorenyl)](**I**),

poly[2,7-(9,9-bis[3,5-bis(benzyloxy)benzyl])fluorenyl-alt-(pyridinyl)](**II**)

and poly[(2,7-(N-(2-ethylhexyl)carbazloyl)-alt-(pyridinyl)] (**III**).

All polymers were prepared by Suzuki cross-coupling reaction and the structures of all polymers were confirmed by ^{1}H-NMR. Their properties such as absorption and emission, thermal stability, electrochemical properties were studied.

The result shows that the different linkage position of pyridinyl unit in the polymer backbone has significant effects on the electronic and optical properties of polymers in solution and in film phases. Meta-linkage(3,5-and 2,6-linkage) of pyridinyl units in the polymer backbone is more favourable to polymer for pure blue emission and prevention of aggregation of polymer chain than para-linkage(2,5-linkage) of the pyridinyl units. These polymers with pyridinyl units possess very low LUMO energy levels for an easy electron injection from a cathode. It also shows that the electronic and optical properties of fluorescent polymers can be well tuned by properly rationalized design of polymer architectures such as the introduction of proper side chain and incorporation of different pyridinyl moieties into polymer backbone.

Chapter 1 Introduction

1.1 General introduction to conjugated polymers

Conjugated polymers have been increasingly attracting interest for the past 50 years. Earlier conventional insulating-polymer systems were used as substitutes for structural materials such as wood, ceramics and metals because of their high strength, light weight, ease of chemical modification/customization, and processibility at low temperature. It was in 1977 that Shirakawa, MacDiarmid, Heeger and coworkers first discovered that the films of polyacetylene (PA) exhibited profound increase in electrical conductivity when exposed to iodine vapor [1]. This discovery opened the modern era of conjugated conducting polymers. Since then, this class of conducting polymers has been greatly enlarged. Many conjugated conducting polymers including polyaniline (PAN) [2], polypyrool (PPyR) [3], polythiophene (PT) [4], poly(*p*-phenylene) (PPP) [5], poly(*p*-phenylene sulphide) [6], and poly(*p*-phenylene vinylene) (PPV) [7] have been synthesized and studied. The electrical conductivities of these polymer systems range from those $<10^{-10}$ S/cm (typical of insulators) to those $>10^4$ S/cm (nearly that of a good metal such as copper, 5×10^5 S/cm).

Apart form syntheses and investigation of potential application of new conjugated materials, a prime focus of the field has been the determination of the mechanisms of charge transfer in these organic semiconductors. Compared to metals and traditional semiconductors, the conducting mechanism of conjugated polymers is obviously different. Metals are intrinsically conducting due to the presence of free electrons. In traditional three-dimentional semiconductors, the fourfold (or sixfold, etc.) coordination of each atom to its neighbor through covalent bonds leads to a rigid structure. In such systems, the electronic excitation can be usually considered in the context of this rigid structure leading to the conventional concepts of electrons and holes as the dominant excitations. However, the essential structural characteristic of conjugated polymers is their conjugated π system extending over a number of recurrent monomeric units. The twofold coordination makes these systems generally more susceptible to structural distortion. This characteristic feature results in low-dimentional materials with a high anisotropy in conductivity, which is higher along the chain direction. As a result, the dominant "electronic" excitations are inherently coupled to chain distortions. The terms, solitons, polarons and bipolarons from solid-state physics are used to interpret the excitations in this class of one-dimentional polymer semiconductors.

When an electron moves in an ionic crystal, its surrounding medium will be polarized with negative ions being repelled away and positive ions being attracted towards it. The relative motion of the opposite ions gives rise to a polarization field, which in turn, affects the motion of the electron itself. This complex—moving electron and its accompanying polarization field----is called a polaron. [8] In conducting polymers, the term polaron is used to denote a localized electron state with accompanying lattice distortion, which forms a cation-radical pair. Because polarons represent localized distortions of the lattice, the associated energy levels must split off from the conduction and valence band. A polaron has a spin state of 1/2 (paramagnetic). In the case of perisitent attractive interaction between two polarons, formation of a stable bound state called a bipolaron is favored. Bipolaron is double charged but spinless. Similarly, because the structural deformation associated with the two charges is stronger than in the case of a polaron, the electronic energy levels of the bipolarons appear further away form the band edges. A charge soliton which is a spinless cation is formed when bipolarons dissociate.

However, the conjugated polymers are well-known insulators in their pure forms. Poly (*p*-phenylenevinylene) has an intrinsic resistivity of $10^{16}\Omega$ cm[7]. In order to achieve (semi)conducting materials, charge carriers have to be introduced in some ways. Normally, three ways of introducing charge carriers are used: 1) Doping-induced charge carriers. 2) Photo- and radiation-induced charge carriers. 3) Charge injection from suitable electrodes.

1.2 Conductivity in conjugated polymers

Similar to semiconductors, the conductivity (σ) of conjugated polymers can be expressed by the following equation: [9]

$$\sigma = n\, e\, \mu \qquad (1.1)$$

Where e is the elementary charge, n is the number of mobile charge carriers and μ is the mobility of the charge carriers. The number and mobility of the charge carriers are the two key factors contributing to the conductivity of polymers. The first (n) is related to the doping levels while the later (μ) is governed by the transport processes of charge carriers.

1.2.1 Conducting mechanism

There are two general classes of conducting polymer structures that lead to qualitatively different electronic properties: (i) Systems in which the ground state is twofold degenerate. For example, undoped trans-polyacetylene (*trans*-PA), the energy gap arises from the pattern of alternating single (long) and double (short) bonds [10] with additional contribution due to electron coulomb repulsion. [11, 12] Interchange of short and long bonds results in an equivalent (degenerate) ground state. At low doping level, polarons states are formed. As doping increases, bipolaron states are formed. The neutral defects are gradually pulled away from the charged defects, approach each other, and finally dissociate to give charged solitons, which states at midgap to form a band that is responsible for the conduction of trans-polyacetylene. [13] So in this case, solitons are the important excitations and the dominant charge-storage species.

(ii) Systems in which the ground-state degeneracy is lifted. In polyheterocycles, such as polythiophene, which containing the similar single and double bonds as PA, however, the interchange of single and double bonds leads to electronic structure of different energy level---quinoid and aromatic structure. In most cases, the quinoid form has a smaller band gap. [14] The obvious consequence of the lack of degeneracy is that the structure cannot support stable soliton excitation. This consequently leads to bipolarons as the lowest energy charge-transfer configurations in such a chain. [15] Both polarons and bipolarons are mobile and they move along the polymer chain by the rearrangement of double and single bounds in the conjugated system in an electric field. If a great number of bipolarons are formed, say as a result of high doping, their energies can start overlapping at the edges, which creates narrow bipolarons bands in the band gap. Very high doping levels can lead to the narrowing of band gap, which is responsible for conductivity of polythiophene. So in this case, polarons and bipolarons are the important excitations with charge storage in bipolarons, and conduction by polaron and bipolaron is now thought to be the dominant mechanism of charge transfer in polymers with nondegenerate ground states.

1.3 Photoluminescence (PL) in conjugated polymers

Photoluminescence is the emission of light by a molecule, which has absorbed radiant energy; the radiation is emitted at a longer wavelength than the incident absorbed energy. Figure 1.1 illustrates absorption from the ground state to various vibrationally excited states of the upper electronic level on the left.

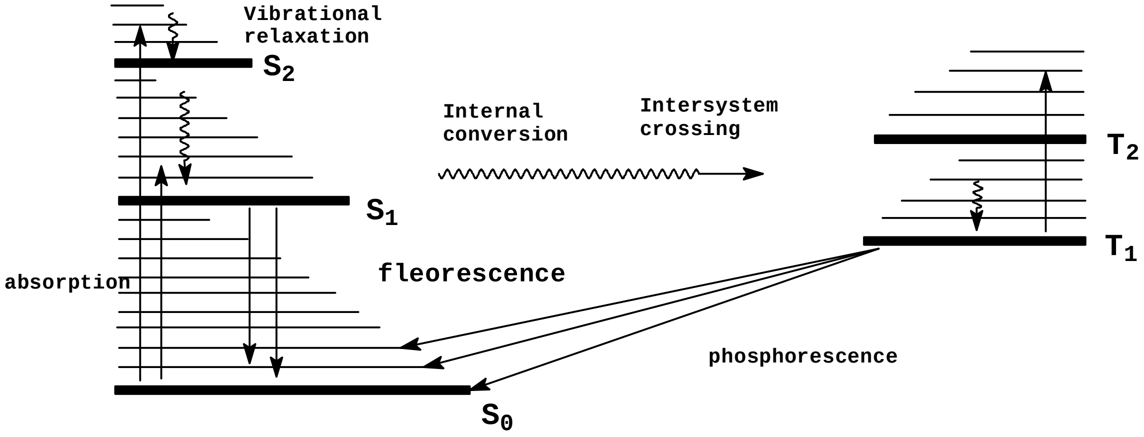

Figure 1.1. Jablonski Diagram

Such a schematic representation of the energy levels and photophysical processes that can occur in the excited molecule is commonly called a Jablonski diagram. In this diagram, the vertical direction corresponds to increasing energy; the horizontal direction has no physical significance. The electronic state are represented by thicker horizontal lines; the symbols S_0, S_1 and S_2 represent the ground state, the first and the second excited states (electron spins paired) respectively, and T_1 and T_2 represent the triplet states (electron spins unpaired).

The physical de-excitation ways are usually classified into three broad categories: radiative, nonradiative and quenching processes. A molecule undergoing a vertical transition upon excitation can arrive in the excited state with an internuclear distance considerably different from that corresponding to the minimum energy for the state. In moving back to the equilibrium nuclear distance, the molecule finds itself a few vibrational levels higher than its minimum energy. The excess energy can be dissipated via bimolecular collisions with solvent molecules. The process is called vibrational relaxation (VR). The excited molecule can also undergo other transitions, such as internal conversion (IC) and intersystem crossing (ISC).

The tendency to re-emit radiation on returning to the ground state is the most interesting of properties for the electronically excited molecules. The emission processes include two different types: fluorescence and phosphorescence. Fluorescence is the radiative emission from an excited state of the same spin multiplicity to the lower state in the transition (usually the ground state). Excitation to the S_1 state of an organic molecule might therefore be followed by the emission of fluorescence accompanying the S_1 to S_0 transition. Since there is no charge of spin multiplicity, the transition is spin-allowed. In the absence of other factors that might make the transition a forbidden one, fluorescence is strongly allowed with the result that it occurs on relatively fast timescales. Typical timescales range from picosecond (10^{-12} s) to microsecond (10^{-6} s).

ISC results in the formation of T_1, which can emit phosphorescence upon returning to the S_0 state. Phosphorescence is less intense than fluorescence and its timescales lie in the range of microseconds to seconds, which is sufficiently sensitive to the human eye.

1.4 Electroluminescence in conjugated polymers

In contrast to photoluminescence, the light emission from an active material as a consequence of optical absorption and relaxation by radiative decay of an excited state, electroluminescence (EL) is a non-thermal generation of light resulting from the application of an electric field to a substrate. [16] In the latter case, excitation is accomplished by recombination of charge carriers of contrary sign (electron and hole) injected into an inorganic or organic semiconductor in the presence of an external circuit.

Electroluminescence from organic crystals was first observed for anthracene in 1963. [17] Since the efficiencies and lifetimes of resulting devices were significantly lower than those obtained for inorganic systems at the same time, research activities were focused on the inorganic materials. In the late 1980s, Tang and VanSlyke, [18] as well as Saito and Tsutsui et al. [19] revived the research on electroluminescence of organic compounds, developing a new generation of light-emitting diodes with organic fluorescent dyes.

Another fundamental work concerning the evolution of organic light-emitting diodes (OLEDs) was published by Friend et al. in 1990. [20] They overcame the drawback of expensive and technologically inconvenient vapor deposition of fluorescent dyes and inorganic semiconductors by using a highly fluorescent conjugated polymer—poly(p-phenylenevinylene) (PPV) —as the active material in a single-layer OLED.

Although PPV itself is insoluble and difficult to process, Friend et al. found a way to build up PPV-OLEDs via the thermoconversion of a processable precursor polymer. Their greatest merit however was that they indicated for the first time the possibility of producing large area displays by simple coating techniques. The PPV diode embodies the prototype of a single-layer OLED and is typically composed of a thin film of the active organic material (30-500 nm) which is sandwiched between two electrodes (Fig. 1.2).

1.4.1 PLED devices

Since one of the electrodes needs to be semitransparent in order to observe light emission from the organic layer, usually an indium tin oxide (ITO)-coated glass substrate is used as the anode. Electropositive metals with low work functions such as Al, Ca, Mg, or In are used as cathodes in order to guarantee efficient electron injection.

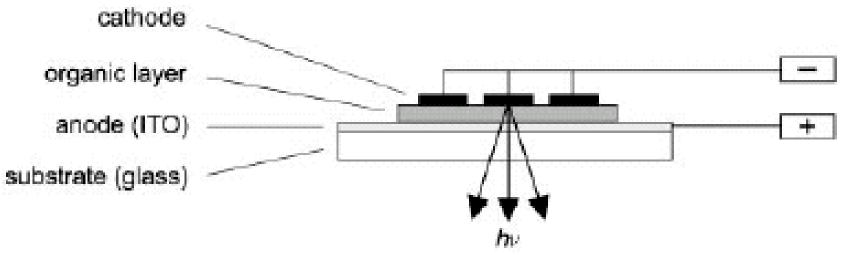

Fig. 1.2 Schematic configuration of a single-layer OLED.

1.4.2 Light generation in PLED

If an external voltage is applied at the two electrodes, charge carriers, i.e. holes, at the anode and electrons at the cathode are injected into the organic layer beyond a specific threshold voltage depending on the organic material applied. In the presence of an electric field the charge carriers move through the active layer and are non-radiatively discharged when they reach the oppositely charged electrode. However, if a hole and an electron encounter one another while drifting through the organic layer, excited singlet and triplet states, so-called excitons, are formed. The singlet state may relax by emission of radiation (fluorescence). [A more detailed explanation of the basics of EL generation from organic materials is provided in ref. 21.]

1.4.3 Quantum efficiency of PLED

The internal EL quantum efficiency η_{int} of an OLED (the ratio of the number of photons emitted per electrons injected) can be calculated from the measured external EL quantum efficiencyη_{ext} using eqn. (1). [21, 22] Due to refraction all photons emitted cannot be perceived by an external observer. External efficencies η_{ext} are accordingly diminished by the factor of $2n^2$ (n=refractive index of the organic layer) with respect to η_{int}.

$$\eta_{int} = 2n^2\eta_{ext} \qquad (1)$$

Power efficiencies η_{pow}, the ratio of output light power to input electric power, can be determined from η_{ext} using the known values of the applied voltage U and the average energy of the emitted photons E_p [eqn. (2)].

$$\eta_{pow} = \eta_{ext} E_p U^{-1} \qquad (2)$$

Luminous efficiencies η_{lum} are determined by multiplication of η_{pow} by the eye sensitivity curve S as defined by the Commission Internationale de L'Eclairage (CIE). This function pays regard to the fact that the human eye possesses distinct sensitivities with respect to different colours [eqn. (3)].

$$\eta_{lum} = \eta_{pow} S \qquad (3)$$

Finally, the brightness of an OLED (given in cd m^{-2}) is also used by several authors to estimate the efficiency of their device. For comparison, the brightness of a conventional laptop display reaches values of approximately 100 cd m^{-2}.

1.5 Application

1.5.1 Organic electroluminescent (EL) devices

Organic EL devices have recently received a great deal of attention for their application as full-colour, flat-panel displays as well as from the standpoint of scientific interest. They are attractive because of low voltage driving, high brightness, capability of multicolour emission by the selection of emitting materials and easy fabrication of large-area and thin-film devices. Following the reports on organic EL devices using single crystals of anthracene, [23] recent pioneering works on organic EL devices using low molecular-weight organic materials [24] and a conjugated polymer [25] have triggered extensive research and development of this field.

The structure of organic EL devices consists of single or multiple layers of organic thin films sandwiched normally between the transparent indium-tin-oxide (ITO) coated glass and vacuum-evaporated metals with low work function such as magnesium (Mg) and aluminium (Al). The operation of organic EL devices involves injection of holes and electrons from the ITO and Mg or Al electrodes, respectively, transport of injected charge carriers, recombination of holes and electrons in the emission layer to generate an electronically excited state molecule, followed by luminescence emission. In order to achieve high performance in organic EL devices, it is necessary to attain charge balance. Generally, layered devices consisting of charge-transport and emitting layers can more readily achieve charge balance than single-layer devices using an emitting material alone. This is because a suitable combination of charge-transporting and emitting materials in layered devices reduces the energy barrier for the injection of charge carriers from the electrodes and because the charge transport layer acts as a blocking layer against the injection of either holes or electrons from the adjoining layer and their subsequent escape from the device.

For the fabrication of high-performance organic EL devices, not only emitting materials but also charge-transporting materials are required. Both polymers and small molecules are candidates for materials in organic EL devices. The materials for organic EL devices should meet the following requirements: (1) to possess a suitable ionisation potential and electron affinity for energy level matching for the injection of charge carriers at the interfaces between the electrode/organic material and organic material/organic material, (2) to permit the formation of a uniform film without pinholes, (3) to be morphologically stable, (4) to be thermally stable, (5) to be electrochemically stable, and (6) to be highly luminescent for emitting materials. In addition, doping of luminescent compounds has been shown to be an effective method for attaining high brightness and desirable emission colour. [26]

For the fabrication of high-performance organic EL devices, development of new materials with high performance and judicious choice of the combination of emitting and charge transporting materials and the combination of emitting and luminescent dopant molecules as well as an understanding of basic processes, such as charge injection from the electrodes, charge transport, recombination of charge carriers to generate the electronically excited-state molecule, are of vital importance. Recent years have witnessed significant progress with regard to brightness, multi- or full-colour emission, and durability and thermal stability of organic EL devices.

1.5.2 Organic photovoltaic devices

Devices for photoelectric conversion using organic materials, which find potential applications as solar cells and photosensors, are mainly classified into photoelectrochemical and photovoltaic devices. Photoelectrochemical cells consist of inorganic semiconductors and organic dyes as a sensitizer immersed in an ionically conductive electrolyte containing a redox couple, where light is absorbed by the organic dye. [27,28] Photovoltaic devices consist of thin films of organic materials sandwiched between two metal electrodes. A built-in electric field, formed in the semiconductor in contact with the electrolyte in the photoelectrochemical cell and in the organic layer at the interface with the metal electrode or with the other organic layer in the photovoltaic device, is responsible for the photogeneration of charge carriers.

Organic solid-state photovoltaic devices have attracted attention because of their light weight, potentially low cost, and ready fabrication of large-area, thin-film devices. Both Schottky-type and p-n heterojunction cells using low molecular-weight organic materials and polymers have been fabricated, and their performance characteristics investigated. In Schottky-type cells, a single-layer organic material is sandwiched between two dissimilar electrodes to form a Schottky barrier in the organic layer at the interface with the metal electrode. On the other hand, p-n heterojunction cells are typically based on a double-layer structure of organic thin films, where the organic/organic interface plays an important role in the performance, the electrodes simply providing ohmic contacts to the organic layers. P-n Heterojunction devices have advantages over Schottky-type devices in that they do not necessarily need the use of low work-function metals that readily undergo air oxidation as electrode materials. It is also expected that a higher quantum yield for photogeneration of charge carriers is attained due to electron donor-acceptor interactions of the two dyes.

The conversion efficiency of organic photovoltaic devices is still lower than that of inorganic photovoltaic devices. The reason for this may be attributed to low photogeneration efficiency of charge carriers and to high electrical resistivity of organic materials which stems from the low mobility and low density of free carriers. The basic processes of the operation of organic photovoltaic devices have been understood in terms of the energy band model for inorganic semiconductors; however, many organic materials do not form energy bands. It is therefore necessary to understand the mechanism of photoelectric conversion in organic photovoltaic devices on the molecular level. It is important to understand what impurity species are involved in the formation of the built-in potential at the interface between the organic material and electrode and two kinds of organic materials as well as the mechanism for the photogeneration of charge carriers in organic materials. Improving the quantum efficiency of the photogeneration of charge carriers is a key issue for the development of organic photovoltaic devices with high conversion efficiency. Recent significant progress in solid-state solar cells using the combination of organic dyes and inorganic semiconductors [29] and using interpenetrating polymer networks [30-32] has attracted renewed interest in this field.

1.5.3 Electrochromic devices

Organic electrochromic devices, which are characterised by low-voltage operation, good optical contrast, and wide viewing angle, can be potentially used as smart windows that control the sun radiation in buildings and cars, rear-view mirrors for cars, and display devices. [33] Low molecular-weight organic compounds, e.g., viologen derivatives and metallophthalocyanines, and polymers including both p-conjugated and pendant polymers have been studied for electrochromic materials. Such organic materials have the potential capability of multi-colour display and in particular, polymer thin films are attractive because they may exhibit a memory effect and have a good cycle life.

Improvement in the cyclability of the colouration and decolouration and the design and synthesis of new redox systems are important issues. [34, 35] All solid-state devices using polymer electrolytes or polymer gel electrolytes [36, 37] as well as electrochromic devices using thin films of organic materials immersed in an electrolyte solution have been studied. Photoinduced electrochromic devices have also been studied. [38]

1.6 Aim of the project

With insights described in this Chapter, specific electronic and optical properties can be obtained by molecular design through modification of polymer side substitutes or backbones. Alternating copolymers are especially interesting in fabrications of LED. Given impetus by this, the attention of this project is focused on:

1) Designing and synthesizing novel, processible, highly fluorescent alternating polymers;
2) Investigating the influence of electron withdrawing pyridinyl units on electrical and optical properties of polymers;
3) Developing short wavelength emission, *e.g.* blue, ultraviolet polymers.
4) Preliminarily probing the potential applications of the derived polymers.

A few series of novel, soluble fluorescent alternating polymers were designed and synthesized. They were poly[2,7-(9,9-bis(2-ethylhexyl)fluorenyl)-alt-(pyridinyl)] &poly[2,7-(9,9-bis(2-ethylhexyl)fluorenyl)](**I**),
poly[2,7-(9,9-bis[3,5-bis(benzyloxy)benzyl])fluorenyl-alt-(pyridinyl)] (**II**)
and poly[(2,7-(N-(2-ethylhexyl)carbazloyl)-alt-(pyridinyl)] (**III**).

All polymers were prepared by Suzuki cross-coupling reaction. The structures of all polymers were confirmed by ^{1}H-NMR. Their properties such as absorption and emission, thermal stability, electrochemical properties were studied.

References

(1) Chiang, C. K.; Fincher, C. R. Jr.; Park, Y. W.; Heeger, A. J. S. H.; Louis, E. J.; Gau, S. C.; MacDiarmid, A.G. *Phys. Rev. Lett.* **1977**, *39*, 1098.

(2) MacDiarmid, A. G.; Chiang, J. C.; Halpern, M.; Huang, W. S.; Mu, S. L.; Somasiri, N. L. D.; Wu, W.; Yaniger, S. *Cryst. Liq. Cryst.* **1985**, *121*,173.

(3) Diaz, A. F.; Kanazawa, K. K.; Gardini, G. P. *J. Chem. Soc*. **1979**, 535.

(4) Yamamoto, T.; Sanechika, K.; Yamamoto, A. *J. Polym. SCi., Polym. Lett. Ed.* **1980**, *18*, 9.

(5) Shacklette, L. W. C. R. R.; Ivory, D. M.; Miller, G. G.; Baughman, R. H. *Synthetic. Metals.* **1980**, *1*, 307.

(6) Wenk, G. E.; Chien, J. C. W.; Karasz, F. E.; Lillya, C. P. *Polymer* **1979**, *20*, 1441.

(7) Tokito, S.; Tsutsui, T.; Saito, S.; Tan, R. *Polym. Commum.* **1986**, *27*, 333.

(8) Kuper, C. G.; Whitfield, G. D. *Polarons and Excitons*; Plenum: New York, **1963**.

(9) Kittel, C. *Introduction to solid state physics*; John Wiley & Sons: New York, **1976**; p 230.

(10) Baeriswyl, D.; Campbell, D. K.; Mazumdar, S. *Conjugated Conducting Polymers*; Springer-Verlag: Berlin, **1992**; p 7.

(11) Hayashi, H.; Nasu, K. *Physical Review B-Condensed Matter* **1985**, *32*, 5295.

(12) Herger, A. J.; Kivelson, S.; Schrieffer, J. R.; Su, W. P. *Reviews of Modern Physics* **1988**, *60*, 781.

(13) Su, W. P.; Schrieffer, J. R.; Heeger, A. J. *Phys. Rev. Lett.* **1979**, *42*, 1698.

(14) Bredas, J. L. *J. Chem. Phys.* **1985**, *82*, 3808.

(15) Chung, T. C.; Kaufman, J. H.; Heeger, A. J.; Wudl, F. *Phys. Rev. B: Condens.*

Matter. **1984**, *30*, 702.

(16) Y. A. Ono, Electroluminescence in Encyclopedia of Applied Physics, ed. G. L. Trigg, VCH, Weinheim, **1993**, vol. 5, p. 295.

(17) (a) M. Pope, H. P. Kallmann and P. Magnante, *J. Chem. Phys.*, **1963**, *38*, 2042; (b) W. Helfrich and W. G. Schneider, *Phys. Rev. Lett.*, **1965**, *14*, 229.

(18) C. W. Tang and S. A. VanSlyke, *Appl. Phys. Lett.*, **1987**, *51*, 913.

(19) (a) C. Adachi, T. Tsutsui and S. Saito, *Appl. Phys. Lett.*, **1990**, *56*, 799; (b) C. Adachi, S. Tokito, T. Tsutsui and S. Saito, *Jpn. J. Appl. Phys.*, **1988**, *28*, L269.

(20) J. H. Burroughes, D. D. C. Bradley, A. R. Brown, R. N. Marks, K. Mackay, R. H. Friend, P. L. Burns and A. B. Holmes, *Nature*, **1990**, *347*, 539.

(21) Reviews concerning OLEDs: A. Kraft, A. C. Grimsdale and A. B. Holmes, *Angew. Chem., Int. Ed.*, **1998**, *37*, 402;

(22) S. Tasch, W. Graupner, G. Leising, L. Pu, M. W. Wagner and R. H. Grubbs, *Adv. Mater.*, **1995**, *7*, 903.

(23) M. Pope, H. P. Kallmann and P. Magnante, *J. Chem. Phys.*, **1963**, *38*, 2042.

(24) C.W. Tang and S. A. Van Slyke, *Appl. Phys. Lett.*, **1987**, *51*, 913.

(25) J. H. Burroughes, D. D. C. Bradley, A. R. Brown, R. N. Marks, K. Mackay, R. H. Friend, P. L. Burn and A. B. Holmes, *Nature*, **1990**, *347*, 539.

(26) C. W. Tang, S. A. Van Slyke and C. H. Chen, *J. Appl. Phys.*, **1989**, *65*, 3610.

(27) B. O'Regan and M. GraÈ tzel, *Nature*, **1991**, *353*, 737.

(28) M. K. Nazeeruddin, A. Kay, I. Roddicio, R. Humphry, E. MuÈ ller, P. Liska, N. Vlachopoulos and M. GraÈ tzel, *J. Am. Chem. Soc.*, **1993**, *115*, 6382.

(29) U. Bach, D. Lupo, P. Comte, J. E. Moser, F. WeissoÈ rtel, J. Salbeck, H. Spreitzer and M. GraÈ tzel, *Nature*, **1998**, *395*, 583.

(30) G. Yu and A. J. Heeger, *J. Appl. Phys.*, **1995**, *78*, 4510.

(31) J. J. M. Halls, C. A. Walsh, N. C. Greenham, E. A. Marseglia, R. H. Friend, A. C. Moratti and A. B. Holmes, *Nature*, **1995**, *376*, 498.

(32) G. Yu, J. Gao, J. C. Hummelen, F. Wudl and A. J. Heeger, *Science*, **1995**, *270*, 1789.

(33) P. M. S. Monk, R. J. Mortimer and D. R. Rosseinsky, *Electrochromism: Fundamentals and Applications*, VCH, Weinheim, **1995**.

(34) A. Kumar, D. M. Welsh, M. C. Morvant, F. Piroux, K. A. Abboud and J. R. Reynolds, *Chem. Mater.*, **1998**, *19*, 896.

(35) J. D. Debad and A. J. Bard, *J. Am. Chem. Soc.*, **1998**, *120*, 2476.

(36) S. A. Sapp, G. A. Sotzing and J. R. Reynolds, *Chem. Mater.*, **1998**, *10*, 2101.

(37) D. L. Meeker, D. S. K. Mudigonda, J. M. Osborn, D. C. Loveday and J. P. Ferraris, *Macromolecules*, **1998**, *31*, 2943.

(38) Y. Lis, J. Hagen and D. Haarer, *Synth. Met.*, **1998**, *94*, 273.

Chapter 2 Experimental Details

2.1 Materials

Solvents, reagents and chemicals were obtained from various chemical companies including Aldrich, Avocado Research Chemicals Ltd., Merck, Fluka, TCI, BDH Laboratory Supplies, JT Baker Inc. EM Science, Across Organics, Goodrich Chemical Enterprise, Comak Chemical Products and Riedel de Haen.

Diethyl ether (J. T. Baker, A. R) was dried over sodium wire. Anhydrous tetrahydrofuran (J. T. Baker, A.R) was obtained by distillation over sodium wire and benzophenone under nitrogen atmosphere. Chloroform (J. T. Baker, A. R) used for polymerization was purified by distillation with calcium hydride and degassed with argon. Acetonitrile (J. T. Baker, A. R) was freshly distilled from calcium hydride before using.

2.2 Characterization Techniques

2.2.1 Nuclear Magnetic Resonance (NMR)

Under appropriate conditions in a magnetic field, a sample can absorb electromagnetic radiation in the radio frequency region at frequencies governed by the characteristics of the sample. Thus, NMR spectrometry is basically another form of absorption spectrometry. [1]

The most common nuclei examined by NMR are ^{1}H and ^{13}C, as these are the NMR sensitive nuclei of the most abundant elements in organic materials. ^{1}H represents over 99% of all hydrogen atoms, while ^{13}C is only just over 1% of all carbon atoms. [2]

^{1}H and ^{13}C NMR spectra were recorded at a 300 MHz Bruker ACF 300 FT-NMR spectrophotometer with chloroform-d as solvent and tetramethylsilane as internal standard.

2.2.2 Gel Permeation Chromatography (GPC)

GPC has developed into one of the most useful methods for routine determination of average molecular weights and molecular weight distributions of polymers. It is a form of liquid chromatography in which the molecules are separated according to their molecular size. The procedure involves injecting a dilute solution of a polydisperse polymer into a continuous flow of solvent passing through a column containing tightly packed microporous gel particles. Separation of the molecules occurs by preferential penetration of the different sized molecules into the pores; small molecules are able to permeate more easily through the pores compared to the larger sized molecules so that their rate of passage through the column is correspondingly slower. Compared with a calibration polymer (often polystyrene), the retention time is converted to a molecular weight. [3]

GPC analyses were carried out using a Perkin-Elmer model 200 HPLC system with Phenogel M×L and M×M columns calibrated using polystyrene as standard and THF as eluent and the flow rate was 0.35ml/min.

2.2.3 Thermogravimetric Analysis (TGA)

TGA makes a continuous weighing of a small sample (ca. 10mg) in a controlled atmosphere (e.g. air or nitrogen) as the temperature is increased at a programmed linear rate. The thermogram illustrates weight lose due to desorption of gases (e.g. moisture) or decomposition. TA is a very simple technique for quantitatively analyzing for filler content of a polymer compound. [4] The basic instrumental requirements are a precision balance, a programmable furnace and a recorder.

Thermogravimetric analysis (TGA) was performed on a TA Instruments with a TGA 2960 thermogravimetric analyzer module at a heating rate of 20℃ min^{-1} with a nitrogen flow of 100 mL min^{-1}. The temperature regime was from room temperature to 800℃.

2.2.4 Differential Scanning Calorimetry (DSC)

The DSC measures the power (heat energy per unit time) differential between a small weighted sample of polymer in a sealed aluminum pan referenced to an empty pan in order to maintain a zero temperature differential between them during programmed heating and cooling temperature scans. The technique is most often used for characterizing the T_g (glass transition temperature), T_m (the heat of fusion on heating) and T_c (the heat of fusion on cooling).

Differential scanning calorimetry (DSC) were runs on a Du Pont DSC 2920 module in conjugation with the Du Pont Thermal analyst system under a heating rate of 20℃/min and a nitrogen flow rate of 70ml/min.

2.2.5 Cyclic Voltammetry (CV)

CV is a dynamic electrochemical method for measuring reduction-oxidation (redox) events. It can be used to study the electrochemical behavior of species diffusing to an electrode surface, interfacial phenomena at an electrode surface and bulk properties of materials in or on electrodes. [5] It gives the values of the oxidation and reduction potentials for a materials in solution relative to a reference redox couple and it is the best way used as a relative measure of the electronic levels for conjugated polymers.

Cyclic voltammetry of polymer films was conducted using a single-compartment, three electrode cell comprising a platinum working electrode with the polymer spin-coated on it, a platinum counter electrode and a silver quasi-reference electrode using a HB-105 Hokuto Denko Ltd. arbitrary function generator and HA-501 Hokuto Denko Ltd. Potentiostat. 0.1 M tetrabutylammonium percholate in acetonitrile was used as the electrolyte solution.

2.2.6 Ultraviolet-Visible Spectroscopy (UV-Vis)

UV-Vis (200 to 800nm) spectroscopy is applied to the qualitative analysis of many organic materials. Molecules with loosely bound electrons absorb energy in the UV-Vis region. Therefore UV-Vis spectra are diagnostic of unsaturation in absorbing molecules (chromophoric groups). [6]

UV-Vis spectra were recorded in a Shimadzu UV-3101 spectrometer. Dilute polymer solutions in spectra-grade chloroform or THF (1×10^{-5}M, based on monomer molecular weight) were used for analysis.

2.2.7 Photoluminescence Spectroscopy (PL)

During the process of absorbing ultraviolet or visible electromagnetic radiation, molecules are elevated to an excited electronic state. Some molecules will emit part of this excess energy as light of a wavelength different from that of absorbed radiation. This process is photoluminescence, which can be considered as a deexcitation process that occur after excitation by photons. [6]

The PL spectra of the polymers were acquired on a Perkin-Elmer LS 55 photoluminescence spectrometer with a xenon lamp as light source.

References

1. *Proton Magnetic Resonance Spectrometry* in *Spectrometric Identification of Organic Compounds,* edited by R. M. Silverstein, G. C. Bassler and T. C. Morrill, 5th edition, John Wiley and Sons, Inc., **1991,** Chapter 4.

2. Nicholas P. Cheremisinoff, *Polymer Characterization Laboratory Techniques and Analysis,* Noyes Publications, **1996.**

3. D. Campbell and J. R. White, *Polymer Characterization, Physical Techniques*, Chapman and Hall, **1989.**

4. N. P. Cheremisinoff, *Polymer Characterization Laboratory Techniques and Analysis,* Noyes Publications, **1996.**

5. J. F Rusling and S.L. Suib, *Adv. Mater.,* **1994,** 6, 922.

6. D. A. Skoog and J. J. Leary, *Principles of Instrumental Analysis,* 4th edition, Saunders College Publishing, **1992.**

Chapter 3 Synthesis and Properties of Poly(fluorenyl-*alt*-pyridinyl)-Based Alternating Copolymers for Light-Emitting Diodes

A novel series of well defined alternating poly[2,7-(9,9-di(2-ethylhexyl)fluorenyl)-alt-pyridinyl] (PDEHFP) were synthesized using palladium(0) catalyzed Suzuki coupling reaction in high yields. In this series of alternating polymers, 2,7-(9,9-di(2-ethylhexyl)fluorenyl was used as light-emitting unit and the electron deficient pyridinyl unit was introduced to tune the wavelength of the emitting light and improve their electron transportation. These polymers were characterized by ^{1}H NMR, thermal analysis, Gel permeation chromatography, UV-vis, fluorescence spectroscopy and cyclic voltammetry. They showed high thermal stabilities with high decomposition temperatures in the range of 360 to 390°C in nitrogen. The difference in linkage position of pyridinyl unit in the polymer backbone has significant effects on the electronic and optical properties of polymers in solution and in film phases. Meta-linkage (3,5- and 2,6-linkage) of pyridinyl units in the polymer backbone is more favourable to polymer for pure blue emission and prevention of aggregation of polymer chain than para-linkage(2,5-linkage) of the pyridinyl units. CV results indicate that these polymers with pyridinyl units possess low LUMO energy levels for an easy electron injection from a cathode.

3.1 Introduction

Since the discovery of polymer-based light-emitting diodes (PLEDs) in 1990, [1] considerable progress has been made in the development of new conjugated polymers and in the performance of related LEDs. [2] Organic luminescent polymers are attractive due to the flexibility in fine-tuning their luminescent properties through the manipulation of chemical structures along with the feasibility of utilizing spin-coating and printing processes for large area display devices. For full-colour display applications, the development of red, green and blue emitting polymers with high efficiency and stability is required. [3,4,5] Among the three primary colours, only red and green PLEDs have sufficient efficiencies and lifetimes to be of commercial value. Polymers with large band gaps that emit blue light efficiently have been the subject of intense academic and industrial research and stable blue PLEDs based on conjugated polymers remains a challenge. This arises because it is hard to achieve a balanced charge injection due to the large band gap between the LUMO and HOMO energy levels.[6] Another problem is that higher thermal and oxidative stabilities are required for the blue light-emitting polymers [7] since blue-light emissions are associated with higher energy band gaps, which requires the application of higher electric field intensities to the light-emitting layer.

Substituted polyfluorenes are promising materials for blue light-emitting active layers in PLEDs, especially because of their blue and strong electroluminescence and their good solubility in organic solvents, which is necessary for the preparation of homogeneous layers with solution-based coating techniques. [8,9,10] However, a major problem with polyfluorenes concerns their tendency to form long-wavelength aggregates/excimers in the solid state, resulting in the appearance of an additional emission band in the long wavelength region of the spectrum and a concomitant drop in electroluminescence (EL) quantum efficiency. [11a-b]

Poly(2,5-pyridinediyl) (PPy)[12a-f] and its derivatives, such as poly(pyridine vinylene) (PPyV)[12a-b] with electron-accepting nature is a family of promising conjugated polymers because of their high luminescence,[12f] excellent electron transporting behaviour and their general resistance to oxidation.[12d] The application of pyridine as the π-deficient moiety in our polymer is driven by the consideration that polypyridinyl (PPy) was used in blue-emitting devices[13,14] and that polymers based on pyridine have been demonstrated to be highly luminescent.[15] Therefore, the incorporation of a pyridinyl unit into polymer backbone increases the electron affinity of the polymers, which not only makes the copolymers to be n-dopable and capable of better electron transportation,[16a-b] but also makes the polymers more resistant to oxidation. These polymers with pyridine units are expected to possess low LUMO energy levels for an easy electron injection from a cathode. Therefore, these copolymers of fluorene unit and pyridine units are expected to possess low HOMO and LUMO energy levels and will achieve a relatively balanced charge injection.

As an extension of our research work concerning polymeric blue light emitting diodes, [17a-e] in the present work, we present the synthesis and characterization of a novel series of blue-emissive alternating copolymers of 9,9-bis(2-ethylhexyl)fluorenyl unit with three different pyridinyl units using the Suzuki cross-coupling approach (Scheme 1). A 1:1

alternating copolymer design was adopted because such arrangement would generally give more consistent physical properties as compared to random copolymers. We have chosen herein 99-bis(2-ethylhexyl)fluorenyl as the π-excessive moiety in the polymer backbone. The incorporation of the pendant 2-ethylhexyl group would serve to improve the solubility of the material and consequently to be processable.

3.2 Experimental Part

3.2.1 Materials. The reagents, 2-ethylhexyl bromide, 2,7-dibromofluorene, n-BuLi, Tetrakis(triphenylphosphine)palladium(0)[$(PPh_3)_4Pd(0)$], 3,5-dibromopyridine, 2-isopropoxy-4,4,5,5-tetramethyl-1,3,2-dioxaborolane and Tetrabutylammonium percholate (Bu_4NClO_4) (AR) were obtained from Aldrich, benzyltriethylammonium chloride, 2,5–dibromopyridine and 2,6-dibromopyridine were from Avocado Research Chemicals Ltd. NaOH(AR), DMSO (AR), toluene(AR), chloroform(AR) and all other reagents were purchased from commercial sources and used without further purification. The solvents, diethyl ether and THF were AR and acetonitrile(HPLC) were dried and distillated prior to use.

3.2.2 Measurements. ^1H NMR and ^{13}C NMR spectra were recorded on a Bruker ACF 300 FT-NMR spectrometer operating at 300 MHz. Deuterated chloroform was used as the solvent and tetramethylsilane (TMS) was used as the internal standard. Weight-average molecular mass (M_w) and number-average molecular mass (M_n) were determined by gel permeation chromatography (GPC) using a Perkin-Elmer mode 200 HPLC system equipped with Phenogel MXL and MXM columns using polystyrene as the standard and THF as the eluant. The thermal properties of the polymers were investigated by DSC and TGA under flowing nitrogen. Thermogravimetric analysis (TGA) was performed on a TA Instruments with a TGA 2960 thermogravimetric analyzer module at a heating rate of 20 °C min^{-1} with a nitrogen flow of 100 mL min^{-1}. The temperature regime was from room temperature to 800℃. Differential scanning calorimetry (DSC) of the polymer podwers was carried out using TA 2920 module. Dilute polymer solution (1×10^{-5}M) was prepared in anhydrous spectrum-grade chloroform, and quinine sulphate (1×10^{-5}M in 0.1 M H_2SO_4) was used as the reference. The thin polymer films were deposited onto quartz glass plates by spin-coating. The absorption and fluorescence spectrum measurements of polymer solution and film were conducted on Shimadzu UV-1601 PC UV-visible spectrophotometer and Perkin Elmer Instrument LS 55 Luminescence spectrometer, respectively. Cyclic voltammetry of polymer films was conducted using a single-compartment, three electrode cell comprising a platinum working electrode with the polymer spin-coated on it, a platinum counter electrode and a silver quasi-reference electrode using a HB-105 Hokuto Denko Ltd. arbitrary function generator and HA-501 Hokuto Denko Ltd. Potentiostat. 0.1 M tetrabutylammonium percholate in acetonitrile was used as the electrolyte solution.

3.2.3 Synthesis.

2,7-Dibromo-9,9-bis(2-ethylhexyl)fluorene (II). This compound was synthesized by a modification method of reference. [18,19] A typical procedure is as following: a mixture of compound **I** (4 g, 12.3 mmol) and benzytrimethylammonium chloride (0.3 g, 1.2 mmol) in 20 ml of DMSO and 8 ml of aqueous NaOH (50 %, w/w) was stirred under N_2 at 80

^{o}C. 2-ethylhexyl bromide (6.8g, 36.8 mmol) was added to the mixture, the resulting mixture was stirred at the same temperature for 3 h before 20 ml of water was added. Then the solution was extracted with three times with diethyl ether (80 ml). The combined organic layers were washed with saturated brine and dried over $MgSO_4$. The solvent was removed under reduced pressure, followed by removal of excess 2-ethylhexyl bromide by distillation under vacuum. The crude product was further purified by column chromatography(silica gel, hexane as eluent) to afford the title product as yellow liquid(Yield: 86%). ^{1}H NMR (300 MHz, $CDCl_3$): δ (ppm) 7.53-7.42(m, 6H), 1.93 (d, 4H), 0.92-0.51 (m, 30H). ^{13}C NMR (300 MHz, $CDCl_3$): δ (ppm) 152.3, 139.1, 130.0, 127.4, 127.3, 121.0, 55.3, 44.2, 34.6, 33.5, 27.9, 27.0, 22.6, 13.9, 10.2.

2,7-Bis(4,4,5,5-tetramethyl-1,3,2-dioxaborolan-2-yl)-9,9-bis(2-ethylhexyl)fluorene (III). **[23a,b]**

A typical synthetic procedure for the synthesis of the fluorene derivative monomer: to a solution of compound **II** (5 g, 9.1 mmol) in anhydrous THF (150 ml) under N_2 at -78 ^{o}C was added 17.1 ml (27mmol) of n-BuLi(1.6 M in hexane) by syringe. The mixture was stirred at -78 ^{o}C and warmed to 0 ^{o}C for 30 mins, and cooled again at -78 ^{o}C, then 2-isopropoxy-4,4,5,5-tetramethyl-1,3,2-dioxaborolane (5.57ml, 27mmol) was rapidly injected into the solution by syringe, the resulting mixture was stirred at -78 ^{o}C for 1 h and left to stir overnight at room temperature. The mixture was poured into water and extracted with ether. The ether extracts were washed with saturated brine and dried over $MgSO_4$. The solvent was removed under reduced pressure, the crude solid product was purified by recrystallized in ethanol to afford 4.7g of the title product as a white solid. (Yield 80%). ^{1}H NMR (300 MHz, $CDCl_3$): δ (ppm) 7.83-7.69 (m, 6H), 2.0 (d, 4H), 1.36 (s, 24H), 0.85-0.46 (m, 30H). ^{13}C NMR (300 MHz, $CDCl_3$): δ (ppm) 150.1, 143.9, 133.4, 130.3, 119.2, 83.5, 54.7, 43.9, 34.6, 33.4, 27.8, 27.1, 24.7, 22.6, 14.0, 10.2.

General Procedure for Polymerization by Suzuki Cross-Coupling Reaction:

Representative procedure for polymerization by Suzuki cross-coupling reaction: compound **III** (1.0 g, 1.6 mmol), benzyltriethylammonium chloride(0.3g, 1.3mmol), 2,5-dibromopyridine (0.38g, 1.6mmol) and $(PPh_3)_4Pd(0)$ (36mg, 0.03 mmol) (1 mol% based on total monomers) were dissolved in a mixture of toluene and aqueous 2 M K_2CO_3(5 ml) (3/2 volume ratio) in a 25 ml three-necked round-bottomed flask. The solution was stirred under N_2 and was heated at 90 ^{o}C with vigorous stirring for 48 h. The resulting mixture was then poured into 100 ml methanol. The precipitate was recovered by filtration and washed with 2 M dilute HCl and methanol respectively. The solid product was extracted with acetone for 24 h in a Soxhlet apparatus to remove oligomers and catalyst residues, 0.65g yellow-green poly[(2,7-(9,9-bis(2-ethylhexyl)fluorenyl-alt-(2,6-pyridinyl)] was obtained. Yield: 89.5%. This polymer was designated as PDEHFP-26, where the number 26 stands for the linking positions of pyridinyl unit in the polymer backbone. The other polymers were synthesized by following a similar procedure.

Poly[2,7-(9,9-bis(2-ethylhexyl)fluorenyl)-alt-(2,6-pyridinyl)] (PDEHFP-26) Yield: 89.5%, yellow-green solid. ^{1}H NMR (300 MHz, $CDCl_3$): δ (ppm), 8.25 (d, 3H), 7.92-7.78 (m, 6H), 2.20(s, 4H), 0.88-0.60 (m, 30H).

Poly[2,7-(9,9-bis(2-ethylhexyl)fluorenyl)-alt-(3,5-pyridinyl)] (PDEHFP-35) Yield: 87%, yellow-green solid. ^{1}H NMR (300 MHz, $CDCl_3$): δ (ppm), 8.90 (s, 2H), 8.19 (s, 1H), 7.92-7.71(m, 6H), 2.15 (s, 4H), 0.89-0.59 (m, 30H).

Poly[2,7-(9,9-bis(2-ethylhexyl)fluorenyl)-alt-(2,5-pyridinyl)] (PDEHFP-25) Yield: 92%, yellow solid. ^{1}H NMR (300 MHz, $CDCl_3$): δ (ppm), 9.06 (s, 1H), 8.16-7.67 (m, 8H), 2.15 (s, 4H), 0.88-0.56(m, 30H).

Poly[2,7-(9,9-bis(2-ethylhexyl)fluorenyl)] (PDEHF) Yield: 77%, yellow solid. ^{1}H NMR (300 MHz, $CDCl_3$): δ (ppm), 7.83-7.63(m, 6H), 2.12 (s, 4H), 0.93-0.60 (m, 30H).

3.3 Result and Discusion

3.3.1 Synthesis and Characterization.

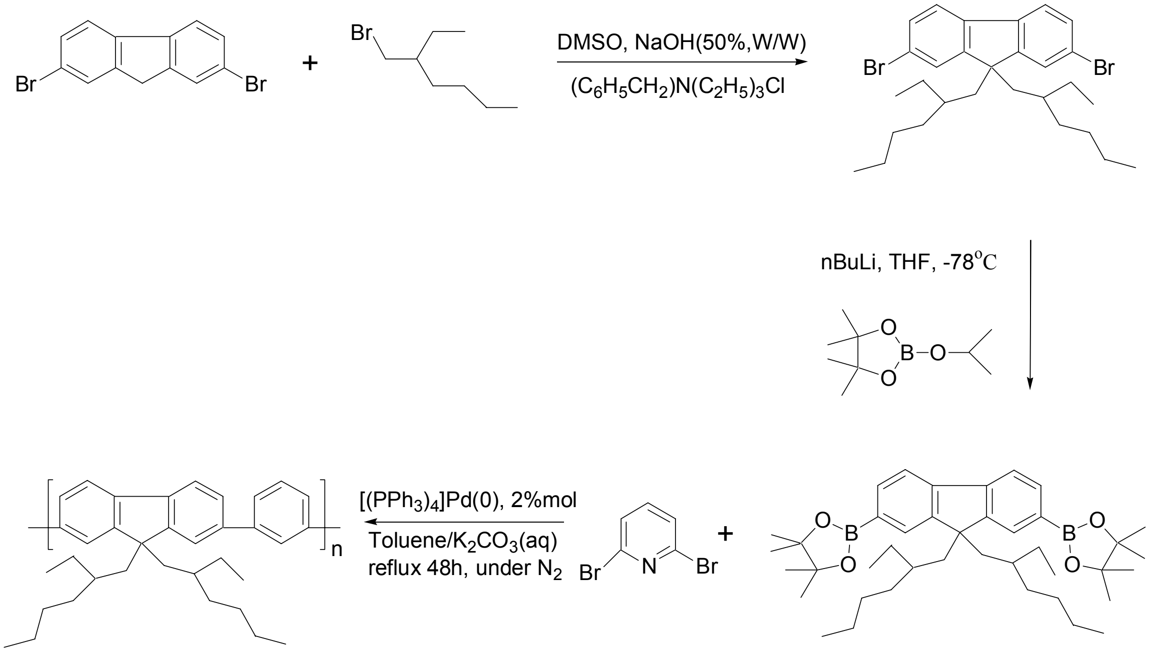

Scheme 1. Synthetic approach to the polymer PDEHFP-26.

The synthetic route for the synthesis of this series of alternating copolymer is outlined in scheme 1. The monomer compound was synthesized in two steps using 2,7-dibromofluorene as the starting material with an overall yield of 68.8% following the procedure reported in the literature. [18,19,20] The polymerization is based on the Suzuki cross-coupling reaction. All three polymers, Poly[2,7-(9,9-bis(2-ethylhexyl)fluorenyl)-alt-(2,6-pyridinyl)] (PDEHFP-26) Poly[2,7-(9,9-bis(2-ethylhexyl)fluorenyl)-alt-(3,5-pyridinyl)](PDEHFP-35), and Poly[2,7-(9,9-bis(2-ethylhexyl)fluorenyl)-alt-(2,5-pyridinyl)](PDEHFP-25) were obtained in high yields of 89.5%, 87%, 92% respectively. For the purpose of contrast, Poly[2,7-(9,9-bis(2-ethylhexyl)fluorenyl)] (PDEHF) was prepared in a similar manner with a yield of 77%, using 2,7-dibromo-9,9-bis(2-ethylhexyl)fluorene as the comonomer. All these polymers were readily soluble in chloroform and THF. The polymerization results are summarized in Table 1.

Table 1 Properties of the Polymers

Polymers	Yield(%)	Colour	Mw[a](kDa)	PDI	DP[b]	Td[c]	Tg[d]
PDEHFP-26	90	yellow-green	16.5	2.34	35	360	120.0
PDEHFP-35	87	yellow-green	18.4	2.15	39	369	108.0
PDEHFP-25	92	yellow	15.7	2.44	34	368	94.3
PDEHF	91	brown	20.5	2.43	53	388	77.3

[a] Weight-average molecular weights determined by GPC using polystyrene standards in THF. [b] Degree of polymerization. [c] Decomposition temperature, determined by TGA in nitrogen, based on 5 % weight loss. [d] Determined by DSC in nitrogen at a scan rate of 20 °C/min.

All the polymers were characterized by ^{1}H NMR and GPC. ^{1}H NMR confirmed the proposed structures of polymers. The molecular weights of polymers were determined by GPC using THF as the eluent and polystyrene as the standard. The results of GPC are also shown in Table 1. The weight-average molecular weight(M_w) of the polymers were ranging from 15700 to 20500 with the polydispersity index of 2.15-2.44.

The thermal stability of polymers in nitrogen was evaluated by thermogravimetric analyses (TGA). The corresponding data are also summarized in Table 1. All the polymers showed weight loss above 360℃ in nitrogen, indicative of good thermal stability. Thermally induced phase transition behavior of the polymers was also investigated with differential scanning calorimetry (DSC) in nitrogen. The DSC data are also shown in table 1. All the three copolymers had a higher glass transition temperature (T_g) than that of the homopolymer. The relative high glass transition temperatures are essential for many applications such as in PLEDs as emissive materials.[21] In all, the PDEHFP series of polymers have excellent thermal stabilities and high T_g.

3.3.2 Optical Properties.

The spectroscopic properties of all four polymers were measured in both solution and in thin films. UV-vis absorption and fluorescence emission spectra of the polymer solution in $CHCl_3$ and that of the polymer films spin-cast from $CHCl_3$ solutions were recorded at room temperature. The optical data are summarized in Table 2.

Table 2 Spectra Properties and Quantum Yield

Polymers	Solution[a]			Film[b]		
	λ_{max}[c]（nm）	λ_{pl}[c]（nm）	Φ[d]	λ_{max}[c]（nm）	λ_{pl}[c]（nm）	Optical band gap(eV)
PDEHFP-26	366	381,401	0.4953	371	407	3.14
PDEHFP-35	343	367,387	0.4426	345	397,417	3.31
PDEHFP-25	381	417,439	0.5193	394	426,449(474)	2.85
PDEHF	379	414,437	0.5463	385	444,513	2.90

[a] 1×10^{-5}M in anhydrous chloroform. [b] Spin-coating on quartz glass from anhydrous chloroform solution. [c] Wavelength of maximum absorbance or emission, wavelength of the shoulder peak is in brackets. [d] Relative to 1×10^{-5}M quinine sulphate in 0.1M H_2SO_4.

The UV-vis absorption and photoluminescence (PL) spectra for all four polymers in chloroform are shown in figure 1. It is evident that the linkage pattern of the pyridinyl moiety in the polymer backbone has a major influence on the absorption maximum of polymer. The absorption maximum of PDEHFP-25 with para-linkage of pyridinyl unit at 381nm is red-shifted in comparison with that of PDEHFP-26 and PDEHFP-35 with metal-linkage of pyridinyl moiety, being 366nm and 343nm, respectively. It is even red-shifted in comparison with that of the homopolymer, being at 379nm, while PDEHFP-26 and PDEHFP-35 is blue-shifted as compared to that of the homopolymer. The difference among the absorption maximum of our PDEHFP series of copolymers is attributed to the lesser extent of π-electron delocalization in the polymer backbone arising from meta-linkages, causing a reduction in the π-conjugation lengths. In the PDEHFP series of polymers, the longer the conjugation length of the conjugated polymers, the more red-shifted of the absorption maximum(λ_{max}). The effect of different linkage position of pyridinyl units on the absorption maximum of polymer is similar to that of our previous report.[22]

The photoluminescence (PL) spectra, which were attributed to fluorescence on account of the short lifetime of the excited state, [23] were obtained by irradiative excitation at the wavelength of the absorption maximum. PDEHFP-25 produce very strong blue fluorescence with emission maximum at 417nm and a shoulder peak at 439nm. For PDEHFP-26 and PDEHFP-35, they produce very strong blue fluorescence which is slightly violet-shifted, with emission maximum at 381 and 401 nm, 367 and 387 nm respectively. As compared to homopolymer PDEHF, PDEHFP-26 and PDEHFP-35 produce blue-shifted fluorescence, while the emission peaks of PDEHFP-25 is almost equivalent with that of homopolymer PDEHF. The effect of different linkage position of pyridinyl units on the emission peaks of polymer is also similar to that of our previous report. [22]

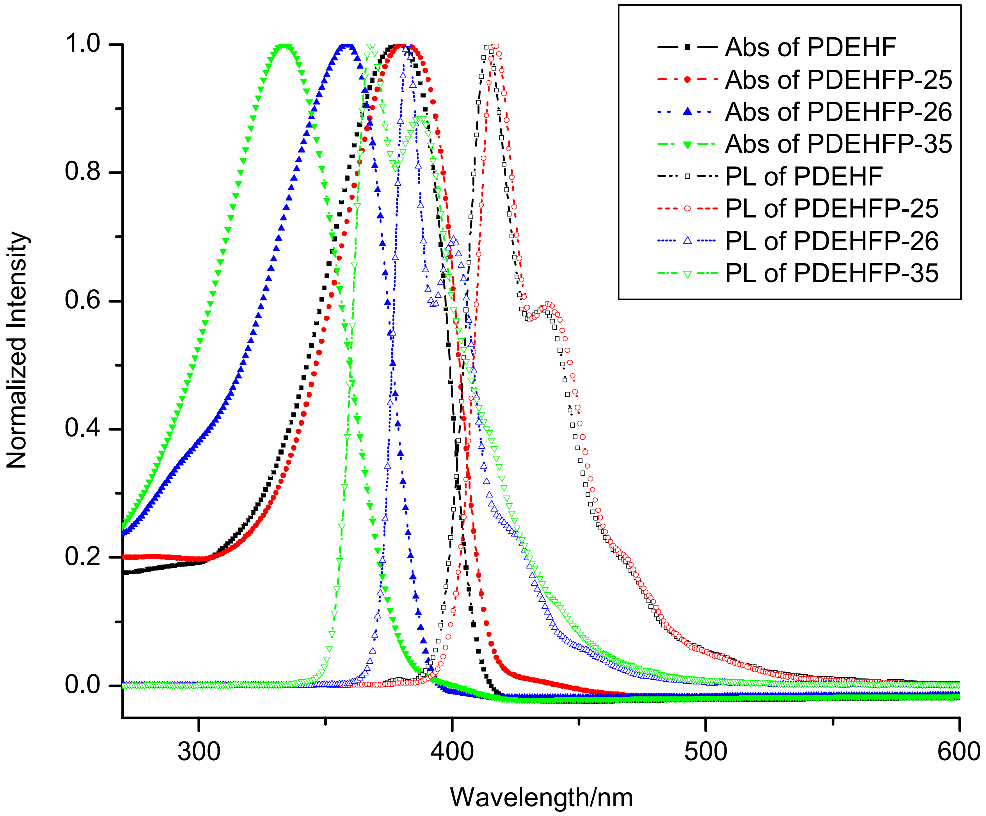

Figure 1. UV-Vis absorption (abs) and photoluminescence (PL) spectra of all the four polymers in $CHCl_3$ solution.

The photoluminescence quantum yields in chloroform solution were measured according to the method described by Davey et al.[24] relative to 10^{-5} M quinine sulphate in 0.1 M H_2SO_4. The results are summarized in Table 2. High quantum yields of all the polymers are obtained, being in the range of 44-55%.

Fig. 2 shows the UV-vis absorption and photoluminescence (PL) spectra of all four polymers in thin films. For PDEHFP-25, in which the pyridinyl unit is para-linked in the polymer main chain, its UV maximum in film at 394 nm is red-shifted in comparison with the UV maxima (at 371nm and 345nm, respectively) of PDEHFP-26 and PDEHFP-35 with meta-linkages of the pyridinyl units. It is even red-shifted in comparison with the UV maxima of the homopolymer, which is at 385nm. While PEEHFP-26 and PDEHFP-35 produce blue-shifted absorption maxima as compared to that of the homopolymer. This is also attributed to the lower extent of π-electron delocalization of the polymer main chain arising from meta-linkages of the pyridinyl moiety, resulting in a reduction in the π-conjugation length.

In the film state, the emission peaks appear at 407, 397(417, shoulder peak) and 426(449,474, shoulder peaks) nm for PDEHFP-26, PDEHFP-35 and PDEHFP-25, respectively. It can be seen that the PL of PDEHFP-25 is very broad and red-shifted in comparison with that of PDEHFP-35 and PDEHFP-26. As compared to the photoluminescence (PL) spectra of the homopolymer, which showed its emission maximum at 444nm (513nm, broad shoulder peak), all three pyridine incorporated copolymers showed blue-shifted emission. The results of PL in film states show that optical properties of fluorene polymers can be well tuned by properly rationalized design of polymer architectures, such as the incorporation of different pyridinyl moieties into polyfluorene backbone.

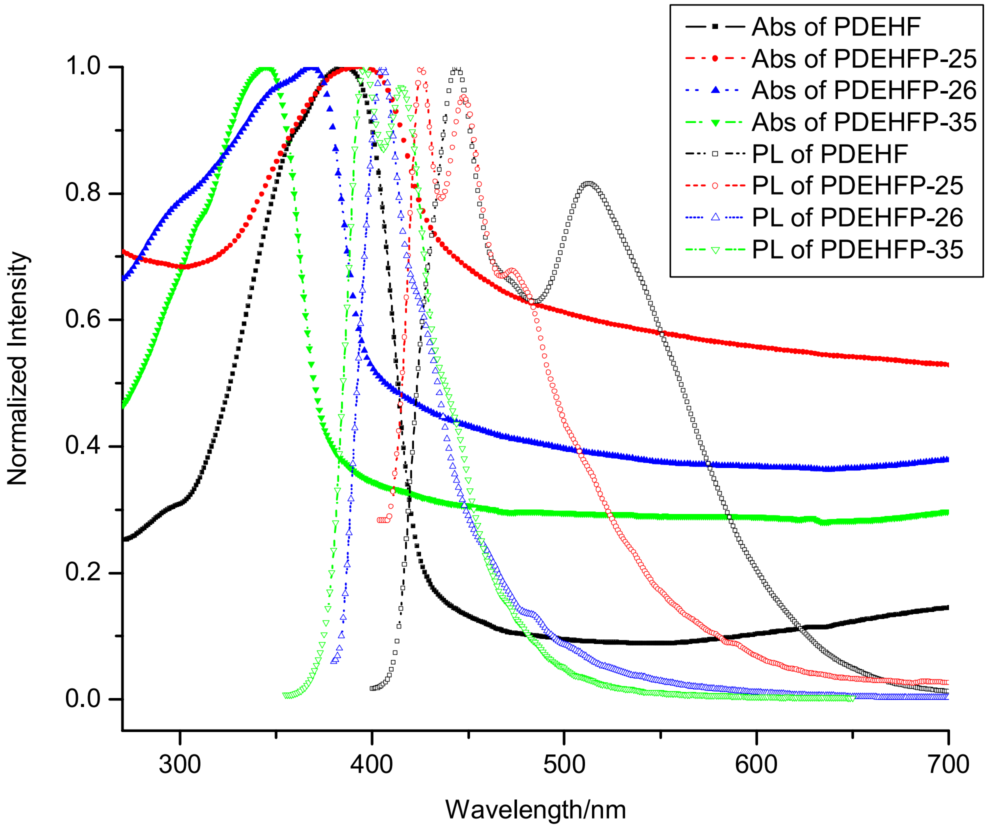

Figure 2. UV-Vis absorption (abs) and photoluminescence (PL) spectra of all the four polymers in thin films.

3.3.3 Electrochemical Properties.

The electrochemical behavior of the polymer was investigated by cyclic voltammetry(CV). CV was performed in a solution of Bu_4NClO_4(0.10M) in acetonitrile at a scan rate of 50mV/s at room temperature under the protection of Nitrogen. A platinum electrode coated with a thin polymer film was used as the working electrode. A Pt wire was used as the counter electrode and an Ag/$AgNO_3$(0.01M) electrode was used as the reference electrode. Figure 3 shows the typical cyclic voltammograms of the polymer PDEHFP-35.

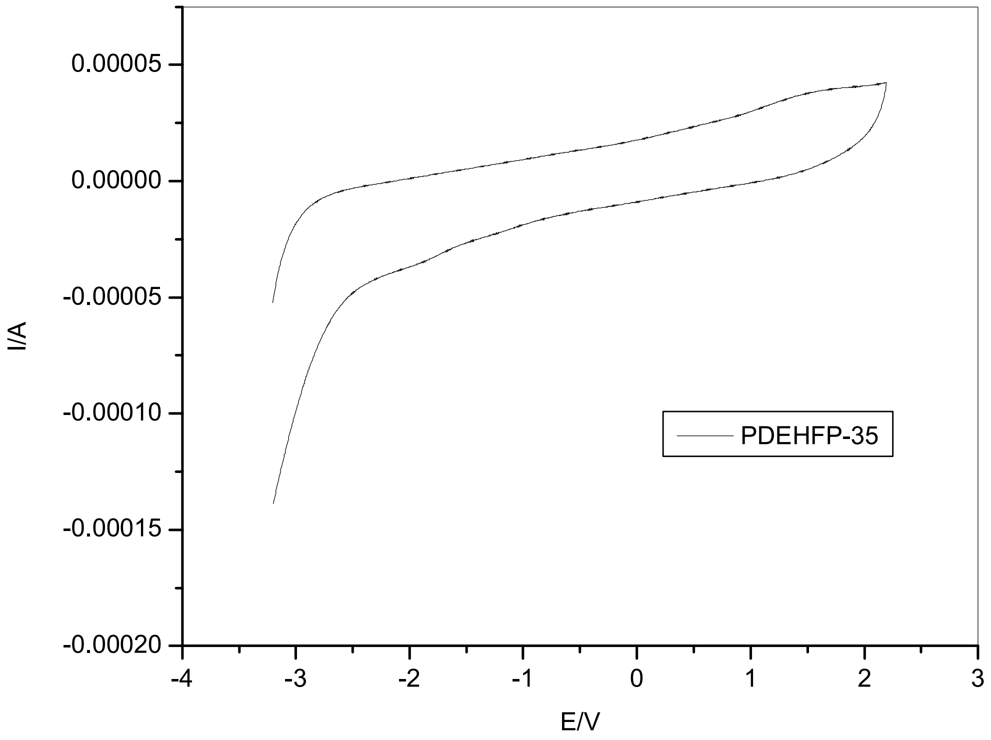

Figure 3. The cyclic voltammograms of PDEHFP-35 films coated on platinum plate electrodes in acetonitrile containing 0.1 M Bu_4NClO_4.

The onset potentials for oxidation were observed to be 1.55, 1.83 and 1.03V for PDEHFP-26, PDEHFP-35, PDEHFP-25 respectively. On the other hand, the onset potentials for reduction were -1.08, -0.78 and -1.25V respectively. From the onset potentials of the oxidation and reduction processes, the band gaps of the polymers were estimated to be 2.63, 2.61 and 2.28eV for PDEHFP-26, PDEHFP-35, PDEHFP-25 respectively. As compared to the homopolymer, PDEHFP-26 and PDEHFP-35 have broader band gaps while PDEHFP-25 has almost the same band gap as the homopolymer, which is 2.3eV. According to the equations [25,26] IP=-($[E_{onset}]^{ox}$+4.4)eV and EA=-($[E_{onset}]^{red}$+4.4)eV, where $[E_{onset}]^{ox}$ and $[E_{onset}]^{red}$ are the onset potentials for the oxidation and reduction of the polymers, the HOMO and LUMO of the polymers were estimated to be -5.95, -6.23 and -5.43eV and -3.32, -3.62 and -3.15eV for PDEHFP-26, PDEHFP-35, PDEHFP-25 respectively. PDEHFP-26 and PDEHFP-35 have lower HOMO and LUMO in comparison with that of the homopolymer, which are -5.36 and -3.06eV respectively, While PDEHFP-25 has almost the same HOMO and LUMO as the homopolymer. The corresponding electrochemical data of the polymers are summarized in Table 3.

Table 3 Electrochemical Properties of the Polymers

polymer	E_{onset}(V) (p-doping)	E_{onset}(V) (n-doping)	Energy levels(eV)		
			HOMO	LUMO	Band gap
PDEHFP-26	1.55	-1.08	-5.95	-3.32	2.63
PDEHFP-35	1.83	-0.78	-6.23	-3.62	2.61
PDEHFP-25	1.03	-1.25	-5.43	-3.15	2.28
PDEHF	0.96	-1.34	-5.36	-3.06	2.3

From table 3, we can see that these copolymers with pyridine units, especially PDEHFP-26 and PDEHFP-35 possess very low LUMO energy levels for an easy electron injection from a cathode, which is consistent with our expectation. We can also find that the HOMO and LUMO energy levels of PDEHFP-26 and PDEHFP-35 are quite similar.

As for PDEHFP-25, its HOMO and LUMO are quite higher and they are close to the HUMO and LUMO of the homopolymer instead. Therefore, the different linkage position of pyridinyl units in the copolymer backbone will affect the energy levels of the polymers.

3.4 Conclusion

In summary, a novel series of well-defined fluorene-pyridine-based alternating copolymers have been synthesized by Suzuki cross-coupling reaction in high yields. These polymers have relatively high molecular weight and have good solubility in common solvents, such as chloroform and THF. All the polymers show good thermal stability and have relatively high T_g. The different linkage position of pyridinyl unit in the polymer backbone has significant effects on the electronic and optical properties of polymers in solution and in film phases. Meta-linkage(3,5-and 2,6-linkage) of pyridinyl units in the polymer backbone is more favourable to polymer for pure blue emission and prevention of aggregation of polymer chain than para-linkage(2,5-linkage) of the pyridinyl units. The result shows that the electronic and optical properties of the polymers are consistent with a rigid-rod conjugated backbone structure. These polymers with pyridine units possess very low LUMO energy levels for an easy electron injection from a cathode. It also shows that the electronic and optical properties of fluorescent polymers can be well tuned by properly rationalized design of polymer architectures such as the incorporation of different pyridinyl moieties into polycarbazole backbone.

References

(1) Burroughes, J. H.; Bradley, D. D. C.; Brown, A. R.; Marks, R. N.; Mackay, K.; Friend, R. H.; Burn, P. L.; Holmes, A. B. *Nature (London)* **1990**, *347*, 539.

(2) (a) Kraft, A.; Grimsdale, A. C.; Holmes, A. B. *Angew. Chem., Int. Ed.* **1998**, *37*, 402. (b) Friend, R. H.; Gymer, R. W.; Holmes, A. B.; Burroughes, J. H.; Marks, R. N.; Taliani, C.; Bradley, D. D. C.; Dos Santos, D. A.; Bre´das, J. L.; Lo¨gdlund, M.; Salaneck, W. R. *Nature (London)* **1999**, *397*, 121. (c) Bernius, M. T.; Inbasekaran, M.; O'Brien, J.; Wu, W. *Adv. Mater.* **2000**, *12*, 1737. (d) Mitschke, U.; Ba¨urele, P. *J. Mater. Chem.* **2000**, *10*, 1471.

(3) Kraft, A.; Grimsdale, A. C.; Holmes, A. B. *Angew. Chem., Int. Ed.* **1998**, *37*, 402.

(4) Segura, J. L. *Acta Polym.* **1998**, *49*, 319.

(5) Friend, R. H.; Gymer, R. W.; Holmes, A. B.; Burroughes, J. H.; Marks, R. N.; Taliani, C.; Bradley, D. A.; Santos, D.; Bre´das, J. L.; Lo¨gdlund, M.; Salaneck, W. R. *Nature* **1999**, *397*, 121.

(6) Chuanjun Xia and Rigoberto C. Advincula, *Macromolecules* **2001,** *34,* 5854.

(7) Jianfu Ding, Michael Day, Gilles Robertson, and Jacques Roovers, *Macromolecules*, **2002**, *35*, 3474-3483

(8) Bernius, M. T.; Inbasekaran, M.; O'Brien, J.; Wu, W. S. *Adv. Mater*. **2000**, *12*, 1737-1750.

(8) Neher, D. *Macromol. Rapid Commun.* **2001**, *22*, 1366-1385.

(10) Scherf, U.; List, E. J. W. *Adv. Mater.* **2002**, *14*, 477-487.

(11) (a). Q. Pei, Y. Yang, *J. Am. Chem. Soc*., **1996**, 118, 7416. (b) M. Kreyenschmidt, G. Klaerner, T. Fuhrer, J. Ashenhurst, S. Karg, W. D. Chen, V. Y. Lee, J. C. Scott, R. D. Miller, *Macromolecules*, **1998**, *31*, 1099.

(12) (a). S. Dailey, M. Halim, E. Rebourt, L. E. Horsburgh, I. D. W. Samuel, A. P. Monkman, *J. Phys. Condens. Matter* 10 (**1998**) 5171; (b). D. D. Gebler, Y. Z. Zhang, J. W. Blatchford, S. W. Jessen, L. B. Lin, T. L. Gustafston, H. L. Wang, T. M. Swager, A. G. Macdiarmid, A. J. Epstein, *J. Appl. Phys*. 78 (**1995**) 4264; (c). Feller, A. P. Monkman, *Synthetic Metals* 116 (**2001**) 149-152; (d). Takakazu Yamamoto, Tsukasa Maruyama, Zhen-hua Zhuo, Takayori Ito, Takashi Fukuda, Yutaka Yoneda, Farida Begum, Tomiki Ikeda, Shintaro Sasaki, Hideo Takezoe, Atsuo Fukuda and Kenji Kubota, *J. Am. Chem. Soc*., **1994**, 116, 4832; (e). Takakazu Yamamoto, Zhen-hua Zhuo, Takaki Kanbara, Masaki Shimura, Kenichi Kizu, Tsukasa Maruyama, Yoshiyuki Nakamura, Takashi Fukuda, Bang-Lin Lee, Naoki Ooba, Satoru Tomaru, Takashi Kurihara, Toshikuni Kaino, Kenji Kubota, and Shintaro Sasaki, *J. Am. Chem. Soc*., **1996**, 118, 10389; (f). L. E. Horsburgh, A. P. Monkman, I. D. W. Samuel, *Synth. Met*. **1999**, 101, 113.

(13) T. Yamamoto, H. Suganuma, Y. Saitoh, T. Maruyama, T. Inoue, *Jpn. J. Appl. Phys*., **1996**, *35*, L1142

(14) T. Kanbara, T. Kushida, N. Saito, I. Kuwajima, K. Kubota, T. Yamamoto, *Chem. Letter*., **1999**, 583.

(15) Y. Z. Wang, D. D. Gebler, D. K. Fu, T. M. Swager, A. G. Macdiarmid, A. J. Epstein, *Synth. Met*., **1997**, *85*, 1179.

(16) (a). M. J. Marsella, D. K. Fu and T. M. Swager, *Adv. Mater.*, **1995**, 7, 145. (b) Jai Kyeong Kim, Jae Woong Yu, Jae Min Hong, Hyun Nam Cho, Dong Young Kim and Chung Yup Kim, *J. Mater. Chem.*, **1999**, 9, 2171.

(17) (a). S. C. Ng, H. F. Lu, H. S. O. Chan, A. Fujii, K. Yoshino, *Adv. Mater.*, **2000**, 12(15), 1122. (b): Fujii, A., R Ootake, T Fujisawa, M Ozaki, Y Ohmori, T Laga, K Yoshino, H. F. Lu, H. S. O. Chan, and S. C. Ng, *Appl. Phys. Lett.*, **2000**, 77(5) 660. (c): S. C. Ng, H. F. Lu, H. S. O. Chan, A. Fujii, L. G. Tong, K. Yoshino, *Macromoleclues*, **2001**, *34*, 6895. (d): R Ootake, T. Fujisawa, T. Sonoda, A. Fujii, T Laga, H. F. Lu, H. S. O. Chan, and S. C. Ng, K. Yoshino, *Synth. Met*. **2001**, 119, 593. (e): Lu H. F., H. S. O. Chan and S. C. Ng, *Macromolecules*, **2003**, 36(5), 1543.

(18)Jianfu Ding, Michael Day, Gilles Robertson, and Jacques Roovers, *Macromolecules*, **2002**, *35*, 3474-3483

(19) Xia, C. J.; Advincula, R. C., *Macromolecules*, **2001**, *34*, 5854.

(20) Maxime Ranger, Dany Rondeau, and Mario leclere*, Macromolecules, **1997,** 30, 7686

(21) T. M. Swager, C. G. Gil, M. S. Wrightton, *J. Phys. Chem.*, **1995**, *99*, 4886.

(22) S. C. Ng, H. F. Lu, H. S. O. Chan, A. Fujii, K. Yoshino, *Adv. Mater.*, 2000, 12(15), 1122.

(23) T. M. Swager, C. G. Gil, M. S. Wrightton, *J. Phys. Chem.*, **1995**, *99*, 4886.

(24)A. P. Davey, S. Elliott, O. O'Connor, W. J. Blau, *Chem. Soc., Chem. Commun*. 1995, 1433.

(25) de Leeuw, D. M.; Simenon, M. M. J.; Brown, A. R.; Einerhand, R. E. F. *Synth. Met.* **1997**,87,53.

(26) Cervini, R.; Li, X. C.; Spencer, G. W. C.; Holmes, A. B.; Moratti, S. C.; Friend, R. H. *Synth. Met.* **1997**, 84, 359.

Chapter 4 Dendronized Fluorenyl-Pyridinyl-Based Alternating Copolymers: Synthesis and Characterization

The synthesis and characterization of a novel series of dendritic, rigid rod poly[2,7-(9,9-bis[3,5-bis(benzyloxy)benzyl])fluorenyl-alt-pyridinyl] via the macromonomer approach were reported. The dendritic intermediate compound (6) was prepared by coupling benzyl bromide functionalized the first generation of benzyl ether dendron (4) with 2,7-dibromofluorene (5) at the 9,9'-position of fluorenyl unit and its further reaction product monomer (7) was subsequently employed in condensation polymerizations with different dibromopyridines via Suzuki coupling reaction to yield alternating copolymers. In this series of alternating copolymers, the fluorene unit was used as light emitting unit and the first generation of benzyl ether dendron attached at the 9,9'-positions of fluorenyl was incorporated to improve polymer solubility and to prevent aggregrate/excimers formation of polymer chain and fluorescence quenching. The electron deficient unit of pyridinyl, on the other hand, was introduced to tune the wavelength of the emitting light and improve their electron transportation. Fluorescence measurements of the materials reveal extensive conjugation along the polymer backbone. Effective suppression of formation of long wavelength emitting aggregates is achieved, thus giving a polymer with pure blue emission. Different linkage position of pyridinyl units in the copolymer backbone has significant effects on the electronic and optical properties in solution and in film phases. For pure blue emission and prevention of aggregation of polymer chain, meta-linkage(3,5- and 2,6- linkage) of pyridinyl units in the polymer backbone is more favourable to polymer than para-linkage (2,5-linkage) of the pyridinyl units. Electrochemical behavior indicated these polymers with pyridinyl units possess very low LUMO energy levels for an easy electron injection from a cathode.

4.1 Introduction

Ever since the first report of the PLED device fabricated from poly(p-phenylenevinylene)(PPV) in 1990,[1] polymeric light-emitting diodes (PLEDs) have attracted significant research attention from both academic community and industry, particularly on account of their potential applications in large-area, flat-panel displays which can be operated at relatively low driving voltages.[2-3] Three primary colors, i.e., blue, green, and red emitting materials, are essential for full-color displays. Among these three colors, green and red light emitting materials have been already achieved with high stability and efficiency. The pursuit of efficient and stable blue PLEDs based on conjugated polymers, however, remains a challenge. A challenging goal in this area is to achieve blue light emitting materials with long-term stability, high efficiency, and free of blue-green emission.[4-5] Highly soluble poly(2,7-(9,9-dialkyl)fluorenyl)s (PFs) and their derivatives are considered as very promising blue light emitting materials because of their excellent chemical and thermal stabilities and exceptionally high solid-state quantum yields not reached with other conjugated polymers.[6] Problems encountered with these rodlike PFs and their copolymers are their tendency to aggregate during operation or annealing in air. Formation of excimers in the solid state leads to blue-green emission and fluorescence quenching. [7] Approaches to avoid the detrimental aggregate/excimer formation have included the use of longer and branched side chains or bulky side chains as solublizers, the incorporation of dendritic endgroups,[8-9] the use of cross-linkable groups,[10-11] the statistical copolymerization of 2,7-dibromocarbazole with other suitable comonomers [12] and the encapsulation of polyfluorene backbones into dendritic envelopes. [13]

The application of pyridine as the π-deficient moiety in our polymer is driven by the consideration that polypyridinyl (PPy) was used in blue-emitting devices [15-16] and that polymers based on pyridine have been demonstrated to be highly luminescent. [17] Therefore, the incorporation of a pyridinyl unit into polymer backbone increases the electron affinity of the polymers, which not only makes the copolymers to be n-dopable and capable of better electron transportation, [18a-b] but also makes the polymers more resistant to oxidation. These polymers with pyridine units will be expected to possess low LUMO energy levels for an easy electron injection from a cathode.

The idea of combining the encapsulation of a linear polymeric emitter with a dendritic structure and incorporation of electron-affinity pyridinyl units led us to synthesize copolymer, which carries in the dendritic side chain that not only serve as solubilizing groups but also hinder aggregation.

4.2 Experimental part

4.2.1 ***Materials.*** The reagents 3,5-(dihydroxy)methylbenzoate, benzyl chloride, lithium aluminium hydride, phosphorus tribromide, n-BuLi, Tetrakis(triphenylphosphine)palladium(0) [$(PPh_3)_4Pd$ (0)], 3,5-dibromopyridine, 2-isopropoxy-4,4,5,5-tetramethyl-1,3,2-dioxaborolane and Tetrabutylammonium percholate (Bu_4NClO_4) (AR) were obtained from Aldrich, benzyltriethylammonium chloride, 2,5–dibromopyridine and 2,6-dibromopyridine were obtained from Avocado Research Chemicals Ltd. NaOH(AR), DMSO (AR), toluene(AR) and all other reagents were purchased from commercial sources and used without further purification. The solvents, diethyl ether, chloroform, and THF were AR and acetonitrile(HPLC) were dried and distillated prior to use.

4.2.2 ***Measurements.*** ^{1}H NMR and ^{13}C NMR spectra were recorded on a Bruker ACF 300 FT-NMR spectrometer operating at 300 MHz. Deuterated chloroform was used as the solvent and tetramethylsilane (TMS) was used as the internal standard. Mass spectra (MS) were obtained using a micrimass VG 7035E mass spectrometer. Weight-average molecular mass (M_w) and number-average molecular mass (M_n) were determined by gel permeation chromatography (GPC) using a Perkin-Elmer mode 200 HPLC system equipped with Phenogel MXL and MXM columns using polystyrene as the standard and THF as the eluant. The thermal properties of the polymers were investigated by DSC and TGA under flowing nitrogen. Thermogravimetric analysis (TGA) was performed on a TA Instruments with a TGA 2960 thermogravimetric analyzer module at a heating rate of 20 ℃ min^{-1} with a nitrogen flow of 100 mL min^{-1}. The temperature regime was from room temperature to 800℃. Differential scanning calorimetry (DSC) of the polymer podwers was carried out using TA 2920 module at a heating rate of 20℃ min^{-1} with a nitrogen flow of 70 mL min^{-1}. Dilute polymer solution (1×10^{-5}M) was prepared in anhydrous spectrum-grade chloroform, and quinine sulphate (1×10^{-5}M in 0.1 M H_2SO_4) was used as the reference. The thin polymer films were deposited onto quartz glass plates by spin-coating. The absorption and fluorescence spectrum measurements of polymer solution and film were conducted on Shimadzu UV-1601 PC UV-visible spectrophotometer and Perkin Elmer Instrument LS 55 Luminescence spectrometer, respectively. Cyclic voltammetry of polymer films was conducted using a single-compartment, three electrode cell comprising a platinum working electrode with the polymer spin-coated on it, a platinum counter electrode and a silver quasi-reference electrode using a HB-105 Hokuto Denko Ltd. arbitrary function generator and HA-501 Hokuto Denko Ltd. Potentiostat. Tetrabutylammonium percholate in acetonitrile was used as the electrolyte solution.

4.2.3 *Synthesis*.

Synthesis of Methyl-α-resorcylate dibenzyl ether (2):

A solution of 20g of methyl-α-resorcylate (1) [3,5-(dihydroxy)methylbenzoate] in 100ml acetone was boiled with 60g benzyl chloride and 30 g K_2CO_3 with vigorous stirring for 72 hours. The reaction was monitored by thin layer chromatography. Filtration was done to remove yellowish-white solid after reaction. All the solvent and the excess benzyl chloride were removed by distillation of the filtrate to give a pale yellow solid product solid (m.p. 77-79° C) with a yield of 88 %. Its structure was confirmed by ^1H NMR. ^1H NMR (300 MHz, $CDCl_3$): δ (ppm) 7.45-7.32(m, 12H) (overlap with signal of $CHCl_3$), 6.82 (s, 1H), 5.08(s, 4H), 3.91(s, 3H).

Synthesis of 3,5-Dibenzyloxybenzyl alcohol ([G-1]-OH) (3):

A mixture of 20g methyl-α-resorcylate dibenzyl ether in 100ml anhydrous diethyl ether was added dropwise to 2.53g lithium aluminium hydride in 100 ml anhydrous ether, which were cooled with ice-water. The reaction system was kept at refluxing at 50-60 ℃ for 24 hrs. Excess $LiAlH_4$ was decomposed first by the addition of ethyl acetate and then 4M HCl. The product was separated by extraction with diethyl ether, was obtained as a white solid with a yield of 90% after distillation of solvent.

^{1}HNMR (300 MHz, $CDCl_3$): δ (ppm) 7.43-7.32(m, 10H) (overlap with signal of $CHCl_3$), 6.63 (d, 2H), 6.55 (t, 1H), 5.04(s, 4H), 4.63(d, 2H), 1.67(s, 1H).

Synthesis of 3,5-Dibenzyloxybenzyl Bromide ([G-1]-Br) (4):

13g phosphorus tribromide (PBr_3) was added dropwise to solution of 10.75g 3,5-dibenzyloxybenzyl alcohol ([G-1]-OH) (3) in 150ml of anhydrous toluene at 0 °C. The reaction was kept at room temperature for 24 hrs with vigorous stirring. Excess PBr_3 was decomposed by addition of water. The product was separated by extraction with toluene and the organic extract was washed by the saturated $NaHCO_3$ and NaCl water solutions, respectively, followed by the removal of the solvent by vacuum distillation to afford crude product as a pale yellow solid. The crude product was purified by recrystallization with hexane, yielding white needle-like crystals (mp: 92-93 °C), Yield: 56 %.

^{1}H NMR (300 MHz, $CDCl_3$): δ (ppm) 7.41-7.34(m, 10H) (overlap with signal of $CHCl_3$), 6.64 (d, 2H), 6.55 (t, 1H), 5.03(s, 4H), 4.41(s, 2H).

Synthesis of 9,9-Bis[3,5-bis(benzyloxy)benzyl]-2,7-dibromofluorene (6):

This compound was synthesized by a modification method of reference.[19,20] A typical procedure is as following: a mixture of 2,7-dibromofluorene (5) (6g, 18.45 mmol) and benzytrimethylammonium chloride (0.35 g, 1.4 mmol) in 30 ml of DMSO and 10 ml of aqueous NaOH (50 %, w/w) was stirred under N_2 at 80 ℃. [G-1]-Br (4) (14g, 36.5 mmol) was added to the mixture, the resulting mixture was stirred at the same temperature for 3 hrs before 20 ml of water was added. Then the solution was extracted with diethyl ether (80 ml) for three times. The combined organic layers were washed with saturated brine and dried over $MgSO_4$. The solvent was removed by rotation evaporation. The crude product was further purified by recrystallization from 2:1 hexane:ethyl acetate to afford 6.77g of the title product as a white crystalline solid. Yield: 51 %

^{1}HNMR (300 MHz, $CDCl_3$): δ (ppm) 7.58 (d, 2H), 7.41-7.28(m, 24H) (overlap with signal of $CHCl_3$), 6.30 (s, 2H), 5.93(d, 4H), 4.74(s, 8H), 3.23(s, 4H).

^{13}C NMR (300 MHz, $CDCl_3$): δ (ppm) 158.84, 150.40, 138.89, 138.11, 136.89, 130.36, 128.42, 128.03, 127.74, 127.25, 121.36, 120.45, 109.14, 101.34, 69.78, 57.05, 45.24.

Synthesis of 2,7-Bis*(4,4,5,5-tetramethyl-1,3,2-dioxaborolan-2-yl)-*9,9-Bis[3,5-bis(benzyloxy)benzyl]fluorene (7):

A typical synthetic procedure for the synthesis of the fluorene derivative monomer: to a solution of compound 6 (18.6 g, 20 mmol) in anhydrous THF (150 ml) under N_2 at –78℃ was added 37.5 ml (60mmol) of n-BuLi (1.6 M in hexane) by syringe. The mixture was stirred at -78℃ and warmed to 0℃ for 30 mins, and cooled again at -78℃, then 2-isopropoxy-4,4,5,5-tetramethyl-1,3,2-dioxaborolane (12.24 ml, 60mmol) was rapidly injected into the solution by syringe, the resulting mixture was stirred at -78.0℃ for 1 h and left to stir overnight at room temperature. The resulting mixture was poured into water and extracted three times with ether (3×150 ml). The combined ether extracts were washed with saturated brine and dried over $MgSO_4$. The solvent was removed by rotation evaporation, the crude solid product was further purified by recrystallization in ethanol to afford 9g of the title product as a white solid with a yield of 44%.

^1H NMR (300 MHz, $CDCl_3$): δ (ppm) 8.03(s, 2H), 7.54 (d, 2H), 7.45(d, 2H), 7.31-7.27(m, 20H) (overlap with signal of $CHCl_3$), 6.17(t, 2H), 5.90(d, 4H), 4.57(s, 8H), 3.41(s, 4H), 1.28(s, 24H).

^{13}C NMR (300 MHz, $CDCl_3$): δ (ppm) 158.45, 148.06, 143.93, 138.98, 137.01, 133.89, 130.66, 128.26, 127.61, 127.35, 127.31, 119.68, 109.01, 101.07, 83.65, 69.64, 57.08, 45.41, 24.73.

General Procedure for Polymerization by Suzuki Cross-Coupling Reaction:

A representative procedure for polymerization by Suzuki cross-coupling reaction is as following:

2,7-bis(4,4,5,5-tetramethyl-1,3,2-dioxaborolan-2-yl)-9,9-bis[(3,5-bis(benzyloxy)benzyl] fluorene (7) (0.37g, 0.36mmol) and 2,6-dibromopyridine (0.084g, 0.36mmol) and $(PPh_3)_4Pd$ (0) (8mg, 0.007mmol) (1 mol% based on total monomers) were dissolved in a mixture of toluene and aqueous 2 M K_2CO_3 (5ml) (3/2 volume ratio) in a 25 ml three-necked round-bottomed flask. The solution was stirred under N_2 and was heated at 95 ℃ with vigorous stirring for 48 h. The resulting mixture was then poured into 100 ml methanol. The precipitate was recovered by filtration and washed with 2 M dilute HCl and methanol respectively. The solid product was collected and dissolved in chloroform.

The resulting solution was added dropwise to methanol to precipitate the polymer again. The precipitated polymer was then collected, washed with methanol, and dried under high vacuum to yield 0.2g white solid of target polymer (8). Yield: 66%. This polymer was designated as PDDFP-26, where the second D stands for dendritic groups and the number 26 stands for the linking positions of pyridinyl unit in the polymer backbone. The other polymers were synthesized by following a similar procedure.

Poly[2,7-(9,9-bis[3,5-bis(benzyloxy)benzyl])fluorenyl-alt-(2,6-pyridinyl)] (PDDFP-26)

Yield: 66%, white solid.

^{1}H NMR(300 MHz, $CDCl_3$): δ(ppm) 8.24-8.19(m, 3H), 7.71-7.66(m, 6H), 7.17-7.11(m, 20H) (overlap with signal of $CHCl_3$), 6.28(m, 2H), 6.05(m, 4H), 4.55(m, 8H), 3.42(m, 4H).

Poly[2,7-(9,9-bis[3,5-bis(benzyloxy)benzyl])fluorenyl-alt-(3,5-pyridinyl)] (PDDFP-35)

Yield: 72.3%, white solid.

^{1}H NMR (300 MHz, $CDCl_3$): δ (ppm) 8.91(s, 1H), 8.03-7.50(m, 8H), 7.25-7.17(m, 20H) (overlap with signal of $CHCl_3$), 6.34(m, 2H), 6.02(m, 4H), 4.66(m, 8H), 3.32(m, 4H).

Poly[2,7-(9,9-bis[3,5-bis(benzyloxy)benzyl])fluorenyl-alt-(2,5-pyridinyl)] (PDDFP-25)

Yield: 91%, yellow-green solid.

^{1}H NMR (300 MHz, $CDCl_3$): δ (ppm) 8.80(s, 1H), 8.02-7.19(m, 28H) (overlap with signal of $CHCl_3$), 6.23(m, 2H), 6.00(m, 4H), 4.63(m, 8H), 3.27(m, 4H).

4.3 Result and Discusion

4.3.1 Synthesis and Characterization.

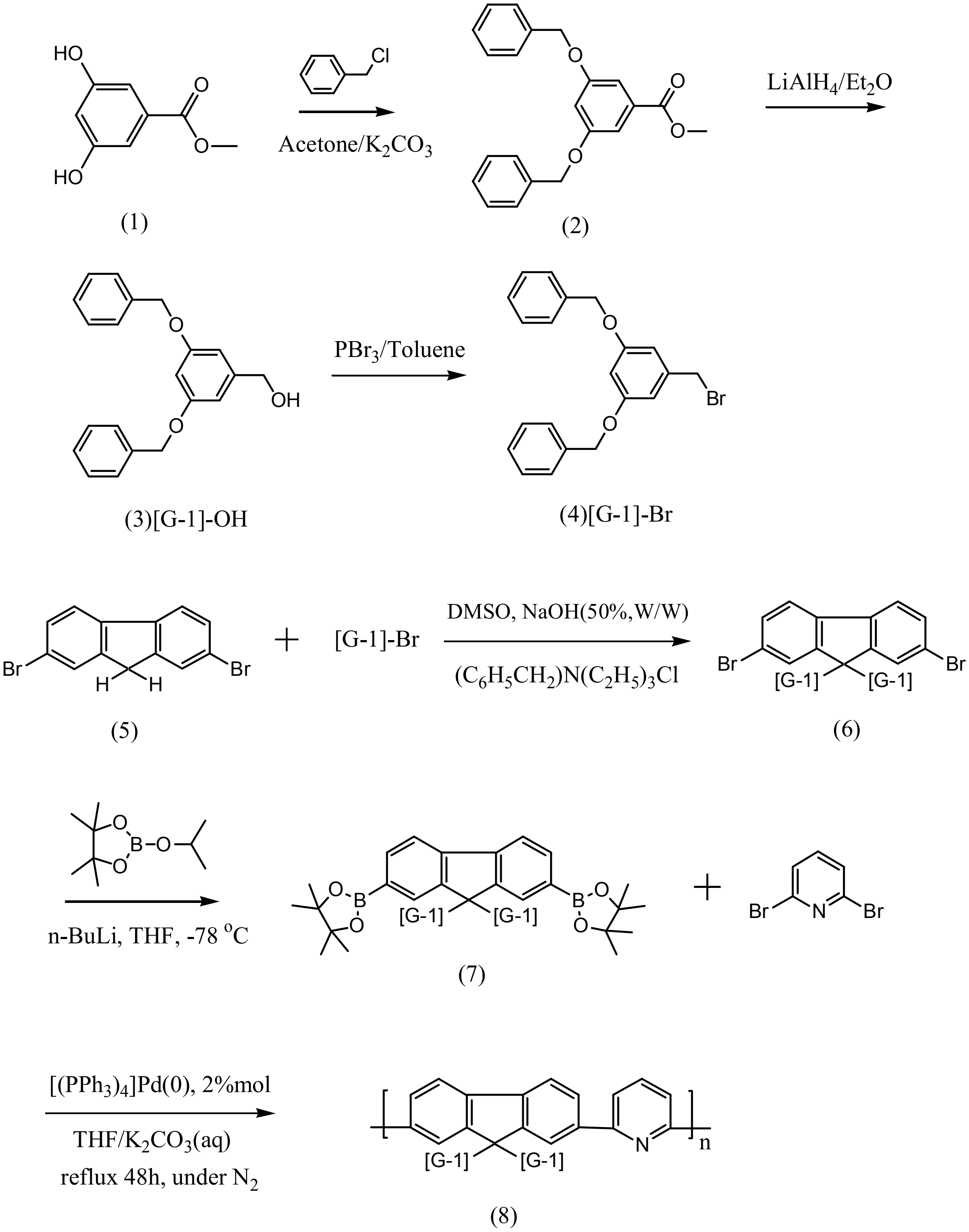

Scheme 1. Synthetic approach to the polymer PDDFP-26.

The synthetic route for the synthesis of monomer and the new series of alternating copolymer is outlined in scheme 1. Compound 9,9-bis[(3,5-bis(benzyloxy)benzyl] -2,7-dibromofluorene (6) is prepared from methyl-α-resorcylate in four steps with a total yield of 23%. Monomer 2,7-bis(4,4,5,5-tetramethyl-1,3,2-dioxaborolan-2-yl)-9,9-bis[(3,5-bis(benzyloxy)benzyl]fluorene (7) was synthesized from compound (6) in a yield of 44% following the procedure reported in the literature. [21] The polymerization is based on the Suzuki cross-coupling reaction. Poly[2,7-(9,9-bis[(3,5-bis(benzyloxy)benzyl])fluorenyl-alt-(2,6-pyridinyl)] (PDDFP-26), PDDFP-35, PDDFP-25 were obtained in good yields of 66%, 72.3% and 91% respectively. All three polymers were easily soluble in chloroform and THF. The polymerization results are summarized in Table 1.

Table 1 Properties of the Polymers

Polymers	Yield(%)	Colour	Mw[a](kDa)	PDI	DP[b]	Td[c]	Tg[d]
PDDFP-26	66	white	5.94	1.46	7	279	83
PDDFP-35	72.3	white	8.82	2.22	10	309	92
PDDFP-25	91	yellow-green	6.37	1.37	8	308	88

[a] Weight-average molecular weights determined by GPC using polystyrene standards in THF. [b] Degree of polymerization. [c] Decomposition temperature, determined by TGA in nitrogen, based on 5 % weight loss. [d] Determined by DSC in nitrogen at a scan rate of 20 °C/min.

All the polymers were characterized by ^{1}H NMR and GPC. ^{1}H NMR confirmed the proposed structures of polymers. The molecular weights of the polymers were determined by gel permeation chromatography (GPC) with THF as the eluent, calibrated against polystyrene standards. The results of GPC are also shown in Table 1.

The thermal stabilities of polymers were evaluated by thermogravimetric analyses (TGA) in nitrogen and the results are also summarized in Table 1. It is apparent that all the polymers exhibited good thermal stability in nitrogen with an onset of decomposition in the range of 270 to 310℃. Thermally induced phase transition behaviour of the polymers was investigated with differential scanning calorimetry(DSC) under nitrogen atmosphere. The glass transition temperatures (T_g) of polymers were also summarized in Table 1. T_g of the polymers was in the range of 80-100℃. The relative high glass transition temperatures are essential for many applications such as in PLEDs as emissive materials. [22]

4.3.2 Optical Properties.

The UV-vis absorption and fluorescence emission spectra of the polymer solution in $CHCl_3$ and that of the polymer films spin-cast from $CHCl_3$ solutions were recorded at room temperature. The optical data are summarized in Table 2.

Table 2 Spectra Properties and Quantum Yield

Polymers	Solution[a]			Film[b]		
	λ_{max}^{c}（nm）	λ_{pl}^{c}（nm）	Φ^{d}	λ_{max}^{c}（nm）	λ_{pl}^{c}（nm）	Optical band gap(eV)
PDDFP-26	365	384(402)	0.32	369	412	3.16
PDDFP-35	342	372(389)	0.34	345	395(416)	3.29
PDDFP-25	379	418(437)	0.30	391	455(487)	2.84

[a] 1×10^{-5}M in anhydrous chloroform. [b] Spin-coating on quartz glass from anhydrous chloroform solution. [c] Wavelength of maximum absorbance or emission, wavelength of the shoulder peak is in brackets. [d] Relative to 1×10^{-5}M quinine sulphate in 0.1M H_2SO_4.

The UV-vis absorption photoluminescence(PL) spectra of the PDDFP series of polymers in chloroform are shown in figure 1. It is evident that the linkage pattern of the pyridinyl moiety in the polymer backbone has a major influence on the absorption maximum of polymer. The absorption maximum of PDDFP-25 with para-linkage of pyridinyl unit at 379 nm is red-shifted in comparison with that of PDDFP-26 and PDDFP-35 with metal-linkage of pyridinyl moiety, being 365 nm and 342nm, respectively. The difference among the absorption maximum of our PDDFP series of copolymers is attributed to the lesser extent of π-electron delocalization in the polymer backbone arising from meta-linkages, causing a reduction in the π-conjugation lengths. The effect of different linkage position of pyridinyl units on the absorption maximum of polymer is similar to that of our previous report. [23]

PDDFP-25 produce very strong blue fluorescence with emission maximum at 418nm and a shoulder peak at 437 nm. For PDDFP-26 and PDDFP-35, they produce very strong blue fluorescence which is slightly violet-shifted, with emission maximum at 384 and 402 nm, 372 and 389 nm respectively.

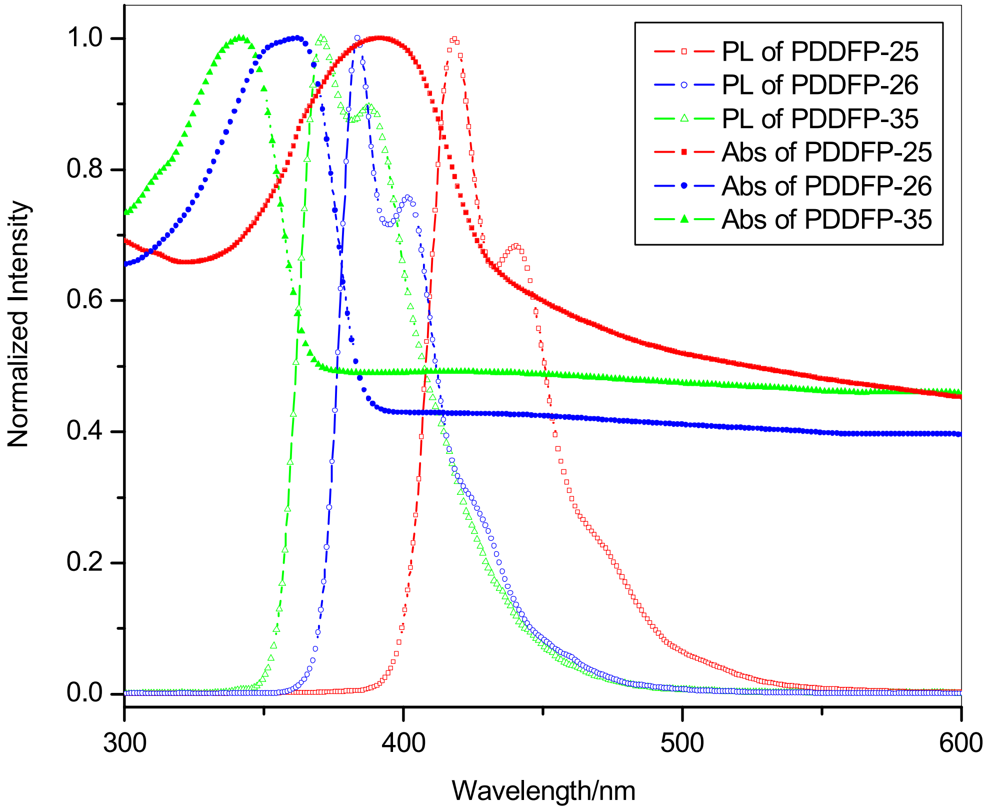

Figure 1. UV-Vis absorption (abs) and photoluminescence (PL) spectra of PDDFP series polymers in $CHCl_3$ solution.

The photoluminescence quantum yields in chloroform solution were measured according to the method described by Davey et al. [24] relative to 10^{-5} M quinine sulphate in 0.1 M H_2SO_4. The results are summarized in Table 2. High quantum yields of all the polymers are obtained, being in the range of 30-35%.

Fig. 2 shows the UV-vis absorption and photoluminescence (PL) spectra of PDDFP series of polymers in thin films. For PDDFP-25, in which the pyridinyl unit is para-linked in the polymer main chain, its UV maximum in film at 391 nm is red-shifted in comparison with the UV maxima (at 369 nm and 345 nm, respectively) of PDDFP-26 and PDDFP-35 with meta-linkages of the pyridinyl units. This is also attributed to the lower extent of π-electron delocalization of the polymer main chain arising from meta-linkages of the pyridinyl moiety, resulting in a reduction in the π-conjugation length.

In the film state, the blue emission peaks appear at 412, 395(416, shoulder peak) and 455(487, shoulder peak) nm for PDDFP-26, PDDFP-35 and PDDFP-25, respectively. It can be seen that the PL of PDDFP-25 is very broad and red-shifted, and has an obvious tailing phenomena beyond 500nm as compared with that of PDDFP-35 and PDDFP-26. The PL of PDDFP-35 and PDDFP-26 showed that the two polymers can emit pure blue light without tailing phenomena as compared with PDEHCP-25. It shows that the incorporation of 3,5-pyridiinyl or 2,6-pyridinyl units into polymers chain prevent the aggregation of polymer chain/interchain excimer formation, which will result in red-shifted peak in the range of 520-550 nm in other polymers.[9a,21b,26,27a] The results of PL in film states show that the encapsulation of a linear polymeric emitter with a dendritic structure and the incorporation of electron-affinity pyridinyl units can well tune the optical properties of fluorene polymers.

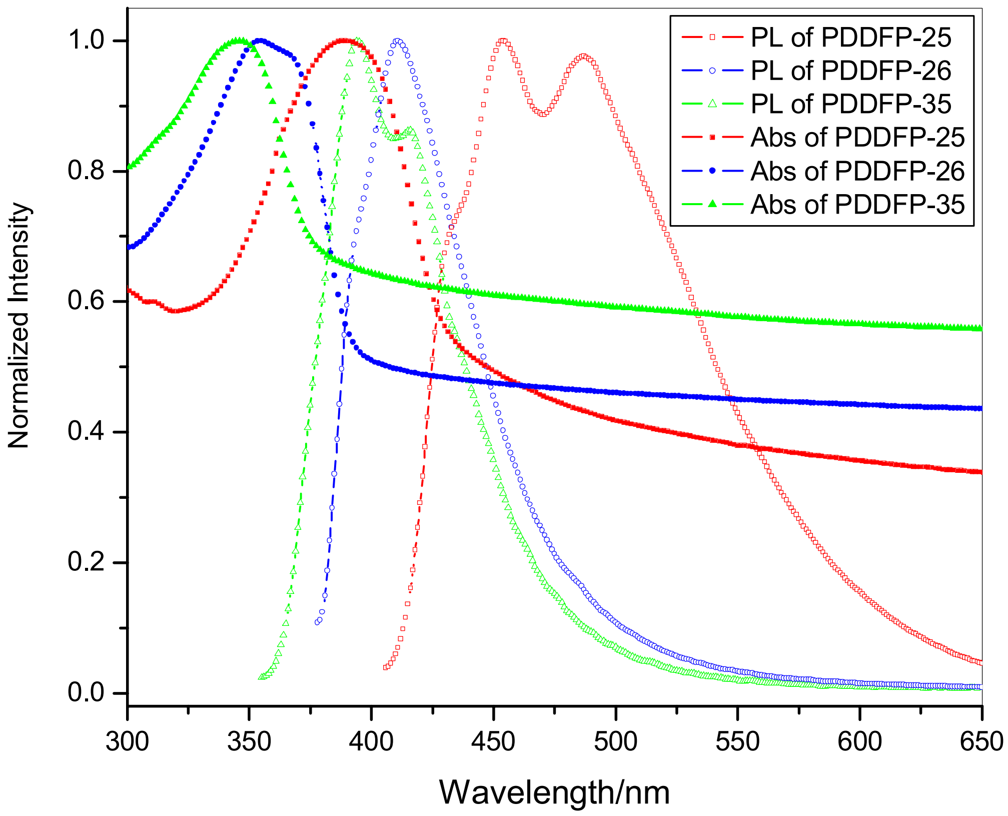

Figure 2. UV-Vis absorption (abs) and photoluminescence (PL) spectra of PDDFP series polymers in thin films.

4.3.3 Electrochemical Properties.

The electrochemical behavior of the polymer was investigated by cyclic voltammetry(CV). CV was performed in a solution of Bu_4NClO_4(0.10M) in acetonitrile at a scan rate of 50mV/s at room temperature under the protection of nitrogen. A platinum electrode coated with a thin polymer film was used as the working electrode. A Pt wire was used as the counter electrode and an $Ag/AgNO_3$(0.01M) electrode was used as the reference electrode. The resulting cyclic voltammograms are outlined in figure 3.

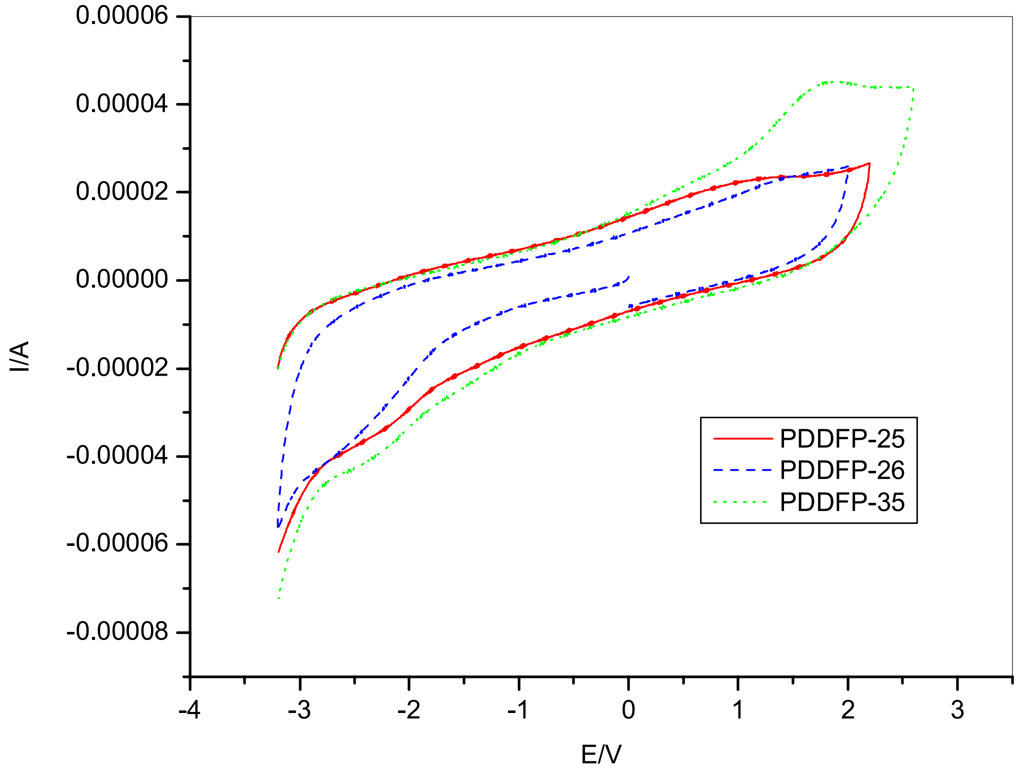

Figure 3. The cyclic voltammograms of PDDFP series polymer films coated on platinum plate electrodes in acetonitrile containing 0.1 M Bu_4NClO_4 .

The onset potentials for oxidation were observed to be 1.77, 1.86 and 1.32V for PDDFP-26, PDDFP-35, PDDFP-25 respectively. On the other hand, the onset potentials for reduction were -1.08, -1.39 and -1.18 respectively. From the onset potentials of the oxidation and reduction processes, the band gaps of the polymers were estimated to be 2.85, 3.25 and 2.50eV for PDDFP-26, PDDFP-35, PDDFP-25 respectively. According to the equations [25,26] IP=-($[E_{onset}]^{ox}$+4.4)eV and EA=-($[E_{onset}]^{red}$+4.4)eV, where $[E_{onset}]^{ox}$ and $[E_{onset}]^{red}$ are the onset potentials for the oxidation and reduction of the polymers, the HOMO and LUMO of the polymers were estimated to be -6.17, -6.26 and -5.72eV and

-3.32, -3.01 and -3.22eV for PDDFP-26, PDDFP-35, PDDFP-25 respectively. The corresponding electrochemical data of the polymers are summarized in Table 3.

Table 3 Electrochemical Properties of the Polymers

polymer	E_{onset}(V) (p-doping)	E_{onset}(V) (n-doping)	Energy levels(eV)		
			HOMO	LUMO	Band gap
PDEHCP-26	1.77	-1.08	-6.17	-3.32	2.85
PDEHCP-35	1.86	-1.39	-6.26	-3.01	3.25
PDEHCP-25	1.32	-1.18	-5.72	-3.22	2.50

From table 3, we can see that these polymers with pyridine units possess very low LUMO energy levels for an easy electron injection from a cathode, which is consistent with our expectation. We can also find that the HOMO and LUMO energy levels of PDDFP-26 and PDDFP-35 are quite similar. As for PDDFP-25, its LUMO is close to the other two polymers while the HUMO is much higher. Therefore, the different linkage position of pyridinyl units in the copolymer backbone will affect the energy levels of the polymers.

4.4 Conclusion

In summary, a novel series of well-defined fluorene-pyridine-based alternating copolymers with dendrimer side chains have been synthesized by Suzuki cross-coupling reaction in good yields. These polymers have high molecular weight and have good solubility in common solvents, such as chloroform and THF. All the polymers show good thermal stability, anti-oxidization and have relatively high T_g. The different linkage position of pyridinyl unit in the polymer backbone has significant effects on the electronic and optical properties of polymers in solution and in film phases. Meta-linkage(3,5-and 2,6-linkage) of pyridinyl units in the polymer backbone is more favourable to polymer for pure blue emission and prevention of aggregation of polymer chain than para-linkage(2,5-linkage) of the pyridinyl units. The result shows that the electronic and optical properties of fluorescent polymers can be well tuned by introduction of dendritic side chain and incorporation of electronic-deficient pyridinyl units.

References

(1) Burroughes, J. H.; Bradley, D. D. C.; Brown, A. R.; Marks, R. N.; Mackay, K.; Friend, R. H.; Burn, P. L.; Holmes, A. B. *Nature (London)* **1990**, *347*, 539.

(2) J. H. Burroughes, D. D. C. Bradley, A. R. Brown, R. N. Mark, K. Mackay, R. H. Friend, P. L. Burn, A. B. Holmes, *Nature*, **1990**, *347*, 539

(3) D. Braun, A. J. Heeger, *Appl. Phys. Lett*. **1991**,*58*, 1982

(4) Jenekhe, S. A.; Osaheni, J. A. *Science* **1994**, *265*, 765.

(5) Samuel, I. D. W.; Rumbles, G.; Collison, C. J. *Phys. Re*V. *B.*, **1995**, *52*, R11573.

(6) (a) Pei, Q.; Yang, Y. *J. Am. Chem. Soc.* **1996**, *118*, 7416. (b) Neher, D. *Macromol. Rapid Commun.* **2001**, *22*, 1365. (c) Scherf, U.; List, E. J. W. *Adv. Mater.* **2002**, *14*, 477. (d) Leclerc, M. *J. Polym. Sci., Part A: Polym. Chem.* **2001**, *39*, 2867.

(7) (a) Prieto, I.; Teetsov, J.; Fox, M. A.; van den Bout, D. A.; Bard, A. J. *J. Phys. Chem. A* **2001**, *105*, 520. (b) Sainova, D.; Miteva, T.; Nothofer, H. G.; Scherf, U.; Glowacki, I.; Ulanski, J.; Fujikawa, H.; Neher, D. *Appl. Phys. Lett.* **2000**, *76*, 1810. (c) Weinfertner, K.-H.; Fujikawa, H.; Tokito, S.; Taga, Y. *Appl. Phys. Lett.* **2000**, *76*, 2502. (d) Grice, A. W.; Bradley, D. D. C.; Bernius, M. T.; Inbasekaran, M.; Wu, W. W.; Woo, E. P. *Appl. Phys. Lett.* **1998**, *73*, 629. (e) Lee, J.-I.; Klaerner, G.; Miller, R. D. *Synth. Met.* **1999**, *101*, 126. (f) Teetsov, J. A.; Vanden Bout, D. A. *J. Am. Chem. Soc.* **2001**, *123*, 3605. (g) Zeng, G.; Yu, W. L.; Chua, S. J.; Huang, W. *Macromolecules* **2002**, *35*, 6907.

(8) G. Klaerner, R. D. Miller, C. J. Hawker, *Polym. Prepr*. **1998**, 1006.

(9) J. I. Lee, G. Klaerner, J. P. Chen, J. C. Scott, R. D. Miller, *Proc. SPIE* **1999**, *3623*, 2.

(10) J. P. Chen, G. Klaerner, J. I. Lee, D. Markiewicz, V. Y. Lee, R. D. Miller, J. C. Scott, *Synth. Met*. **1999**, *107*, 129.

(11) G. Klaerner, J. I. Lee, E. Chan, J. P. Chen, A. Nelson, D. Markiewicz, R. Siemens, J. C. Scott, R. D. Miller, *Chem. Mater*. **1999**, *11*, 1800.

(12) G. Klaerner, M. H. Davey, W. D. Chen, J. C. Scott, R. D. Miller, *Adv. Mater*. **1998**, *10*, 993.

(13) (a) Setayesh, S.; Grimsdale, A. C.; Weil, T.; Enkelmann, V.; Mu¨ llen, K.; Meghdadi, F.; List, E. J. W.; Leising, G. *J. Am. Chem. Soc.* **2001**, *123*, 946. (b) Marsitzky, D.; Vestberg, R.; Blainey, P.; Tang, B. T.; Hawker, C. J.; Carter, K. R. *J. Am. Chem. Soc.* **2001**, *123*, 6965. (c) Chou, C. H.; Shu, C. F. *Macromolecules* **2002**, *35*, 9673.

(14) (a) Zhang, A. F.; Shu, L. J.; Bo, Z. S.; Schlu¨ ter, A. D. *Macromol. Chem. Phys.* **2003**, *204*, 328. (b) Schlu¨ ter, A. D.; Rabe, J. P. *Angew. Chem., Int. Ed.* **2000**, *39*, 864.

(15) T. Yamamoto, H. Suganuma, Y. Saitoh, T. Maruyama, T. Inoue, *Jpn. J. Appl. Phys*., **1996**, *35*, L1142

(16) T. Kanbara, T. Kushida, N. Saito, I. Kuwajima, K. Kubota, T. Yamamoto, *Chem. Letter*., **1999**, 583.

(17) Y. Z. Wang, D. D. Gebler, D. K. Fu, T. M. Swager, A. G. Macdiarmid, A. J. Epstein, *Synth. Met*., **1997**, *85*, 1179.

(18) (a). M. J. Marsella, D. K. Fu and T. M. Swager, *Adv. Mater*., **1995**, 7, 145. (b) Jai Kyeong Kim, Jae Woong Yu, Jae Min Hong, Hyun Nam Cho, Dong Young Kim and Chung Yup Kim, *J. Mater. Chem*., **1999**, 9, 2171.

(19)Jianfu Ding, Michael Day, Gilles Robertson, and Jacques Roovers, *Macromolecules*, **2002**, *35*, 3474-3483

(20) Xia, C. J.; Advincula, R. C., *Macromolecules*, **2001**, *34*, 5854.

(21) Maxime Ranger, Dany Rondeau, and Mario leclere*, Macromolecules, **1997,** 30, 7686

(22) T. M. Swager, C. G. Gil, M. S. Wrightton, *J. Phys. Chem*., **1995**, *99*, 4886.

(23) S. C. Ng, H. F. Lu, H. S. O. Chan, A. Fujii, K. Yoshino, *Adv. Mater*., **2000**, 12(15), 1122.

(24)A. P. Davey, S. Elliott, O. O'Connor, W. J. Blau, *Chem. Soc., Chem. Commun*. 1995, 1433.

(25) de Leeuw, D. M.; Simenon, M. M. J.; Brown, A. R.; Einerhand, R. E. F. *Synth. Met.* **1997**,87,53.

(26) Cervini, R.; Li, X. C.; Spencer, G. W. C.; Holmes, A. B.; Moratti, S. C.; Friend, R. H. *Synth. Met.* **1997**, 84, 359.

Chapter 5 Novel Fluorescent Carbazolyl-Pyridinyl Alternating Copolymers: Synthesis, Characterization and Properties

A novel series of AB type polymers comprising of alternating carbazolyl and pyridinyl units were synthesized using palladium(0)-catalyzed Suzuki cross-coupling reaction in good to high yields. In this series of alternating copolymers, the electron-rich 2,7-(N-(2-ethylhexyl)carbazolyl) unit was used as lighting emitting unit and the electron deficient unit of pyridinyl was introduced to tune the wavelength of the emitting light and improve their electron transportation. These polymers were characterized by ^{1}HNMR and ^{13}CNMR, gel permeation chromatography(GPC), thermal analysis, UV-vis, fluorescence spectroscopy and cyclic voltammetry(CV). The glass transition temperature of these polymers ranged from 120 ℃ to 150 ℃ and the polymers showed high thermal stability with decomposition temperatures in the range of 370 to 400℃ in nitrogen. Different linkage pattern of pyridinyl units in the copolymer backbone has significant effect on the electronic and optical properties in solution and in film phases. For pure blue emission and prevention of aggregation of polymer chain, meta-linkage pattern (3,5- and 2,6-linkage) of pyridinyl units in the polymer backbone is more favorable to polymer than para-linkage pattern (2,5-linkage) of the pyridinyl units. CV results indicate that these polymers with pyridinyl units possess lower LUMO energy levels for an easy electron injection from a cathode than poly[3,6-(N-octyl)carbazolyl] and its derivatives do.

5.1 Introduction

Ever since the first report of the polymeric light-emitting diodes (PLED) device fabricated from poly(p-phenylenevinylene)(PPV) in 1990,[1] PLEDs have attracted significant research attention from both academic community and industry, particularly on account of their potential applications in large-area, flat-panel displays which can be operated at relatively low driving voltages.[1,2] For full-colour display applications, the development of red, green and blue emitting materials (either polymers or oligomers or small organic molecules) with high efficiency and stability is required.[3,4,5] Among the three primary colours, only red and green PLEDs have sufficient efficiencies and lifetimes to be of commercial value. The pursuit of efficient and stable blue PLEDs based on conjugated polymers remains a challenge. This arises because it is hard to achieve a balanced charge injection due to the large band gap between the LUMO and HOMO energy levels.[6]

Recently, increasing interest has been paid to carbazole-based polymers because of their optical properties and good hole-transporting ability in light-emitting devices.[7] Among the carbazole-derivatived polymers, poly(N-alkyl-2,7-carbazolyl)s (PCs) have emerged as a promising class of conjugated polymers, which can be utilized as the blue light-emitting active layers in PLEDs.[8] However, poly(N-alkyl-2,7-carbazolyl) exhibits additional emission bands in the long wavelength region of the spectrum(453nm, 492nm) in solid states, possibly because of the their tendency to form π-aggregates/excimers in the solid state.[8]

Poly(2,5-pyridinediyl)(PPy) and its derivatives[9] such as poly(pyridine vinylene) (PPyV)[9a-b] with electron-accepting nature is a family of promising conjugated polymers because of their high luminescence,[9f] excellent electron transporting behaviour and their general resistance to oxidation.[9d] The application of pyridinyl as the π-deficient moiety in this novel series of polymer is driven by the consideration that polypyridinyl (PPy) was used in blue-emitting devices[10-11] and that polymers based on pyridine have been demonstrated to be highly luminescent.[12] Therefore, the incorporation of a pyridinyl unit into polymer backbone increases the electron affinity of the polymers, which not only makes the copolymers to be n-dopable and capable of better electron transportation,[13] but also makes the polymers more resistant to oxidation. These polymers with pyridine units are expected to possess low LUMO energy levels for an easy electron injection from a cathode. Therefore, these copolymers of carbazolyl unit and pyridinyl units are expected to possess low HOMO and LUMO energy levels and will achieve a relatively balanced charge injection.

As an extension of our research work concerning polymeric blue light emitting diodes,[14] in the present work, we first present the synthesis and characterization of a novel series of blue-emissive alternating copolymers of N-(2-ethylhexyl)carbazolyl unit with three different pyridinyl units using the Suzuki cross-coupling approach (Scheme 1). A 1:1 alternating copolymer design was adopted because such arrangement would generally give more consistent physical properties as compared to random copolymers.

5.2 Experimental Part

5.2.1 Materials. The reagents, 2-ethylhexyl bromide, 4,4'-dinitro-2-azidobiphenyl, n-BuLi, Tetrakis(triphenylphosphine)palladium(0) [$(PPh_3)_4Pd$ (0)], 3,5-dibromopyridine, 2-isopropoxy-4,4,5,5-tetramethyl-1,3,2-dioxaborolane and Tetrabutylammonium percholate (Bu_4NClO_4) (AR) were obtained from Aldrich; benzyltriethylammonium chloride, 2,5–dibromopyridine and 2,6-dibromopyridine were obtained from Avocado Research Chemicals Ltd. NaOH(AR), $NaNO_2$(AR), NaN_3, $SnCl_2$(AR), KI(AR), DMSO (AR), toluene(AR), acetonitrile and all other reagents were purchased from commercial sources and used without further purification. The solvents, diethyl ether, chloroform, and THF were AR and were dried and distillated prior to use.

5.2.2 Measurements. ^1H NMR and ^{13}C NMR spectra were recorded on a Bruker ACF 300 FT-NMR spectrometer operating at 300 MHz. Deuterated chloroform was used as the solvent and tetramethylsilane (TMS) was used as the internal standard. Weight-average molecular mass (M_w) and number-average molecular mass (M_n) were determined by gel permeation chromatography (GPC) using a Perkin-Elmer mode 200 HPLC system equipped with Phenogel MXL and MXM columns using polystyrene as the standard and THF as the eluant. The thermal properties of the polymers were investigated by DSC and TGA under flowing nitrogen. Thermogravimetric analysis (TGA) was performed on a TA Instruments with a TGA 2960 thermogravimetric analyzer module at a heating rate of 20℃ min^{-1} with a nitrogen flow of 100 mL min^{-1}. The temperature regime was from room temperature to 800℃. Differential scanning calorimetry (DSC) of the polymer powers was carried out using TA 2920 module at a heating rate of 20℃

min^{-1} with a nitrogen flow of 70 mL min^{-1}. Dilute polymer solution (1×10^{-5}M) was prepared in anhydrous spectrum-grade chloroform, and quinine sulphate (1×10^{-5}M in 0.1 M H_2SO_4) was used as the reference. The thin polymer films were deposited onto quartz glass plates by spin-coating. The absorption and fluorescence spectrum measurements of polymer solution and film were conducted on Shimadzu UV-1601 PC UV-visible spectrophotometer and Perkin Elmer Instrument LS 55 Luminescence spectrometer, respectively. Cyclic voltammetry of polymer films was conducted using a single-compartment, three electrode cell comprising a platinum working electrode with the polymer spin-coated on it, a platinum counter electrode and a silver quasi-reference electrode using a HB-105 Hokuto Denko Ltd. arbitrary function generator and HA-501 Hokuto Denko Ltd. Potentiostat. 0.1 M tetrabutylammonium percholate in acetonitrile was used as the electrolyte solution.

5.2.3 Synthesis

4,4'-Dinitro-2-azidobiphenyl (II) To a solution of 10.0g (38.6mmol) of 4,4'-dinitro-2-biphenylamine in a mixture of 200ml of acetic acid and 40ml of sulfuric acid at 0 ℃ was added dropwise 5.32g (77.1mmol) of sodium nitrite. The mixture was stirred at 5-10 ℃ for 2h before approximately 5.00g of urea (to destroy the excess of nitrous acid), 500ml of ice water and 5.00g of activated carbon were added. The mixture was stirred again for 20 minutes and filtrated rapidly through a Buchner funnel into a flask immersed in an ice bath. A solution of 5.07g (78.0mmol) of sodium azide in 100ml of water was added dropwise to the clear yellow filtrate. The resulting solution was stirred at 0℃ for 1h and at room temperature for 24h. The mixture was quenched with

500 ml of a solution of $NaHCO_3$ in water and extracted three times with ethyl acetate. The organic layer was dried over magnesium sulfate and the solvent was removed under vacuum. Recrystallization from ethanol afford 8.81g of the title product as a yellow solid. (Yield: 80.1%)

^{1}H NMR (300 MHz, $CDCl_3$): δ (ppm) 8.33 (d, 2H), 8.16 (d, 1H), 8.10 (dd, 1H), 7.64(d, 2H), 7.53(d, 1H).

^{13}C NMR (300 MHz, Acetone-d_6): δ (ppm) 150.30, 149.49, 144.42, 140.94, 138.57, 133.79, 132.40, 124.89, 121.30, 116.04.

2,7-Dinitrocarbazole (III) To 600ml of boiling kerosene (first washed with concentrated sulfuric acid) was added very slowly 6.00g (21.0mmol) of 4,4'-dinitro-2-azidobiphenyl. The resulting solution was maintained to reflux for 1h. After cooling, the solution was kept at 0℃ for 24h. The precipitate was filtered through a Buchner funnel and the solid was washed with petroleum ether. Final purification was obtained by recristallization from ethanol to afford 4.66g of the title product. (Yield: 86%)

^{1}H NMR (300 MHz, D_6-Acetone): δ (ppm) 11.35 (s, 1H), 8.53 (dd, 4H), 8.16 (dd, 2H).

^{13}C NMR (300 MHz, Acetone-d_6): δ (ppm) 148.81, 142.63, 127.93, 123.65, 116.32, 109.28.

2,7-Diaminocarbazole (IV) To a solution of 2,7-dinitrocarbazole (6.00g, 23.3mmol) in a mixture of acetic acid (200ml) and hydrochloric acid 8N (70ml) was added 44.3g (0.23mol) 0f tin (II) chloride. The mixture was refluxed for 24h under nitrogen. After cooling, the precipitate was separated from the solvent by filtration and washed several times with cold acetic acid. The resulting diammonium salt was dissolved in water followed by addition of an aqueous solution of sodium hydroxide until the PH reached a value of 10. The precipitate was collected by filtration and dried under reduced pressure. Recrystallization in ethanol afforded 3.08g of the title product as a shiny gray solid. (Yield: 67%)

^{1}H NMR (300 MHz, D_6-Acetone): δ (ppm) 9.42 (s, 1H), 7.53 (d, 2H), 6.63 (dd, 2H), 6.47 (dd, 2H), 4.43(s, 4H).

^{13}C NMR (300 MHz, Acetone-d_6): δ (ppm) 147.22, 143.19, 120.39, 117.22, 109.34, 97.05.

2,7-Diiodocarbazole (V) To a solution of 1.50g (7.61mmol) of 2,7-diaminocarbazole in 100ml of 3M HCl solution at 0℃ was added very slowly 1.10g (15.9mmol) of sodium nitrite in 5ml of water. The mixture was stirred at 0℃ for 2h and then added to 100ml of a solution of potassium iodide. The precipitate was collected by filtration and washed with aqueous solution of $NaHCO_3$. The solid was dried under vacuum for 24h and use directly in the next reaction without further purification.

N-(2-ethylhexyl)-2,7-diiodocarbazole (VI) This compound was synthesized by a modification method of reference. [15] A typical procedure is as following: a mixture of 2,7-diiodocarbazole (6g, 14.3 mmol) and benzytrimethylammonium chloride (0.35 g, 1.4 mmol) in 30 ml of DMSO and 10 ml of aqueous NaOH (50 %, w/w) was stirred under N_2 at 80℃. 2-Ethylhexyl bromide(7.0g, 36.3 mmol) was added to the mixture, the resulting mixture was stirred at the same temperature for 3 h before 20 ml of water was added. Then the solution was extracted three times with diethyl ether (80 ml). The combined organic layers were washed with saturated brine and dried over $MgSO_4$. The solvent was removed under reduced pressure. The crude product was further purified by column chromatography(silica gel, hexane as eluent) followed by recrystallization in ethanol to afford 1.57g of the title product as a white solid. (Global yield for the last two steps: 38.5%).

^{1}H NMR (300 MHz, $CDCl_3$): δ (ppm) 7.78 (d, 2H), 7.71 (d, 2H), 7.52 (dd, 2H), 4.05 (dd, 2H), 2.01(m, 1H), 1.34(m, 8H) 0.90(m, 6H).

^{13}C NMR (300 MHz, $CDCl_3$): δ (ppm) 141.6, 128.1, 121.6, 118.2, 90.7, 47.4, 39.0, 30.6, 28.4, 24.2, 22.9, 13.9, 10.8.

2,7-Bis(4,4,5,5-tetramethyl-1,3,2-dioxaborolan-2-yl)-N-(2-ethylhexyl)carbazole (VII)

A typical synthetic procedure for the synthesis of the carbazole derivative monomer: to a solution of N-(2-ethylhexyl)-2,7-diiodocarbazole (10.6 g, 20 mmol) in anhydrous THF (150 ml) under N_2 at -78℃, was added 37.5 ml (60mmol) of n-BuLi(1.6 M in hexane) by syringe. The mixture was stirred at -78℃ and warmed to 0℃ for 30 mins, and cooled again at -78℃, then 2-isopropoxy-4,4,5,5-tetramethyl-1,3,2-dioxaborolane (12.24 ml, 60mmol) was rapidly injected into the solution by syringe, the resulting mixture was stirred at -78.0℃ for 1 h and left to stir overnight at room temperature. The resulting mixture was poured into water and extracted with ether. The ether extracts were washed with saturated brine and dried over $MgSO_4$. The solvent was removed under reduced pressure, the crude solid product was further purified by column chromatography(silica gel, hexane:dichloromethane=2:1 as eluent) followed by recrystallization in ethanol to afford 4.5g of the title product as a white solid. (Yield 42.4%).

^{1}H NMR (300 MHz, $CDCl_3$): δ (ppm) 8.11 (d, 2H), 7.88 (s, 2H), 7.66 (d, 2H), 4.26 (m, 2H), 2.12 (m, 1H), 1.39(m, 32H), 0.90(m, 6H).

^{13}C NMR (300 MHz, $CDCl_3$): δ (ppm) 140.82, 124.91, 124.62, 119.82, 115.53, 83.64, 47.04, 39.10, 30.56, 28.40, 24.85, 24.31, 22.94, 14.01, 10.88.

General Procedure for Polymerization by Suzuki Cross-Coupling Reaction

Representative procedure for polymerization by Suzuki cross-coupling reaction: 2,7-bis(4,4,5,5-tetramethyl-1,3,2-dioxaborolan-2-yl)-N-(2-ethylhexyl)carbazole (VII) (0.2g, 0.36mmol) and 2,6-dibromopyridine (0.084g, 0.36mmol) and $(PPh_3)_4Pd(0)$ (8mg, 0.007mmol) (1 mol% based on total monomers) were dissolved in a mixture of THF and aqueous 2 M K_2CO_3(5ml) (3/2 volume ratio) in a 25 ml three-necked round-bottomed flask. The solution was stirred under N_2 and was heated at 95℃ with vigorous stirring for 48 h. The resulting mixture was then poured into 100 ml methanol. The precipitate was recovered by filtration and washed with 2 M dilute HCl and methanol respectively. The solid product was extracted with acetone for 24 h in a Soxhlet apparatus to remove oligomers and catalyst residues, 0.125g yellow-green poly[(2,7-(N-(2-ethylhexyl)carbazloyl)-alt-(2,6-pyridinyl)] (VIII) was obtained. Yield: 94%. This polymer was designated as PEHCP-26, where the number 26 stands for the linkage pattern of pyridinyl unit in the polymer backbone. The other polymers were synthesized by following a similar procedure.

Poly[(2,7-(N-(2-ethylhexyl)carbazolyl)-alt-(2,6-pyridinyl)] (PEHCP-26) (VIII) Yield: 94%, yellow-green solid. ^{1}H NMR (300 MHz, $CDCl_3$): δ (ppm), 7.86-8.32 (m, 9H, proton of pyridinyl unit and carbazolyl unit), 4.42 (m, 2H), 2.28(m, 1H), 0.83-1.50(m, 14H).

Poly[(2,7-(N-(2-ethylhexyl)carbazolyl)-alt-(3,5-pyridinyl)] (PEHCP-35) Yield: 80%, brown-yellow solid. ^{1}H NMR (300 MHz, $CDCl_3$): δ (ppm), 9.0(s,1H), 8.28(dd, 3H), 7.57-7.70(m, 5H), 4.33 (m, 2H), 2.20(m, 1H), 0.82-1.46(m, 14H).

Poly[(2,7-(N-(2-ethylhexyl)carbazolyl)-alt-(2,5-pyridinyl)] (PEHCP-25) Yield: 47%, yellow solid. ^{1}H NMR (300 MHz, $CDCl_3$): δ (ppm), 7.57-9.12(m, 9H, proton of pyridinyl unit and carbazolyl unit), 4.34(m, 2H), 2.21(m, 1H), 0.90-1.44(m, 14H).

5.3 Result and Discusion

5.3.1 Synthesis and Characterization.

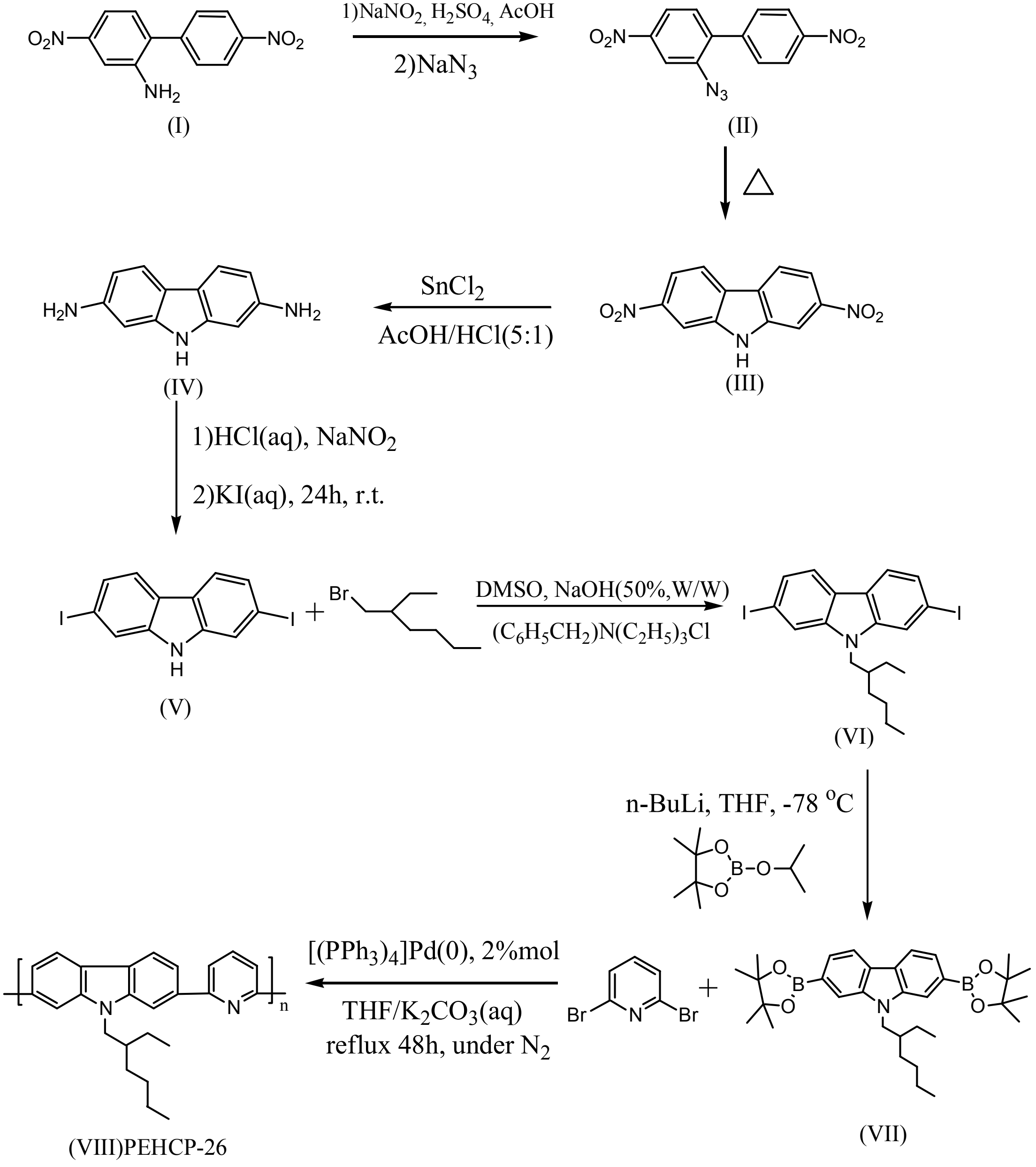

Scheme 1. Synthetic approach to the polymer PEHCP-26.

The synthetic route for the synthesis of this series of alternating copolymer is outlined in scheme 1. The compound N-(2-ethylhexyl)-2,7-diiodocarbazole (VI) was prepared from 4,4'-dinitro-2-azidobiphenyl (I) in five steps with a total yield of 18% according to reference.[8,15] The monomer compound (VII) was synthesized with a yield of 42.4% using N-(2-ethylhexyl)-2,7-diiodocarbazole (VI) as the starting material following the procedure reported in the literature.[14f,16] The polymerization is based on the Suzuki cross-coupling reaction. Poly[(2,7-(N-(2-ethylhexyl)carbazloyl)-alt-(2,5-pyridinyl)] (PEHCP-25) (VIII) was obtained in moderate yield of 47%, poly[(2,7-(N-(2-ethylhexyl)carbazloyl)-alt-(3,5-pyridinyl)](PEHCP-35) and poly[(2,7-(N-(2-ethylhexyl)carbazloyl)-alt-(2,6-pyridinyl)](PEHCP-26) were obtained in high yields of 80 and 94%, respectively. All three polymers were easily soluble in chloroform and THF. The polymerization results are summarized in Table 1.

Table 1 Properties of the Polymers

Polymers	Yield(%)	Colour	Mw[a](kDa)	PDI	DP[b]	T_d[c]	T_g[d]
PEHCP-26	94	bellow-green	4.9	1.56	14	400	145.3
PEHCP-35	80	brown-yellow	4.3	1.35	12	392	128.3
PEHCP-25	47	yellow	1.4	1.22	4	372	121.7

[a] Weight-average molecular weights determined by GPC using polystyrene standards in THF. [b] Degree of polymerization. [c] Decomposition temperature, determined by TGA in nitrogen, based on 5 % weight loss. [d] Determined by DSC in nitrogen at a scan rate of 20 °C/min.

All the polymers were characterized by ^{1}H NMR and GPC. ^{1}H NMR confirmed the proposed structures of polymers. The molecular weights of polymers were determined by GPC using THF as the eluent and polystyrene as the standard. The results of GPC are also shown in Table 1. PEHCP-26 and PEHCP-35 were found to be polymers with relatively low weight-average molecular weight (M_w) of ca. 4900 and 4300, corresponding to a polymerization degree of approximate 14 and 12, and a polydispersity index of 1.56 and 1.35, respectively. PEHCP-25 was actually an oligomer with a polymerization degree of 4.

The thermal stabilities of polymers were evaluated by thermogravimetric analyses (TGA) in nitrogen and the results are also summarized in Table 1. It is apparent that all the polymers exhibited excellent thermal stability with an onset of decomposition in the range of 370 to 400℃. Thermally induced phase transition behaviour of the polymers was investigated with differential scanning calorimetry(DSC) under nitrogen atmosphere. The glass transition temperatures (T_g) of polymers were also summarized in Table 1. T_g of the polymers was in the range of 120-150℃. The relative high glass transition temperature of fluorescent polymer is essential for its potential application, such as in PLEDs as emissive materials.[17] In all, the PEHCP series of polymers have excellent thermal stability and high T_g.

5.3.2 Optical Property.

The UV-vis absorption and fluorescence emission spectra of the polymer solution in $CHCl_3$ and the polymers films, which were spin-cast from $CHCl_3$ solutions, were recorded at room temperature. The optical data are summarized in Table 2.

Table 2. Spectra Properties and Quantum Yield

Polymers	Solution[a]			Film[b]		
	λ_{max}[c] (nm)	λ_{pl}[c] (nm)	Φ[d]	λ_{max}[c] (nm)	λ_{pl}[c] (nm)	Optical band gap(eV)
PEHCP-26	355	411,428	0.395	361	436	2.97
PEHCP-35	337	403(418)	0.458	344	431	3.02
PEHCP-25	365	420(438)	0.376	376	463(488)	2.77

[a] 1×10^{-5}M in anhydrous chloroform. [b] Spin-coating on quartz glass from anhydrous chloroform solution. [c] Wavelength of maximum absorbance or emission, wavelength of the shoulder peak is in brackets. [d] Relative to 1×10^{-5}M quinine sulphate in 0.1M H_2SO_4.

The UV-vis absorption and photoluminescence (PL) spectra of the PEHCP series of polymers solutions are depicted in Fig. 1. It is evident that the linkage pattern of the pyridinyl moiety in the polymer backbone has a major influence on the absorption maximum of polymer. The absorption maximum of PEHCP-25 with para-linkage of pyridinyl unit at 365 nm is blue-shifted in comparison with that of poly(N-octyl-2,7-carbazole)[8] and poly(pyridine-2,5-diyl) (PPy), [13] being at 380 nm and 373 nm, respectively. The absorption maximum of PEHCP-26 and PEHCP-35 with para-linkage of pyridinyl unit, being at 355 nm and 337nm, respectively is much blue-shifted in comparison with that of poly(N-octyl-2,7-carbazole) and poly(pyridine-2,5-diyl) (absorption maximums of poly(pyridine-2,6-diyl) and poly(pyridine-3,5-diyl) were unavailable). The difference among the absorption maximum of the PEHCP series of copolymers is attributed to the lesser extent of π-electron delocalization in the polymer backbone arising from meta-linkages, causing a reduction in the π-conjugation lengths. The effect of different linkage position of pyridinyl units on the absorption maximum of polymer is similar to that one in our previous report.[14a,f,g]

The photoluminescence (PL) spectra, which were attributed to fluorescence on account of the short lifetime of the excited state, [18] were obtained by irradiative excitation at the wavelength of the absorption maximum. PEHCP-25 produce very strong blue fluorescence with emission maximum at 420nm and a small shoulder peak at 438 nm. For PEHCP-26 and PEHCP-35, they produce very strong blue fluorescence which is slightly violet-shifted, with emission maximum at 411 and 428 nm, 403 and 418 nm respectively. The emission maximum of PEHCP-25 with para-linkage of pyridinyl unit in the polymer backbone is almost equivalent with that of poly(N-octyl-2,7-carbazole),[8] while copolymers with meta-linkage of pyridinyl unit in the polymer backbone is violet-shifted as compared to that of poly(N-octyl-2,7-carbazole).[8]

The photoluminescence quantum yields in chloroform solution were measured according to the method described by Davey et al.[19] relative to 10^{-5} M quinine sulphate in 0.1 M H_2SO_4. The results are summarized in Table 2. High quantum yields of all the polymers are obtained, being in the range of 35-50%.

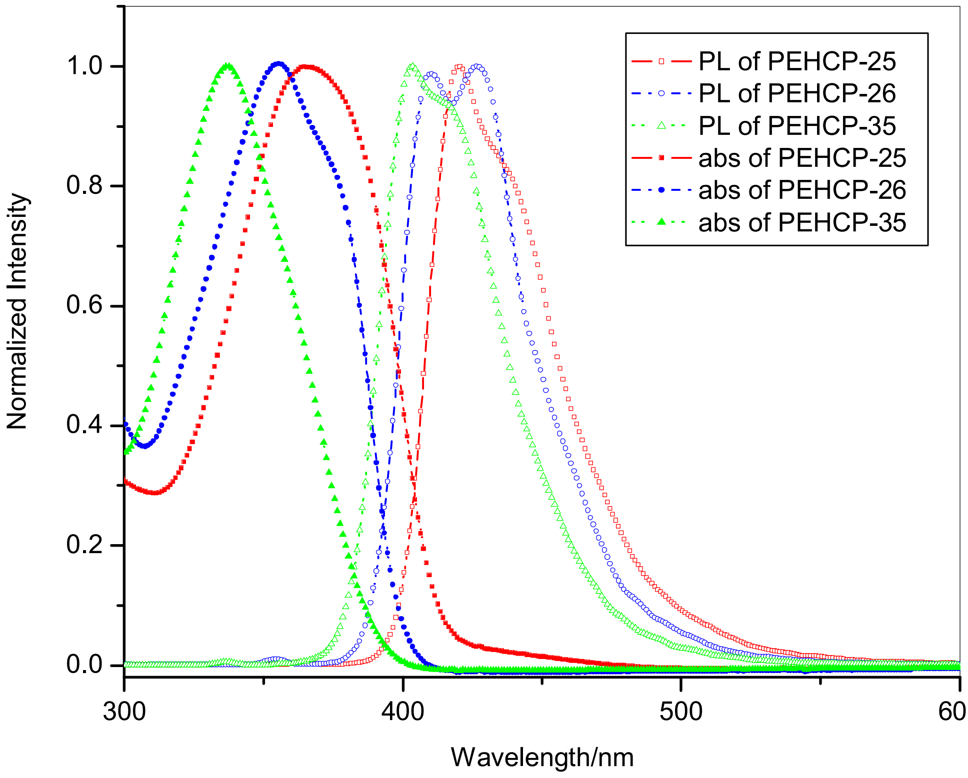

Figure 1. UV-Vis absorption (abs) and photoluminescence (PL) spectra of PEHCP series polymers in $CHCl_3$ solution.

Fig. 2 shows the UV-vis absorption and photoluminescence (PL) spectra of the PEHCP series of polymers in thin films. As compared to the poly(N-octyl-2,7-carbazole),[8] this series of pyridinyl containing copolymer show blue-shifted absorption maxima. For PEHCP-25, in which the pyridinyl unit is para-linked in the polymer main chain, its absorption maximum in film at 376 nm is red-shifted in comparison with the absorption maxima (at 361 nm and 344 nm, respectively) of PEHCP-26 and PEHCP-35 with meta-linkages of the pyridinyl units. This is attributed to the lower extent of π-electron delocalization of the polymer main chain arising from meta-linkages of the pyridinyl moiety, resulting in a reduction in the π-conjugation length.

In the film state, the blue emission peaks appear at 436, 431 and 463(488, shoulder peak) nm for PEHCP-26, PEHCP-35 and PEHCP-25, respectively. The PL of PEHCP-35 and PEHCP-26 showed that the two polymers can emit purer blue light without tailing phenomena and additional red-shifted peak in the long wavelength region of the spectrum (such as 453nm, 492nm for poly(N-octyl-2,7-carbazole), 500-520 nm for poly(N-octyl-3,6-carbazole), 488 nm for PEHCP-25) as compared with poly(N-octyl-2,7-carbazole),[8] poly(N-octyl-3,6-carbazole)[7a] and PEHCP-25. Therefore, PEHCP-35 and PEHCP-26 can emit purer blue light without any evidence of π-aggregates/excimers in the solid state as compared to the PL of poly(N-octyl-2,7-carbazole). The results of PL in film states also show that optical properties of carbazole polymers can be well tuned by properly rational design of polymer architectures, such as the incorporation of different pyridinyl moieties into polymer backbone.

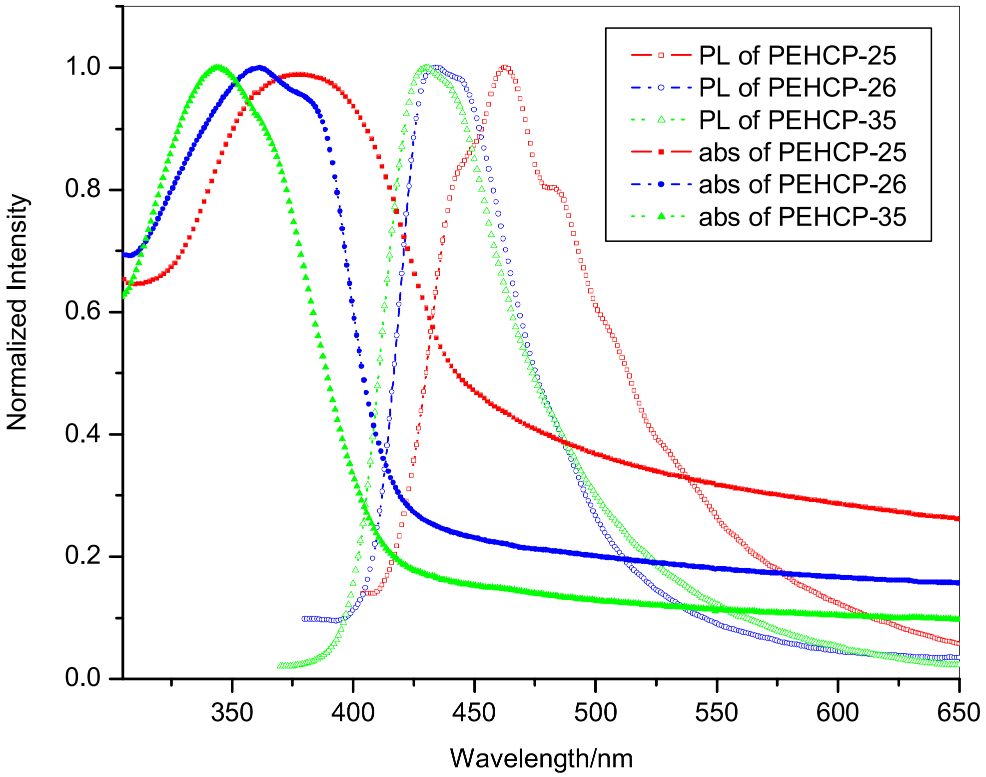

Figure 2. UV-Vis absorption (abs) and photoluminescence (PL) spectra of PEHCP series polymers in thin films.

5.3.3 Electrochemical Property.

The electrochemical behavior of the polymers was investigated by cyclic voltammetry(CV). CV was performed in a solution of Bu_4NClO_4(0.10M) in acetonitrile at a scan rate of 50mV/s at room temperature under the protection of nitrogen. A platinum electrode coated with a thin polymer film was used as the working electrode. A Pt wire was used as the counter electrode and an Ag/$AgNO_3$(0.01M) electrode was used as the reference electrode. The resulting cyclic voltammograms are outlined in figure 3.

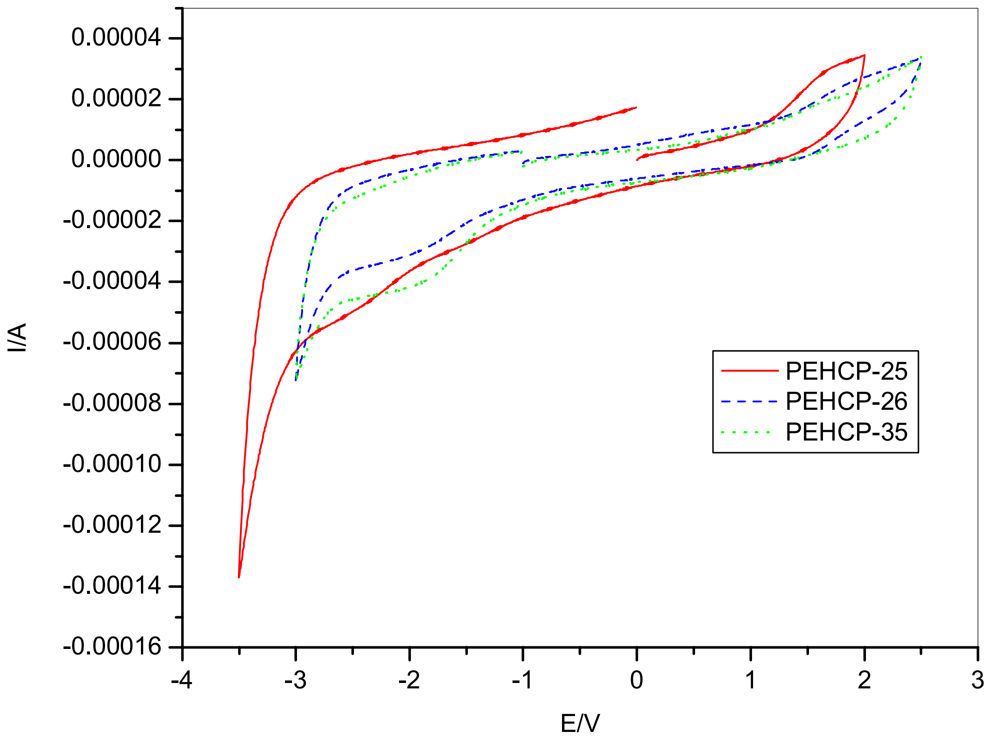

Figure 3. The cyclic voltammograms of PEHCP series polymer films coated on platinum plate electrodes in acetonitrile containing 0.1 M Bu_4NClO_4.

The onset potentials for oxidation were observed to be 2.09, 2.01 and 1.86V for PEHCP-26, PEHCP-35, PEHCP-25, respectively. On the other hand, the onset potentials for reduction were -0.72, -0.55 and -1.26, respectively. From the onset potentials of the oxidation and reduction processes, the band gaps of the polymers were estimated to be 2.81, 2.56 and 3.12eV for PEHCP-26, PEHCP-35, PEHCP-25, respectively. According to the equations [20,21] IP = $-([E_{onset}]^{ox}+4.44)$ eV and EA = $-([E_{onset}]^{red}+4.44)$ eV, where $[E_{onset}]^{ox}$ and $[E_{onset}]^{red}$ are the onset potentials for the oxidation and reduction of the polymers, the HOMO and LUMO of the polymers were estimated to be -6.49, -6.41 and

-6.26eV and -3.68, -3.85 and -3.14eV for PEHCP-26, PEHCP-35, PEHCP-25, respectively. The corresponding electrochemical data of the polymers are summarized in Table 3. The HOMO and LUMO of this series of polymers are much lower than those of polymers derived from carbozole and benzothiadiazole, the HOMO and LUMO of the latter were in the range of -5.25 – -5.40 and -2.00 - -3.12, respectively.[7a]

Table 3 Electrochemical Properties of the Polymers

polymer	E_{onset}(V) (p-doping)	E_{onset}(V) (n-doping)	Energy levels(eV)		
			HOMO	LUMO	Band gap
PEHCP-26	2.09	-0.72	-6.49	-3.68	2.81
PEHCP-35	2.01	-0.55	-6.41	-3.85	2.56
PEHCP-25	1.86	-1.26	-6.26	-3.14	3.12

From table 3, we can see that these polymers with pyridine units possess very low LUMO energy levels for an easy electron injection from a cathode, which is consistent with our expectation. We can also find that the HOMO and LUMO energy levels of PEHCP-26 and PEHCP-35 are quite similar. As for PEHCP-25, its HOMO is close to the other two polymers while the LUMO is much higher. Therefore, the different linkage position of pyridinyl units in the copolymer backbone will affect the energy levels of the polymers.

5.4 Conclusion

In summary, a novel series of well-defined carbazole-pyridine-based alternating copolymers have been synthesized by Suzuki cross-coupling reaction in good to high yields. These polymers have relatively low molecular weight and have good solubility in common solvents, such as chloroform and THF. All the polymers show good thermal stability and have relatively high T_g. The different linkage position of pyridinyl unit in the polymer backbone has significant effects on the electronic and optical properties of polymers in solution and in film phases. Meta-linkage(3,5-and 2,6-linkage) of pyridinyl units in the polymer backbone is more favourable to polymer for pure blue emission and prevention of aggregation of polymer chain than para-linkage(2,5-linkage) of the pyridinyl units. The result shows that the electronic and optical properties of the polymers are consistent with a rigid-rod conjugated backbone structure. These polymers with pyridine units possess very low LUMO energy levels for an easy electron injection from a cathode. It also shows that the electronic and optical properties of fluorescent polymers can be well tuned by properly rationalized design of polymer architectures such as the incorporation of different pyridinyl moieties into polycarbazole backbone.

References

(1) Burroughes, J. H.; Bradley, D. D. C.; Brown, A. R.; Marks, R. N.; Mackay, K.; Friend, R. H.; Burn, P. L.; Holmes, A. B. *Nature (London)* **1990**, *347*, 539.

(2) D. Braun, A. J. Heeger, *Appl. Phys. Lett*. **1991**,*58*, 1982

(3) Kraft, A.; Grimsdale, A. C.; Holmes, A. B. *Angew. Chem., Int. Ed.* **1998**, *37*, 402.

(4) Segura, J. L. *Acta Polym.* **1998**, *49*, 319.

(5) Friend, R. H.; Gymer, R. W.; Holmes, A. B.; Burroughes, J. H.; Marks, R. N.; Taliani, C.; Bradley, D. A.; Santos, D.; Bre´das, J. L.; Lo¨gdlund, M.; Salaneck, W. R. *Nature* **1999**, *397*, 121.

(6) Chuanjun Xia and Rigoberto C. Advincula, *Macromolecules* **2001,** *34,* 5854.

(7) (a) Jian Huang, Yuhua Niu, Wei Yang, Yueqi Mo,Ming Yuan, and Yong Cao, *Macromolecules* **2002,** *35,* 6080; (b). Lee J. H., Park J. W., Ko J. M., Chang Y. H., *Polym. Bull.* **1993**, 31, 339. (c). Justin Thomas K. R., Lin Jiann T., *J. Am. Chem. Soc.* 2001, 123, 9404. (d). Lee J. H., Park J. W., Choi S. K., *Synth. Met*., **1997**, 88, 31. (e). Meng H., Chen Z. K. *J. Phys. Chem. B*, **1999**, 103, 6429. (f). Chao C. S., Whang W. T., *Macromo. Chem. Phys*., **2001**, 202, 2864.

(8) Jean-Francüois Morin and Mario Leclerc**,** *Macromolecules* **2001,** *34,* 4680.

(9) (a). S. Dailey, M. Halim, E. Rebourt, L. E. Horsburgh, I. D. W. Samuel, A. P. Monkman, *J. Phys. Condens. Matter* 10 (**1998**) 5171; (b). D. D. Gebler, Y. Z. Zhang, J. W. Blatchford, S. W. Jessen, L. B. Lin, T. L. Gustafston, H. L. Wang, T. M. Swager, A. G. Macdiarmid, A. J. Epstein, *J. Appl. Phys*. 78 (**1995**) 4264; (c). Feller, A. P. Monkman, *Synthetic Metals* 116 (**2001**) 149-152; (d). Takakazu Yamamoto, Tsukasa Maruyama, Zhen-hua Zhuo, Takayori Ito, Takashi Fukuda, Yutaka Yoneda, Farida Begum, Tomiki

Ikeda, Shintaro Sasaki, Hideo Takezoe, Atsuo Fukuda and Kenji Kubota, *J. Am. Chem. Soc.*, **1994**, 116, 4832; (e). Takakazu Yamamoto, Zhen-hua Zhuo, Takaki Kanbara, Masaki Shimura, Kenichi Kizu, Tsukasa Maruyama, Yoshiyuki Nakamura, Takashi Fukuda, Bang-Lin Lee, Naoki Ooba, Satoru Tomaru, Takashi Kurihara, Toshikuni Kaino, Kenji Kubota, and Shintaro Sasaki, *J. Am. Chem. Soc.*, **1996**, 118, 10389; (f). L. E. Horsburgh, A. P. Monkman, I. D. W. Samuel, *Synth. Met.* **1999**, 101, 113.

(10)T. Yamamoto, H. Suganuma, Y. Saitoh, T. Maruyama, T. Inoue, *Jpn. J. Appl. Phys.*, **1996**, *35*, L1142

(11) T. Kanbara, T. Kushida, N. Saito, I. Kuwajima, K. Kubota, T. Yamamoto, *Chem. Letter.*, **1999**, 583.

(12)Y. Z. Wang, D. D. Gebler, D. K. Fu, T. M. Swager, A. G. Macdiarmid, A. J. Epstein, *Synth. Met.*, **1997**, *85*, 1179.

(13) (a). M. J. Marsella, D. K. Fu and T. M. Swager, *Adv. Mater.*, **1995**, 7, 145. (b) Jai Kyeong Kim, Jae Woong Yu, Jae Min Hong, Hyun Nam Cho, Dong Young Kim and Chung Yup Kim, *J. Mater. Chem.*, **1999**, 9, 2171.

(14) (a). S. C. Ng, H. F. Lu, H. S. O. Chan, A. Fujii, K. Yoshino, *Adv. Mater.*, **2000**, 12(15), 1122. (b): Fujii, A., R Ootake, T Fujisawa, M Ozaki, Y Ohmori, T Laga, K Yoshino, H. F. Lu, H. S. O. Chan, and S. C. Ng, *Appl. Phys. Lett.*, **2000**, 77(5) 660. (c): S. C. Ng, H. F. Lu, H. S. O. Chan, A. Fujii, L. G. Tong, K. Yoshino, *Macromoleclues*, **2001**, *34*, 6895. (d): R Ootake, T. Fujisawa, T. Sonoda, A. Fujii, T Laga, H. F. Lu, H. S. O. Chan, and S. C. Ng, K. Yoshino, *Synth. Met.* **2001**, 119, 593. (e): Lu H. F., H. S. O. Chan and S. C. Ng, *Macromolecules*, **2003**, 36(5), 1543. (f): Shouping Liu, S. C. Ng, Hardy S. O. Chan, *Journal of Polymer Science, Part A: Polymer Chemistry*, 2004, 42,

4792-4801. (g): Shouping Liu, S. C. Ng, Hardy S. O. Chan, *Synth. Met*, 2005, 129(1) (In Press).

(15)(a)Jianfu Ding, Michael Day, Gilles Robertson, and Jacques Roovers, *Macromolecules*, 2002, *35*, 3474-3483 (b)Xia, C. J.; Advincula, R. C., *Macromolecules*, 2001, *34*, 5854.

(16) Maxime Ranger, Dany Rondeau, and Mario leclere*, Macromolecules, **1997,** 30, 7686

(17) Tokito S., Tanaka H, Noda K., Okada A., Taga Y., *Appl. Phys. Lett.*, **1997**, 70, 1929.

(18) T. M. Swager, C. G. Gil, M. S. Wrightton, *J. Phys. Chem.*, **1995**, *99*, 4886.

(19) A. P. Davey, S. Elliott, O. O'Connor, W. J. Blau, *Chem. Soc., Chem. Commun*. **1995**, 1433.

(20) de Leeuw, D. M.; Simenon, M. M. J.; Brown, A. R.; Einerhand, R. E. F. *Synth. Met.* **1997**,87,53.

(21) Cervini, R.; Li, X. C.; Spencer, G. W. C.; Holmes, A. B.; Moratti, S. C.; Friend, R. H. *Synth. Met.* **1997**, 84, 359.

Appendix NMR spectrums of intermediate compounds, monomers and polymers

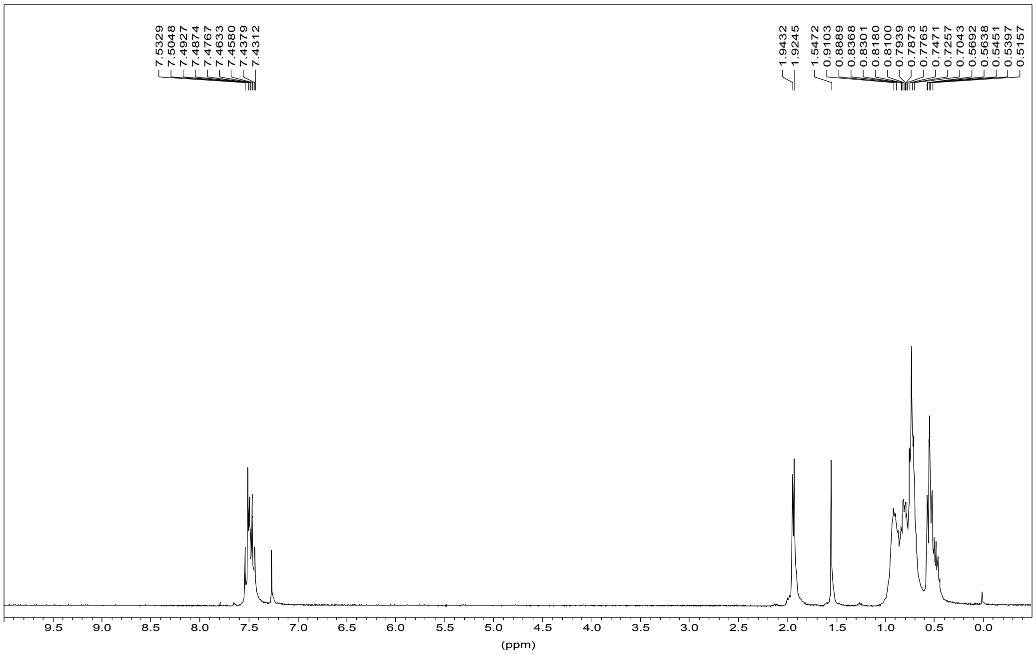

(1) 2,7-Dibromo-9,9-bis(2-ethylhexyl)fluorene

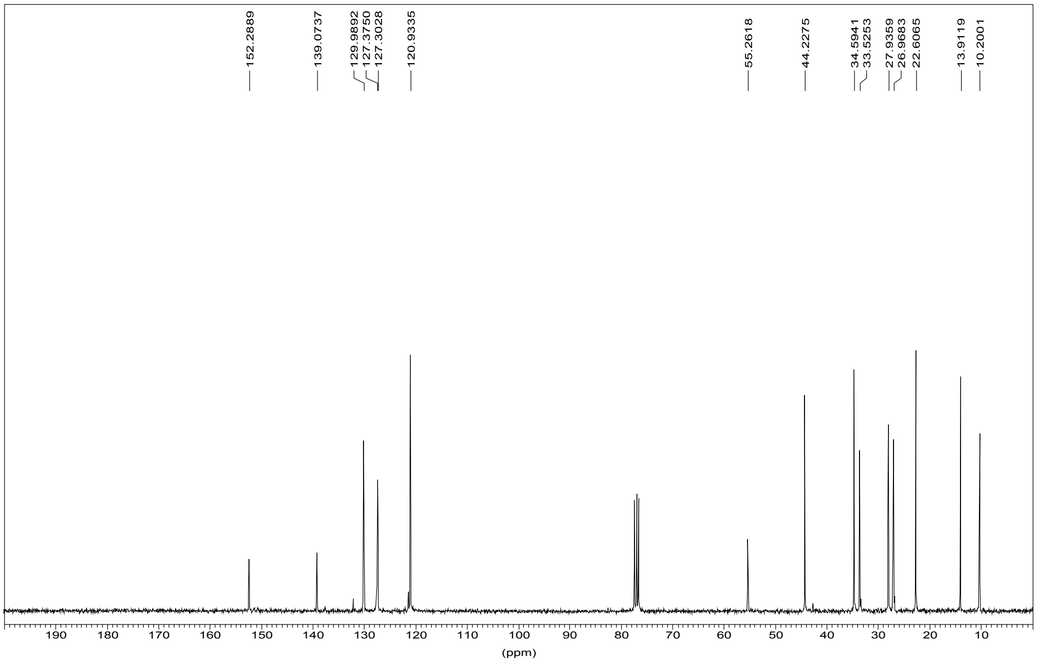

(1) 2,7-Dibromo-9,9-bis(2-ethylhexyl)fluorene

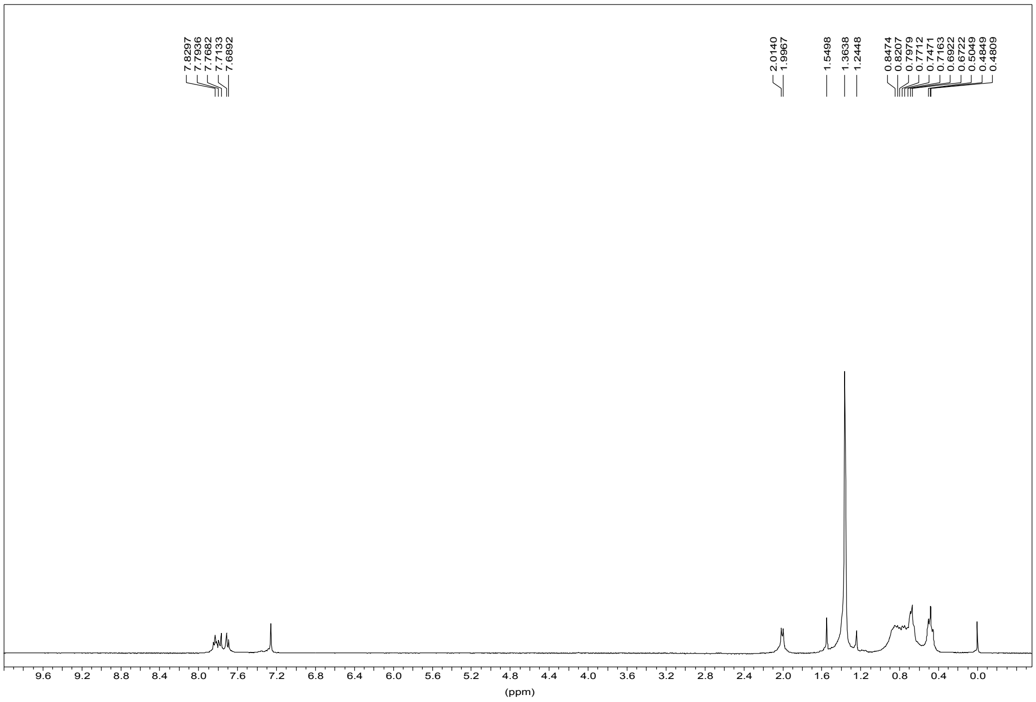

(2) 2,7-Bis(4,4,5,5-tetramethyl-1,3,2-dioxaborolan-2-yl)-9,9-bis(2-ethylhexyl)fluorene

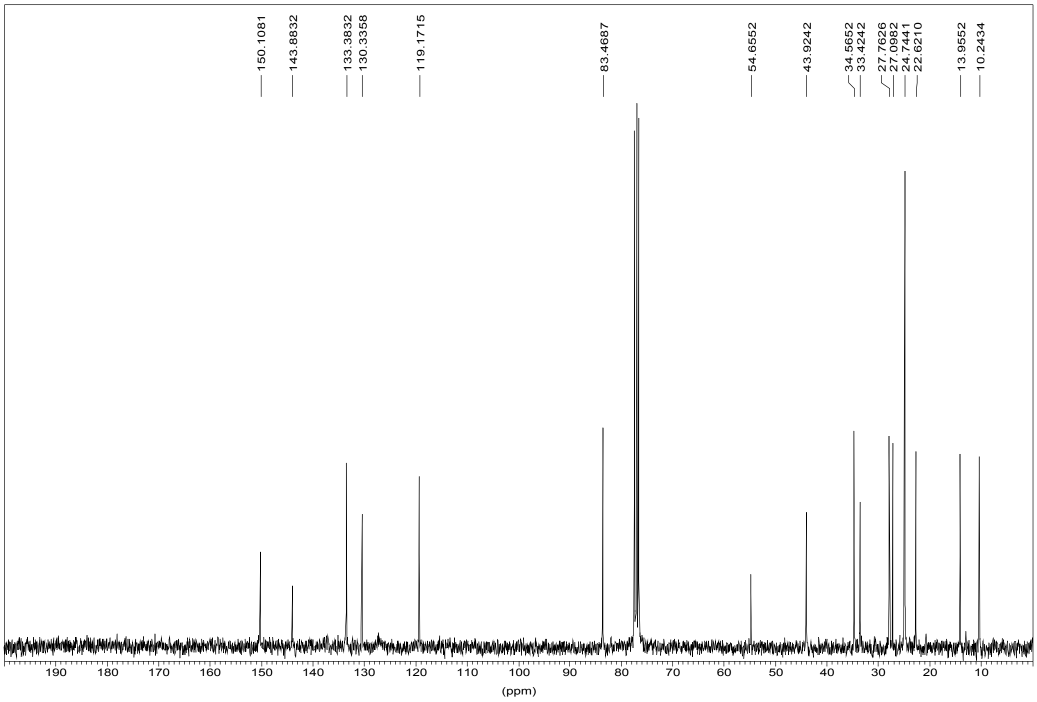

(2) 2,7-Bis(4,4,5,5-tetramethyl-1,3,2-dioxaborolan-2-yl)-9,9-bis(2-ethylhexyl)fluorene

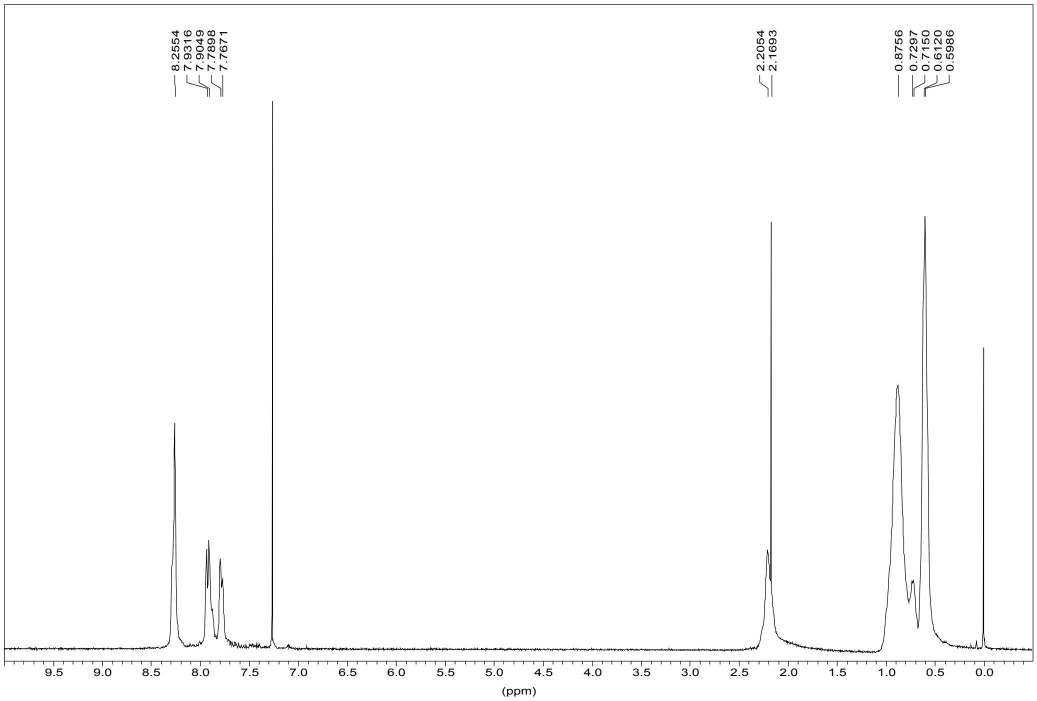

(3) Poly[2,7-(9,9-bis(2-ethylhexyl)fluorenyl)-alt-(2,6-pyridinyl)](PDEHFP-26)

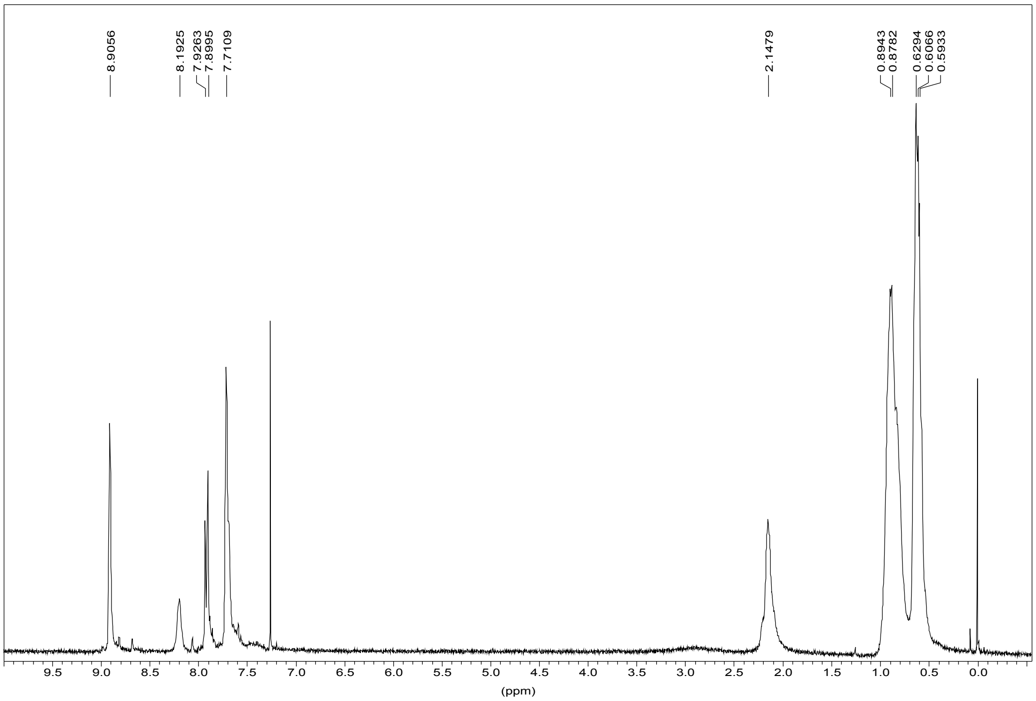

(4) Poly[2,7-(9,9-bis(2-ethylhexyl)fluorenyl)-alt-(3,5-pyridinyl)] (PDEHFP-35)

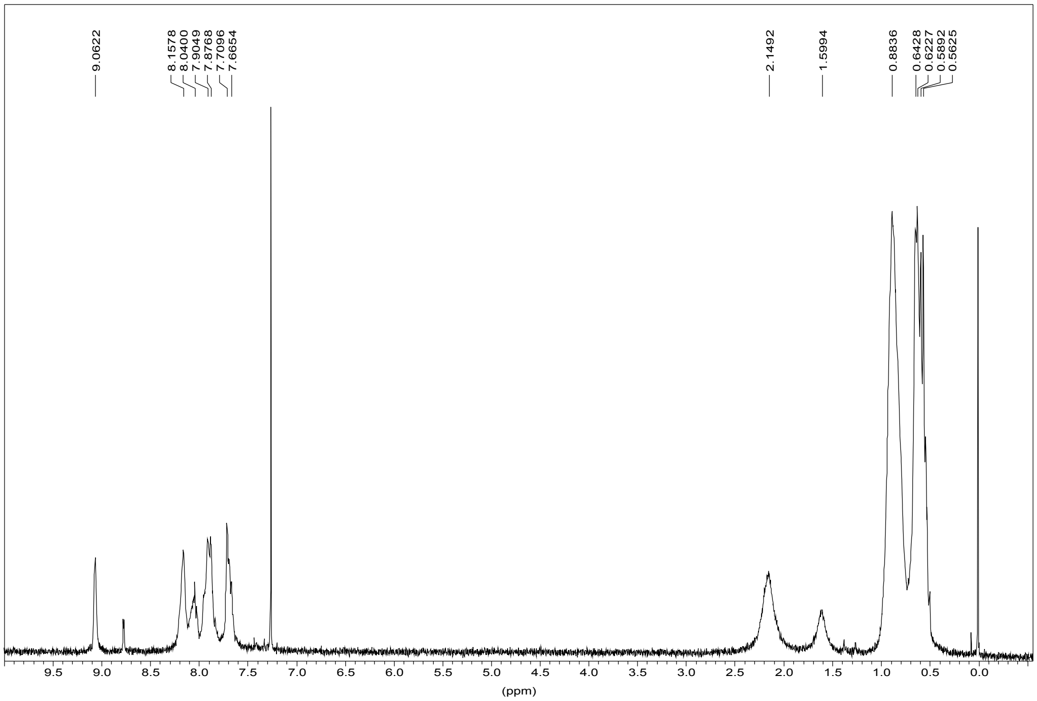

(5) Poly[2,7-(9,9-bis(2-ethylhexyl)fluorenyl)-alt-(2,5-pyridinyl)] (PDEHFP-25)

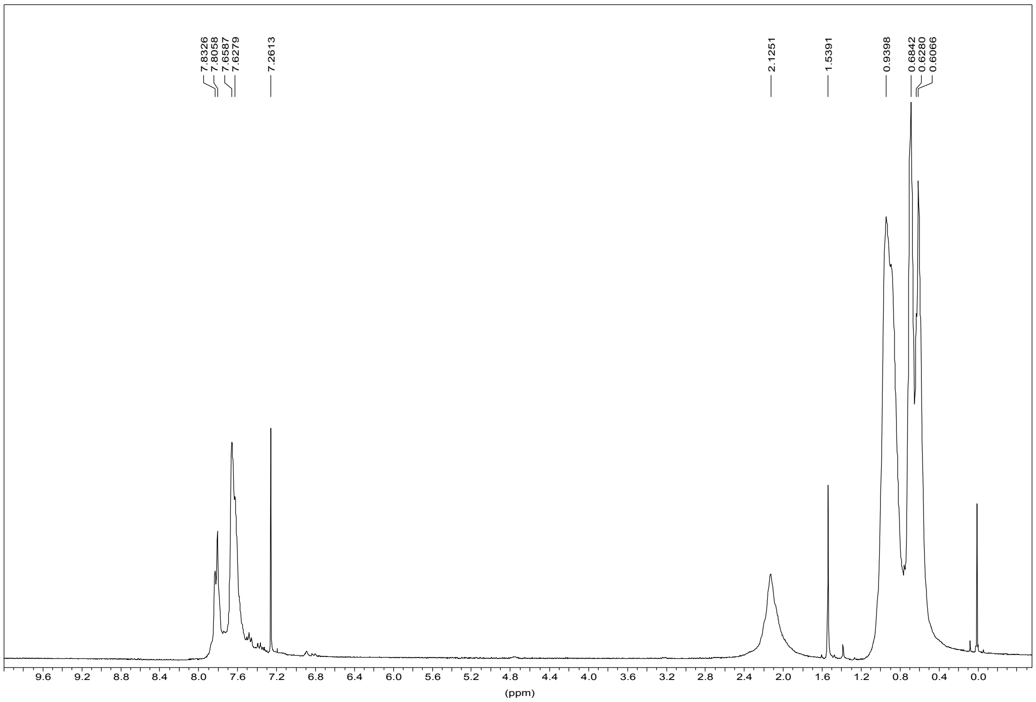

(6) Poly[2,7-(9,9-bis(2-ethylhexyl)fluorenyl)] (PDEHF)

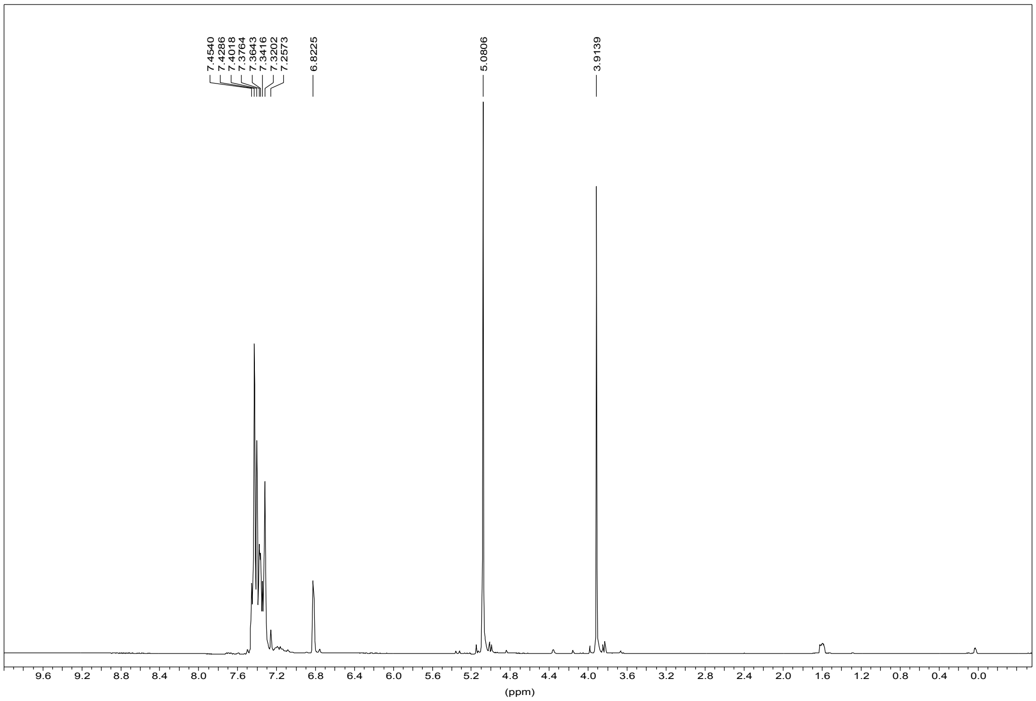

(7) Methyl--α-resorcylate dibenzyl ether

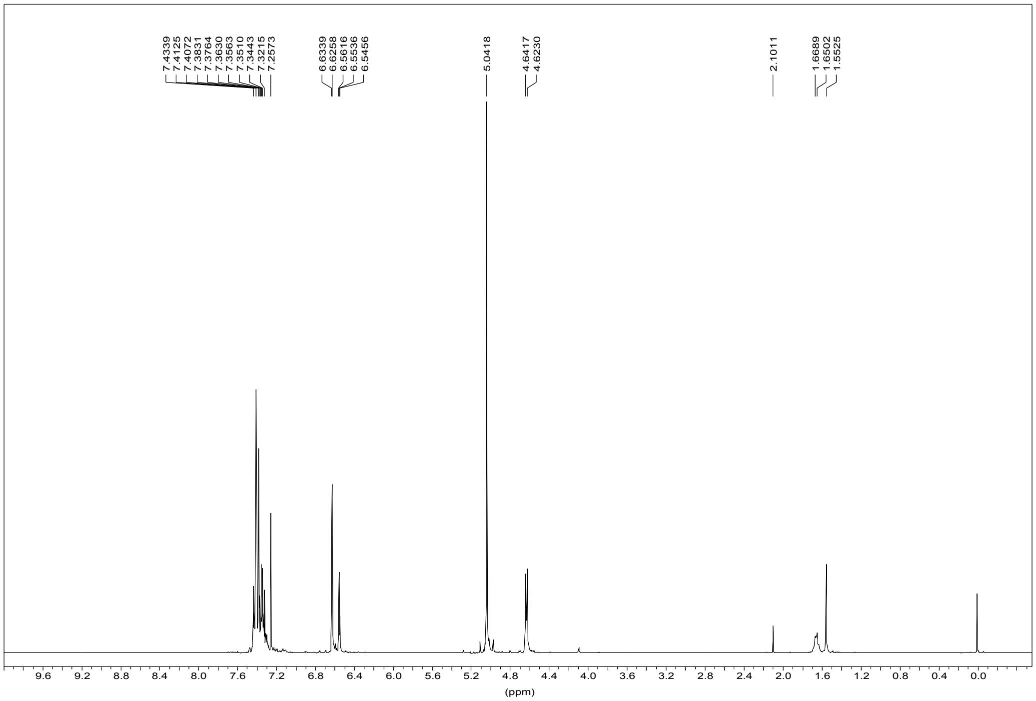

(8) 3,5-Dibenzyloxybenzyl alcohol ([G-1]-OH)

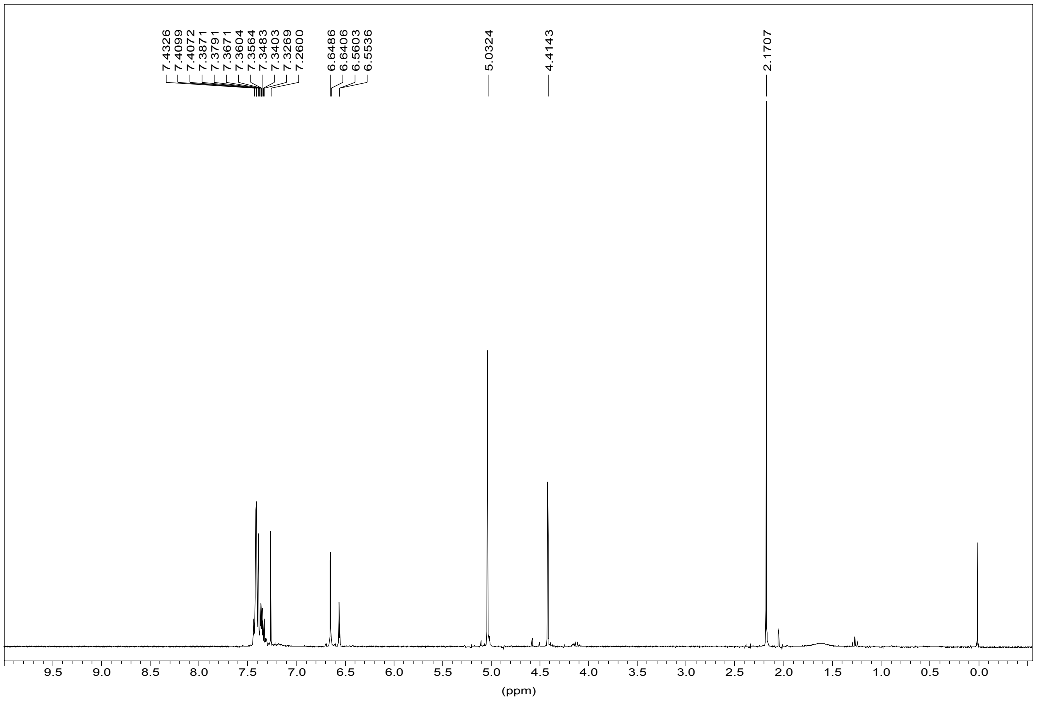

(9) 3,5-Dibenzyloxybenzyl Bromide ([G-1]-Br

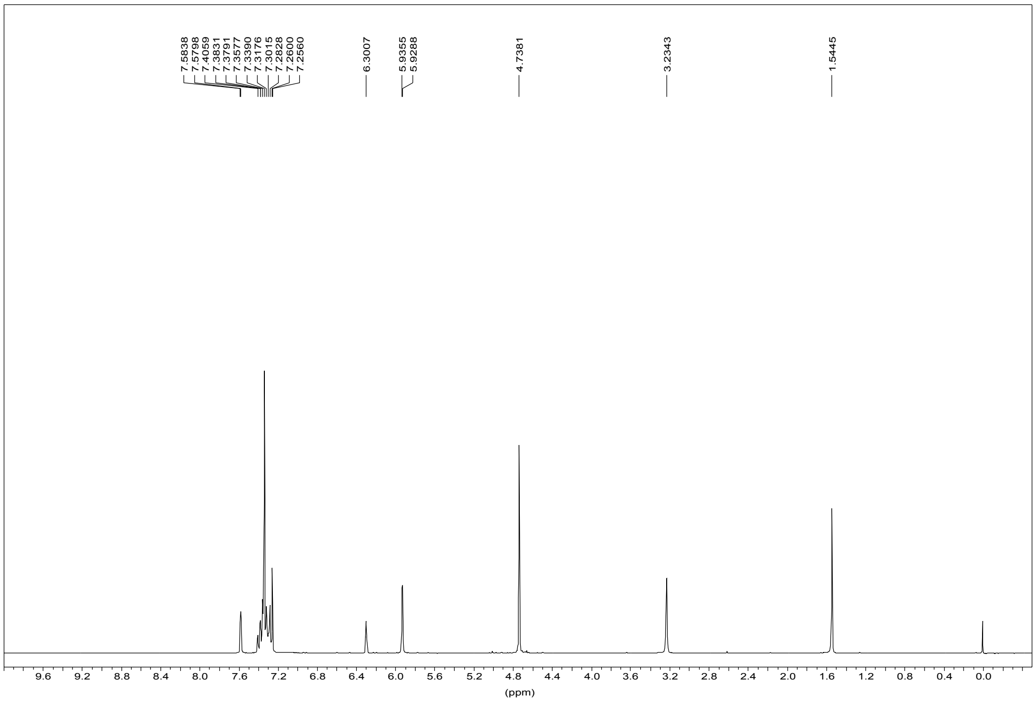

(10) 9,9-Bis[3,5-bis(benzyloxy)benzyl]-2,7-dibromofluorene

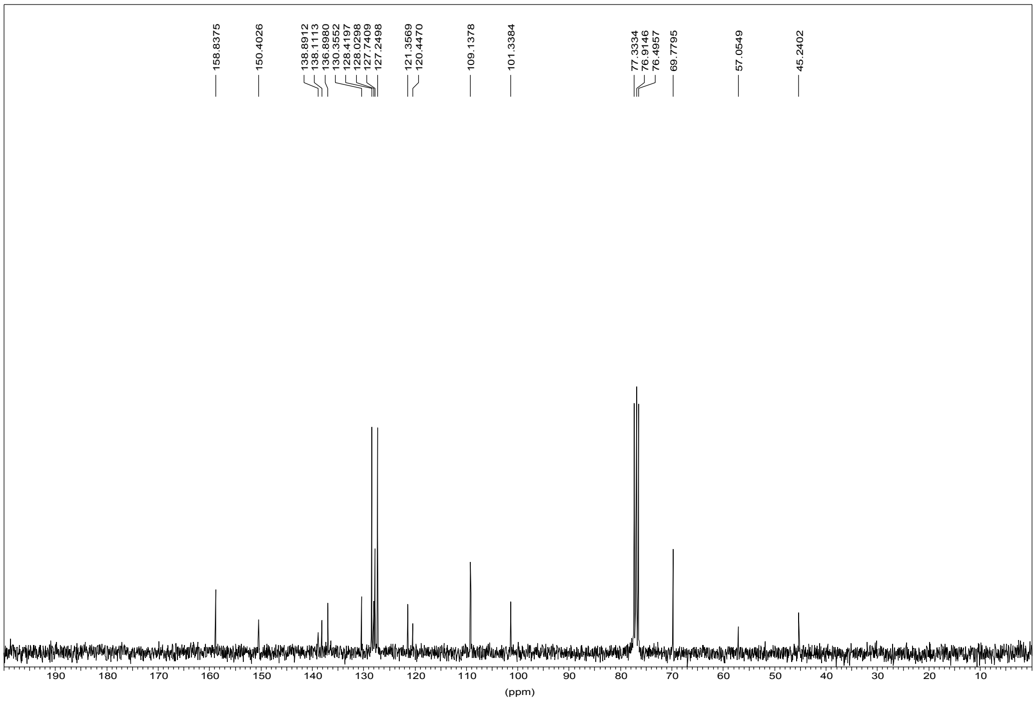

(10) 9,9-Bis[3,5-bis(benzyloxy)benzyl]-2,7-dibromofluorene

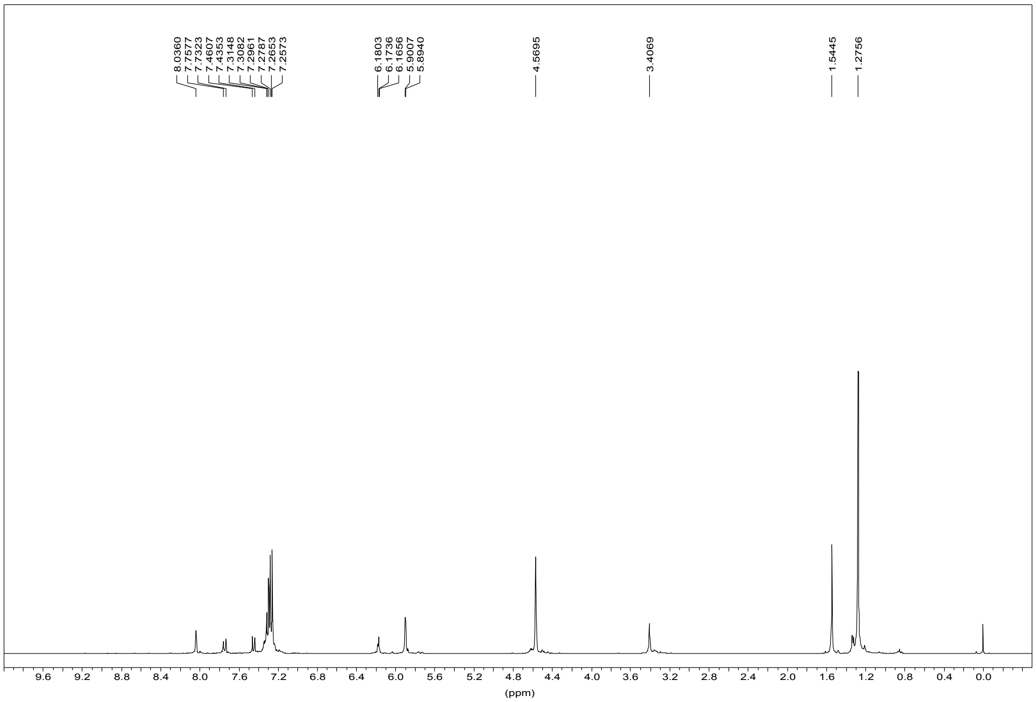

(11)2,7-Bis(4,4,5,5-tetramethyl-1,3,2-dioxaborolan-2-yl)-9,9-Bis[3,5-bis(benzyloxy)benzyl]fluorene

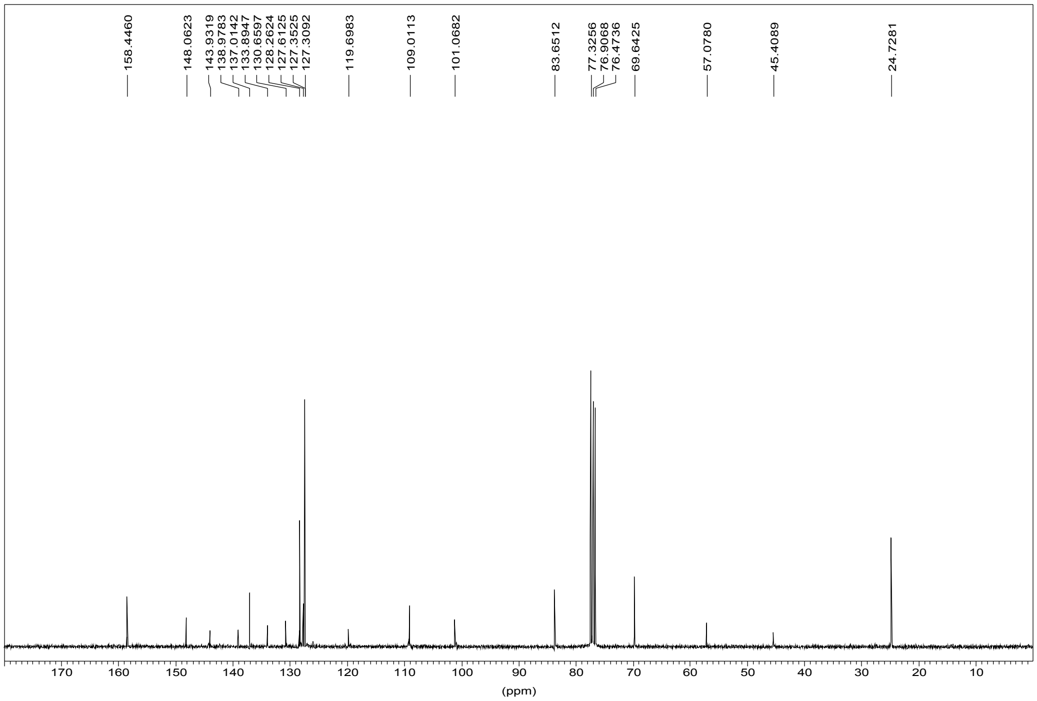

(11)2,7-Bis(4,4,5,5-tetramethyl-1,3,2-dioxaborolan-2-yl)-9,9-Bis[3,5-bis(benzyloxy)benzyl]fluorene

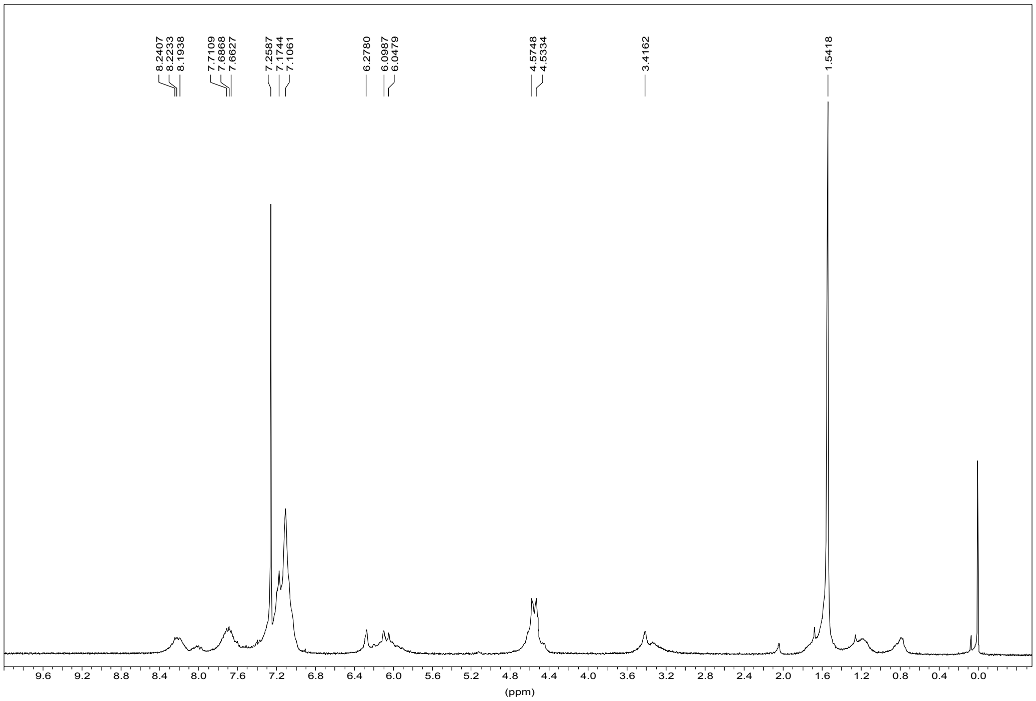

(12)Poly[2,7-(9,9-bis[3,5-bis(benzyloxy)benzyl])fluorenyl-alt-(2,6-pyridinyl)]

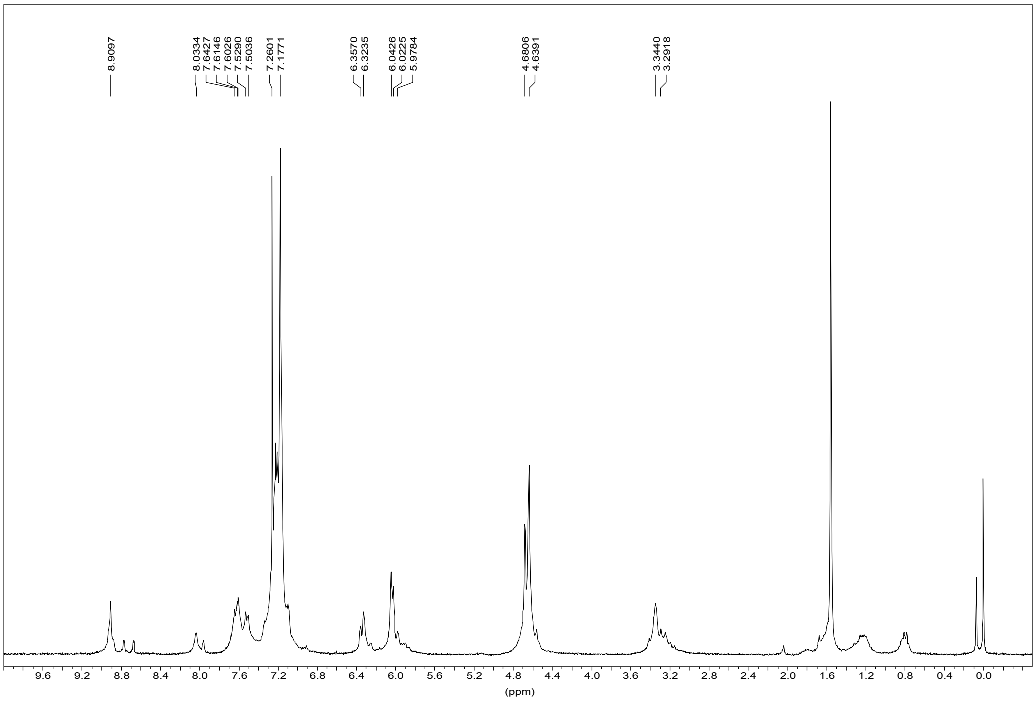

(13) Poly[2,7-(9,9-bis[3,5-bis(benzyloxy)benzyl])fluorenyl-alt-(3,5-pyridinyl)]

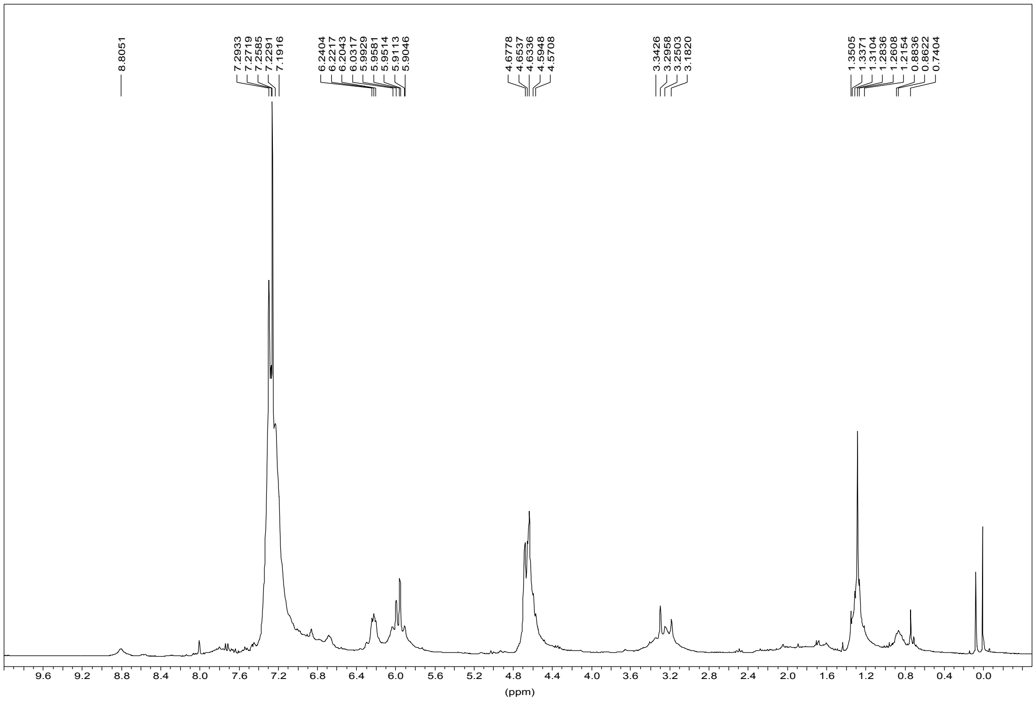

(14) Poly[2,7-(9,9-bis[3,5-bis(benzyloxy)benzyl])fluorenyl-alt-(2,5-pyridinyl)]

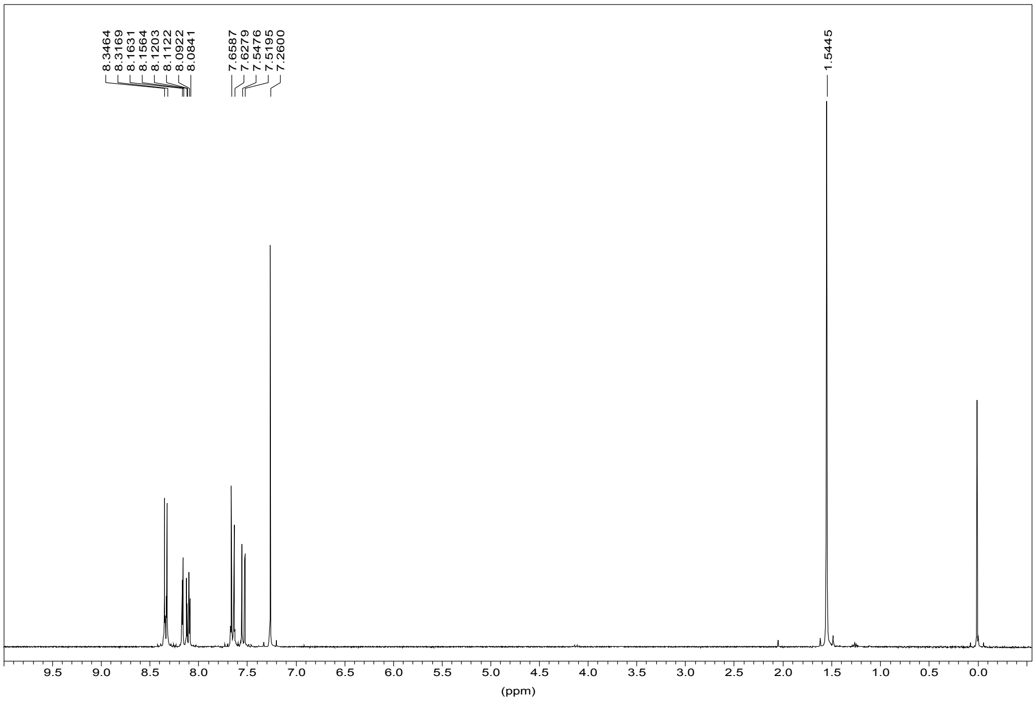

(15) 4,4'-Dinitro-2-azidobiphenyl

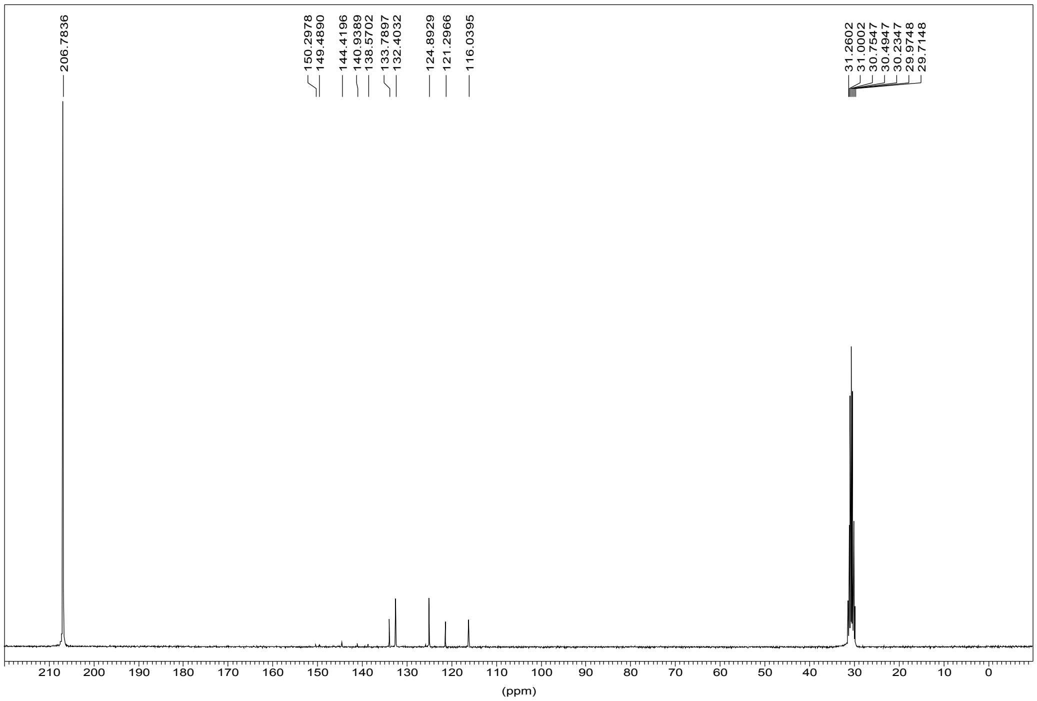

(15) 4,4'-Dinitro-2-azidobiphenyl

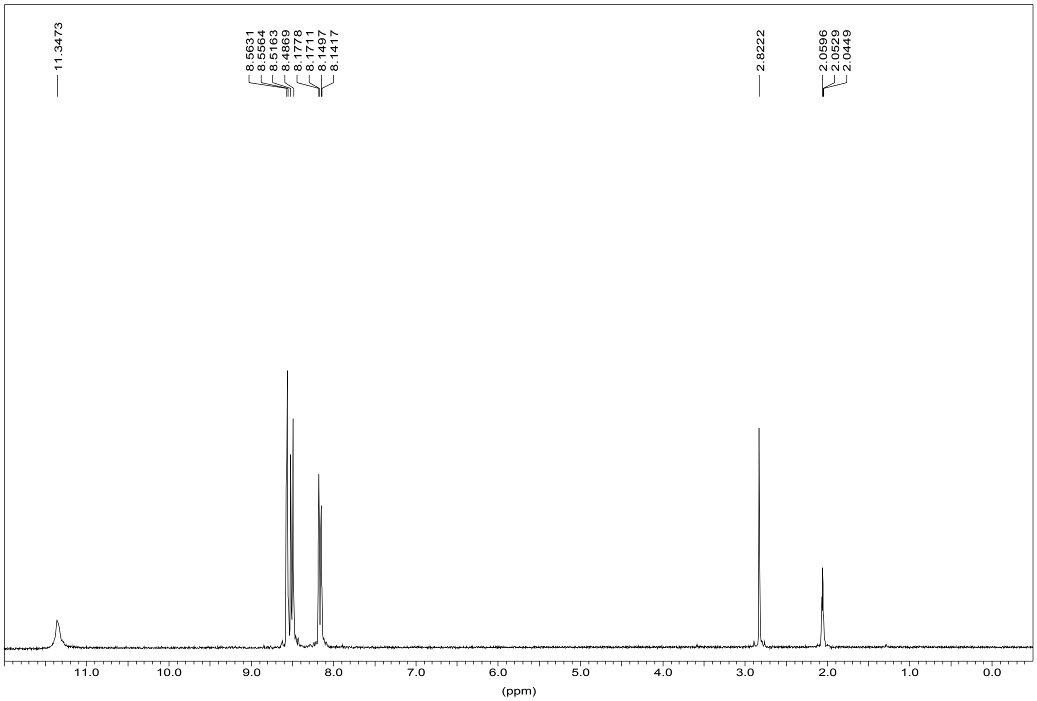

(16) 2,7-Dinitrocarbazole

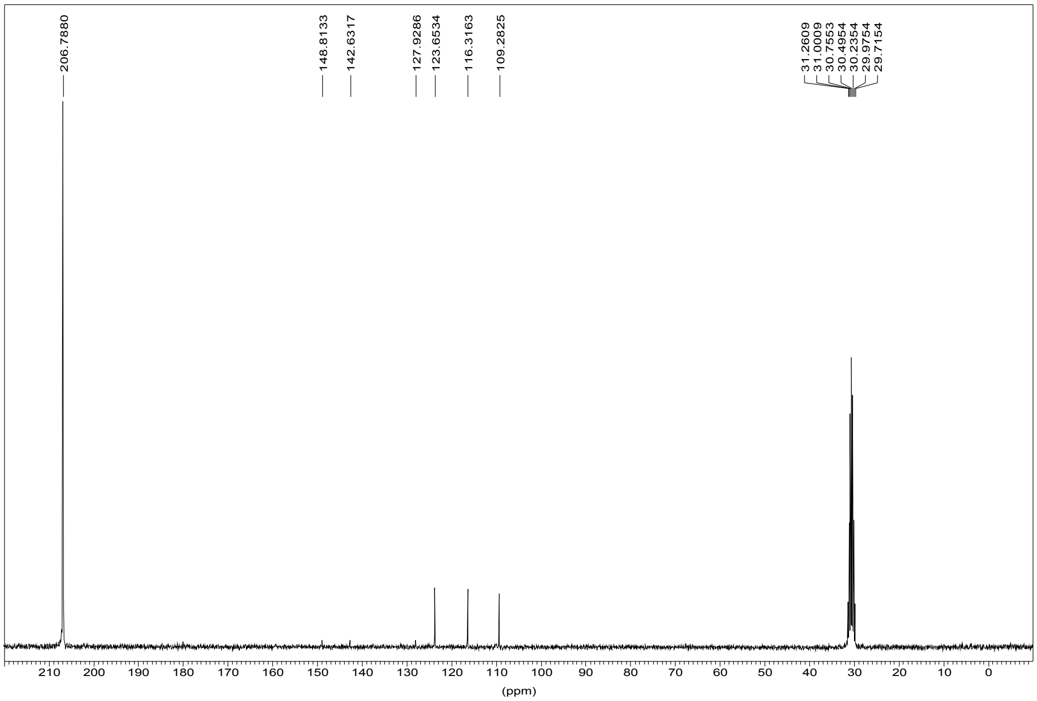

(16) 2,7-Dinitrocarbazole

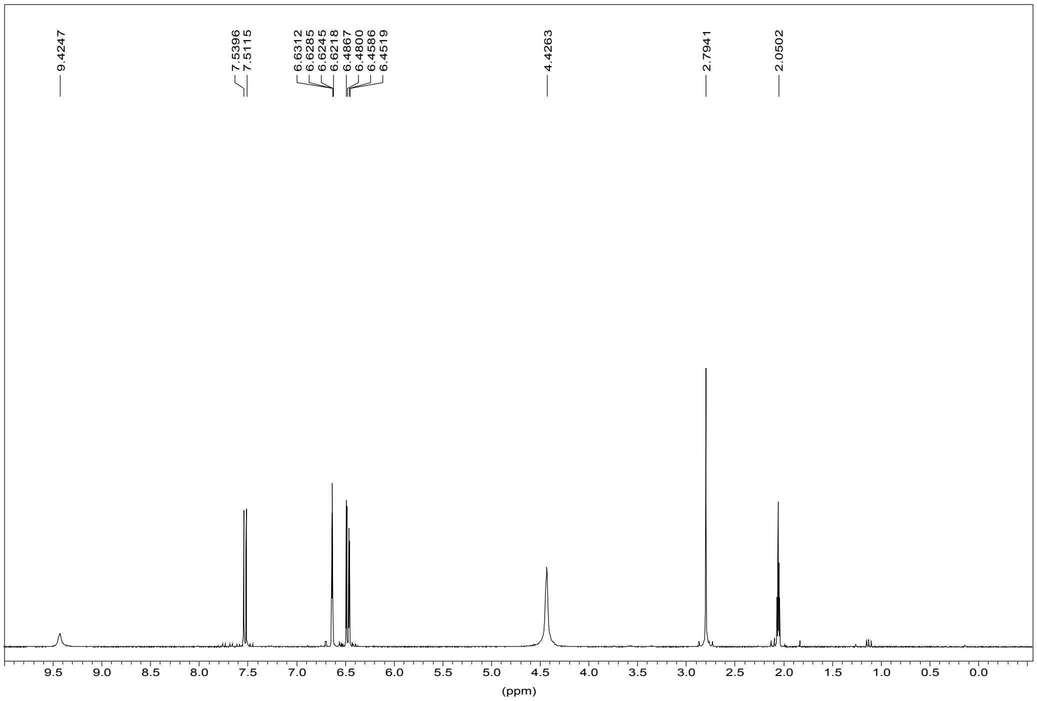

(17) 2,7-Diaminocarbazole

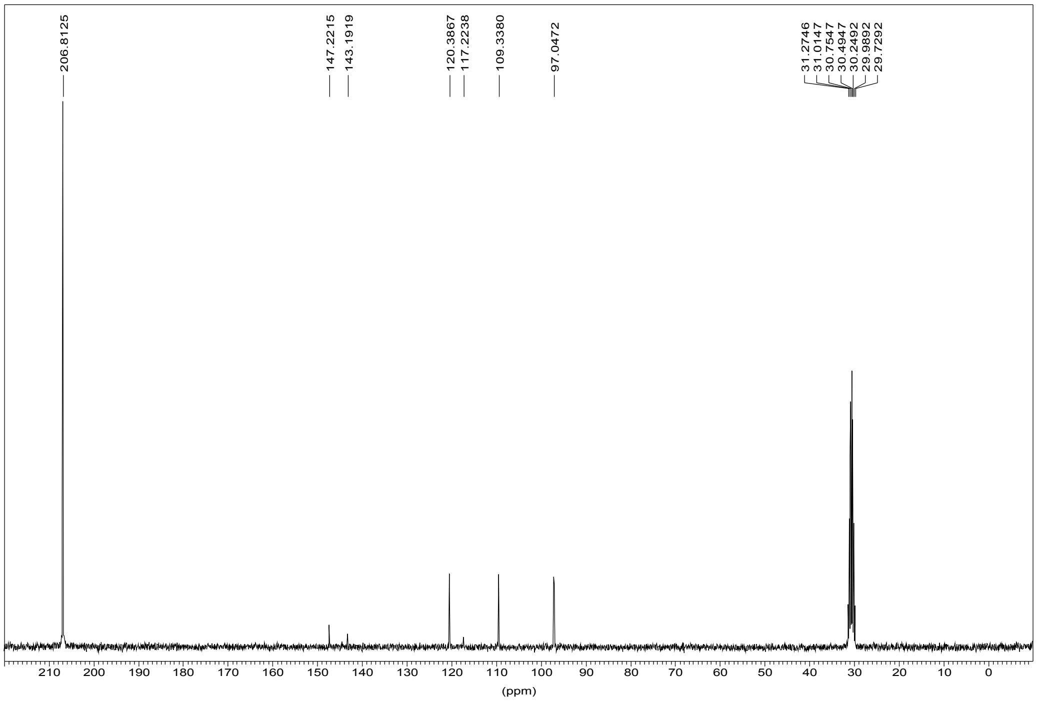

(17) 2,7-Diaminocarbazole

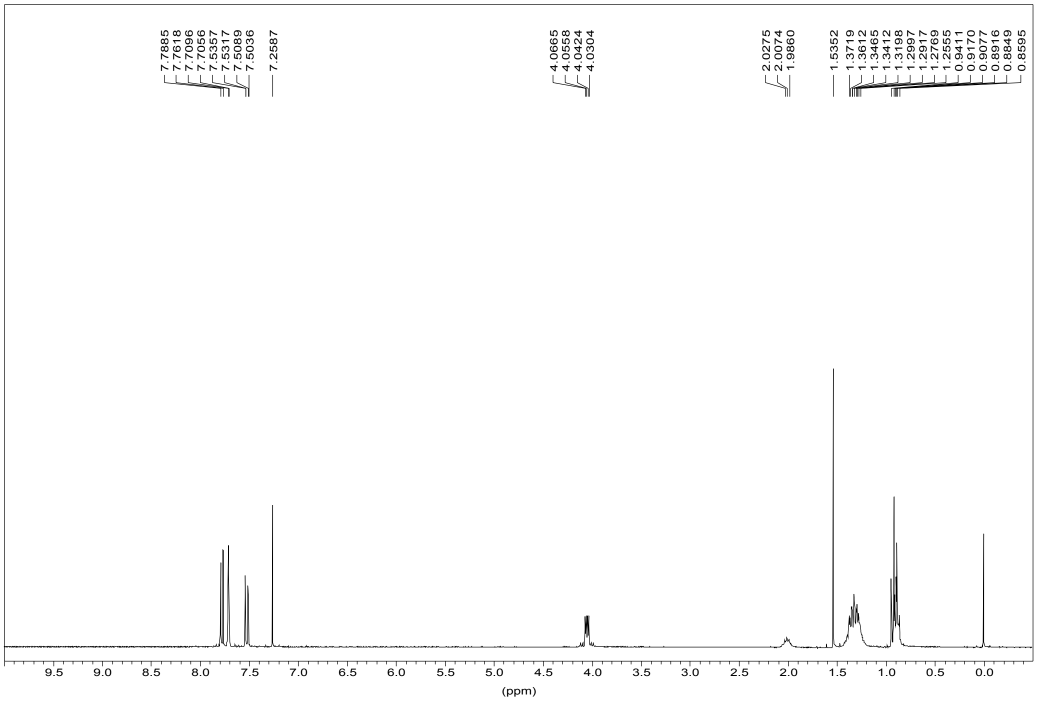

(18) N-(2-ethylhexyl)-2,7-diiodocarbazole

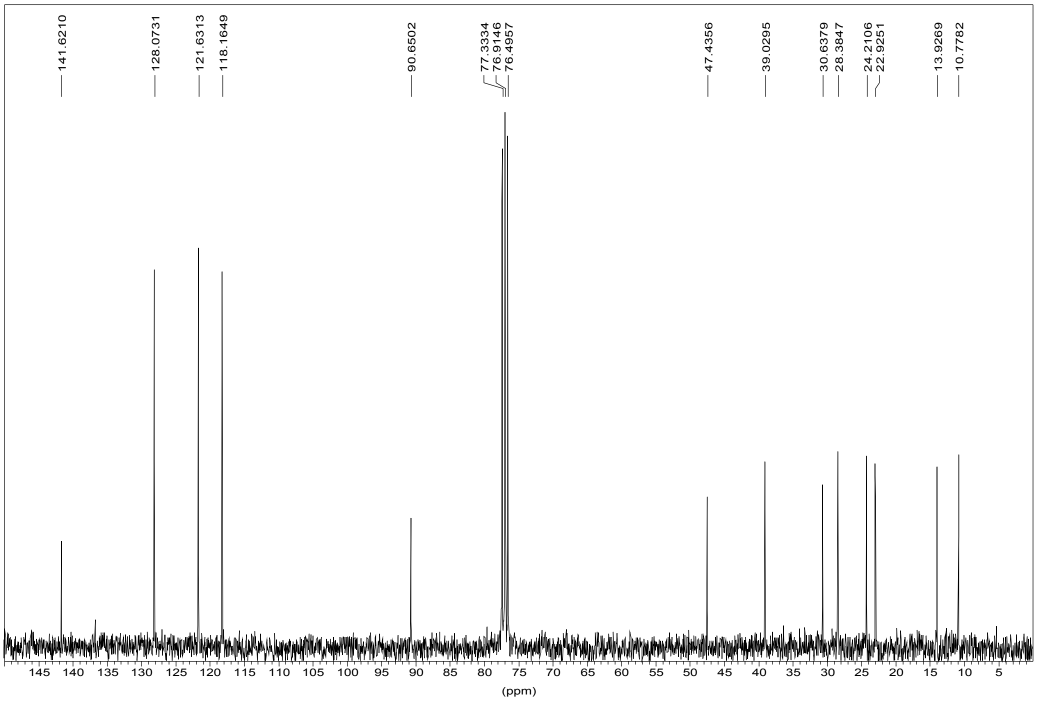

(18) N-(2-ethylhexyl)-2,7-diiodocarbazole

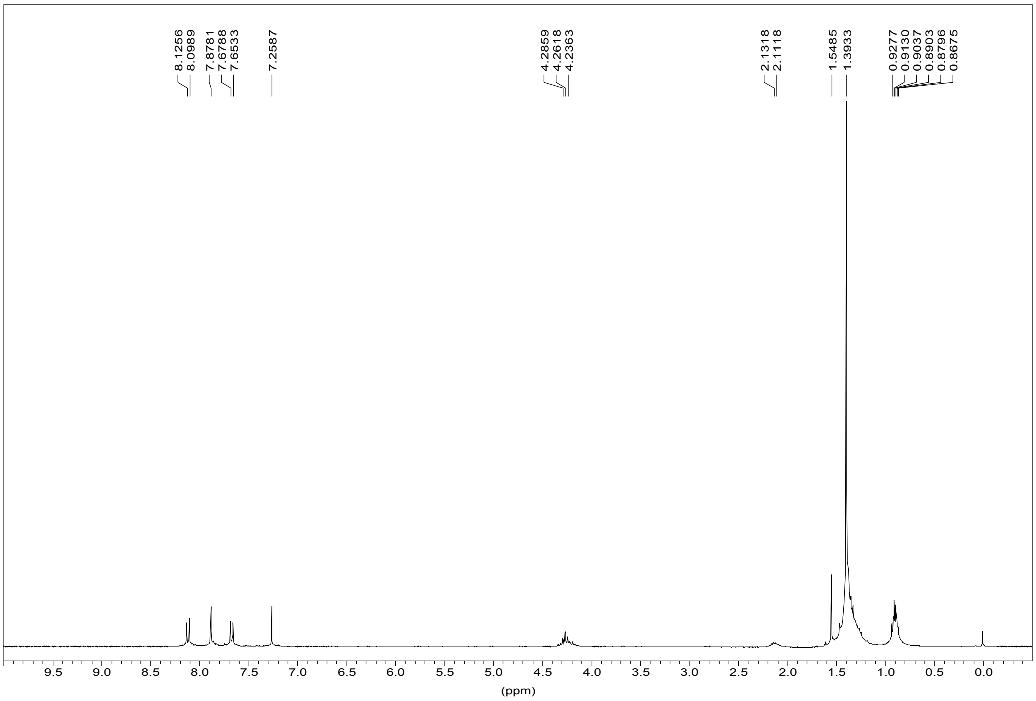

(19) 2,7-Bis(4,4,5,5-tetramethyl-1,3,2-dioxaborolan-2-yl)-N-(2-ethylhexyl)carbazole

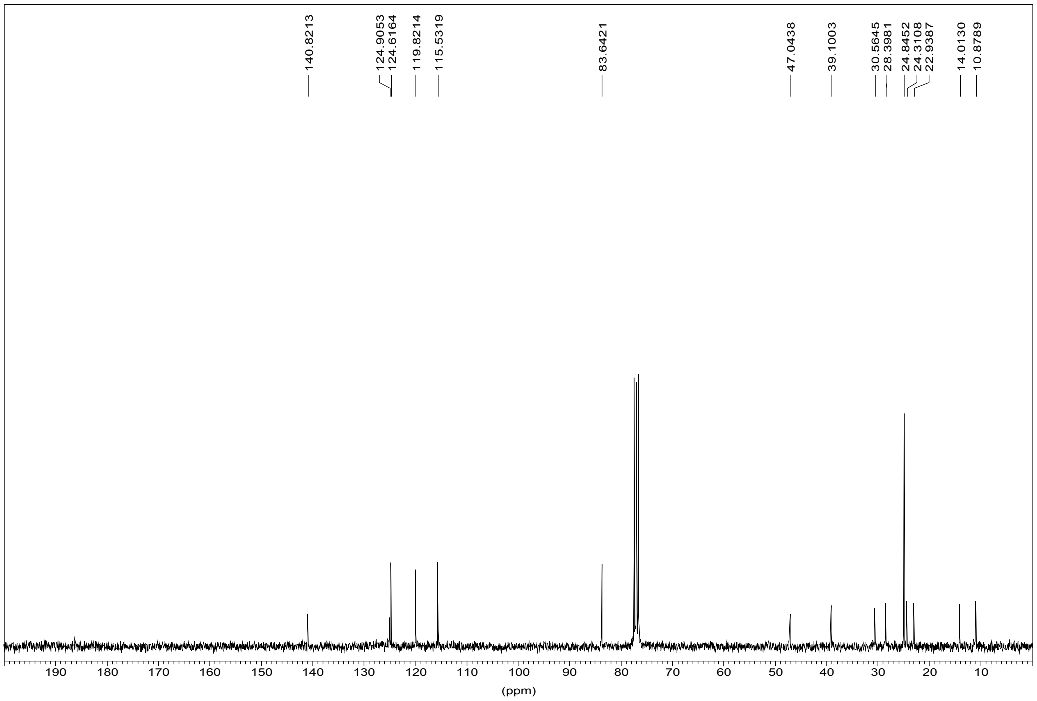

(19) 2,7-Bis(4,4,5,5-tetramethyl-1,3,2-dioxaborolan-2-yl)-N-(2-ethylhexyl)carbazole

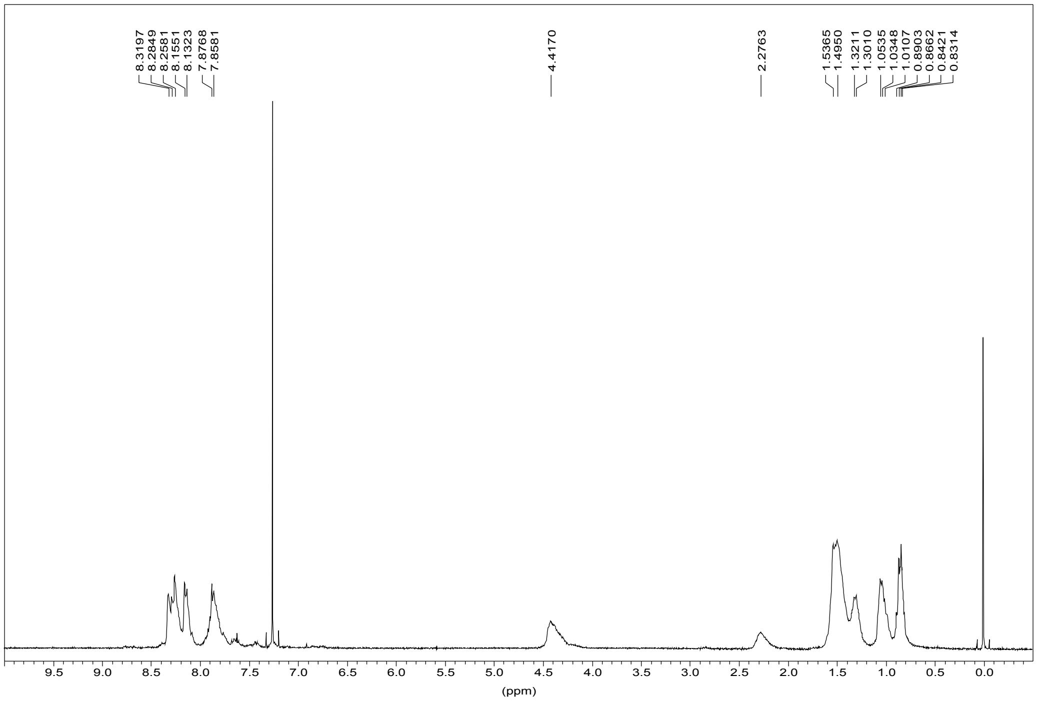

(20) Poly[(2,7-(N-(2-ethylhexyl)carbazolyl)-alt-(2,6-pyridinyl)]

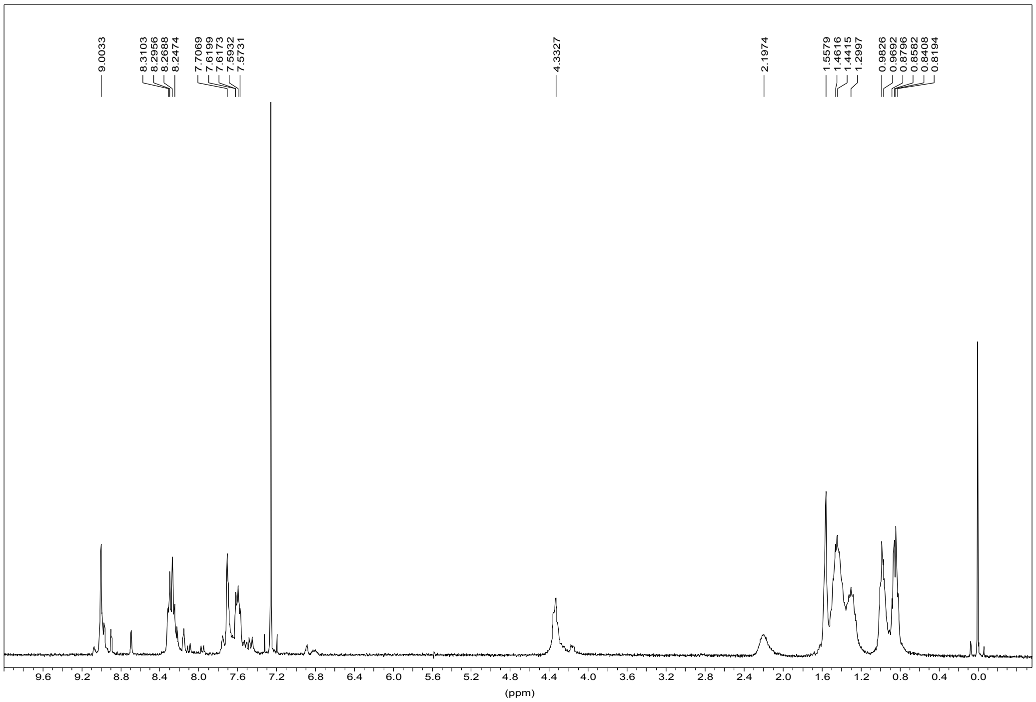

(21) Poly[(2,7-(N-(2-ethylhexyl)carbazolyl)-alt-(3,5-pyridinyl)]

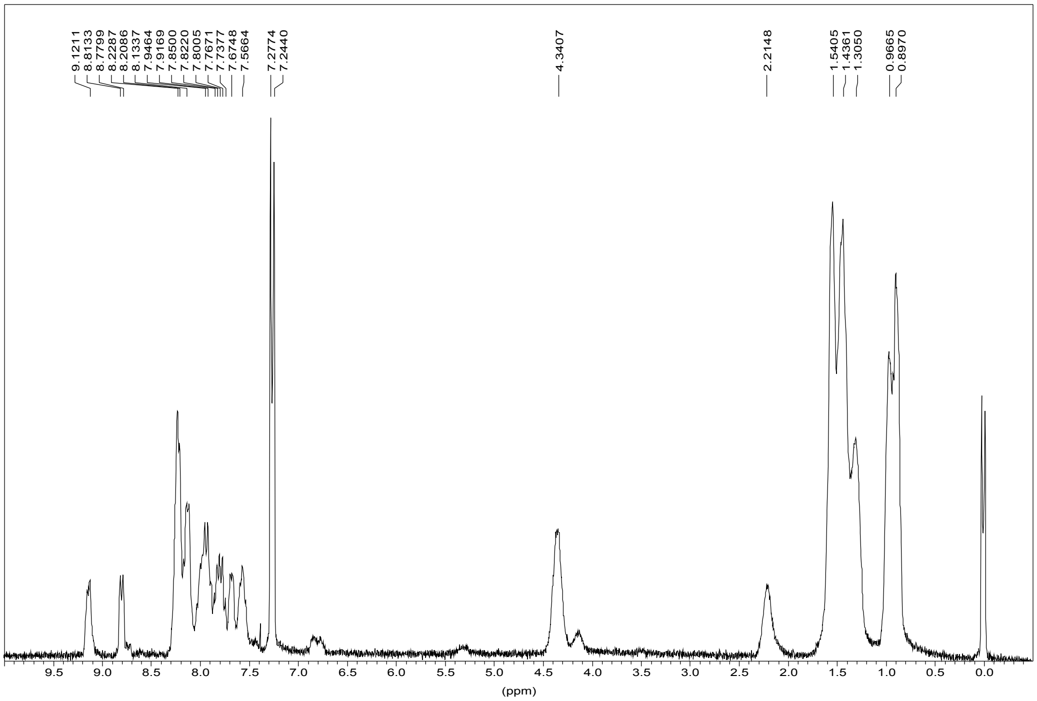

(22) Poly[(2,7-(N-(2-ethylhexyl)carbazolyl)-alt-(2,5-pyridinyl)]